EXPERIMENTAL INVESTIGATION OF PIN PLATES

David Duerr

George Pincus

February 1985

University of Houston - University Park
Department of Civil Engineering
Research Report No. UHCE 85-3

EXPERIMENTAL INVESTIGATION

OF PIN PLATES

by

David Duerr
George Pincus

Report No. UHCE 85-3
Department of Civil Engineering
Cullen College of Engineering
University of Houston - University Park
Houston, Texas 77004
February 1985

EXPERIMENTAL INVESTIGATION OF PIN PLATES

David Duerr
Graduate Student
University of Houston
Houston, Texas 77004

George Pincus
Professor of Civil Engineering
University of Houston
Houston, Texas 77004

ABSTRACT

Current procedures commonly in use for the design of pinned connections are based on limited research and investigation results which have been reported in the literature over the years. The structural specifications, such as AISC and AASHTO, provide empirical design formulas and/or proportion requirements for pin plates which are valid for basic rectangular link plates, but are of questionable suitability when applied to the many non-rectangular shapes encountered in practice, e.g., asymmetrical lifting eyes.

This report presents the results of a two-phase investigation of the behavior of pin plates under static loading. The first phase presents a summary of major theoretical and experimental work conducted by previous investigators. Methods of calculating elastic stresses and ultimate loads are presented, and comparisons of the various formulas are made. The second phase reports the results of pin plate tests conducted by the authors. Asymmetrical shapes, large pin-to-hole clearances, and high strength steels are all addressed in these tests.

Conclusions are drawn where appropriate, and recommendations for additional areas of research of pin plates are made in the final section. General purpose design methods are not developed in this paper.

INTRODUCTION

Techniques currently in common use for the design of pinned connections are based on rather limited research and investigation results that have been published over the years. The bulk of this work falls into two general categories. Theoretical studies, as well as some of the reported experimental work, only considered behavior of pin plates in the elastic range. The balance of the experimental work considered only test specimens of one basic configuration: rectangular plates of constant thickness, hole centered in the plate, and load applied along the longitudinal axis of the plate. In all but one study, the pin through which the load was applied fit relatively closely in the hole. Thus, a rather large amount of extrapolation has been made by practitioners to develop methods by which pin plates may be designed.

In many cases, structural systems using pinned connections possess very little redundancy. One of the most common examples of such a system is an assemblage of lifting equipment, i.e., rigging. The manufactured rigging, such as slings and shackles, are often connected to the lifted load by means of a pin plate, commonly referred to as a lifting eye or padeye. Similarly, a pinned truss, such as an eyebar bridge, has little or no redundancy; failure of one connection could result in complete collapse of the structure. Thus, such members and their connections are often designed with relatively high factors of safety with respect to their ultimate loads.

The working load and ultimate strength behavior of simple pin-connected structural elements, such as eyebars and flat link plates, has been investigated in the past and reported in the literature. The structural steel codes and specifications, such as AISC and AASHTO, give simple design requirements for such members which provide factors of safety considered to be adequate for the intended service. However, due to the limited nature of the investigations into the behavior of pinned connections, the application of the resulting design methods to all types of pin plates is inappropriate.

Some elements of a pinned connection, most notably the aforementioned lifting eyes, may vary in configuration dramatically from the standard link plate or eyebar shape which has been investigated in the literature and addressed in the codes. These plates may be asymmetrical in outline and/or in application of load. The main plate may be reinforced in the area of the pin hole with doubler plates. There may be a relatively large clearance between the pin and the hole; this is particularly common in lifting eyes where a loose fit is desirable to facilitate easy insertion and removal of a shackle pin. It is intuitively obvious that each of these changes in pin plate configuration will affect structural performance. It is thus necessary to investigate each of these areas of pin plate configuration in order to be able to quantify their effects on plate behavior.

This investigation into the behavior of pin plates summarizes past research and presents the results of new tests. A group of specimens were instrumented with resistance-type strain gages and loaded to failure. These specimens were designed to investigate the effects of

varying pin-to-hole clearance, symmetrical but non-rectangular shape, asymmetrical shape and loading, and pin hole area reinforcement. For reference, the ultimate loads of the specimens are compared to the empirical formulas developed by previous investigators.

PREVIOUS PIN PLATE INVESTIGATIONS

Theoretical Studies. There have been a number of purely mathematical investigations of pin plates presented in the literature. Almost without exception, the work presented considers only behavior in the elastic range. Discussions which include plasticity are limited to simply the effect of a plastic hinge; i.e., the effects of strain hardening are not considered. Thus, these techniques, so limited, cannot serve to determine the true ultimate load of a pinned connection. The published work in this category is still useful, however, in analyzing gross section stresses at working loads and for evaluating general patterns of behavior under load.

Eshwar (1978) presents a theoretical analysis of the stresses around a pin hole in an infinite elastic plate. A rigid pin with a radial clearance is fitted in the hole. An absence of friction between pin and plate is assumed.

Two general load conditions are considered. In the first (Fig. 1a), the plate is subject to uniform biaxial stresses at infinity. The inequality of the stresses causes an elliptical deformation of the hole, resulting in bearing between pin and hole edge at two opposite points. No load is applied to the system through the pin. The second condition (Fig. 1b) considers an infinite plate loaded through the rigid pin. It is this second load condition that is of most interest to the present study.

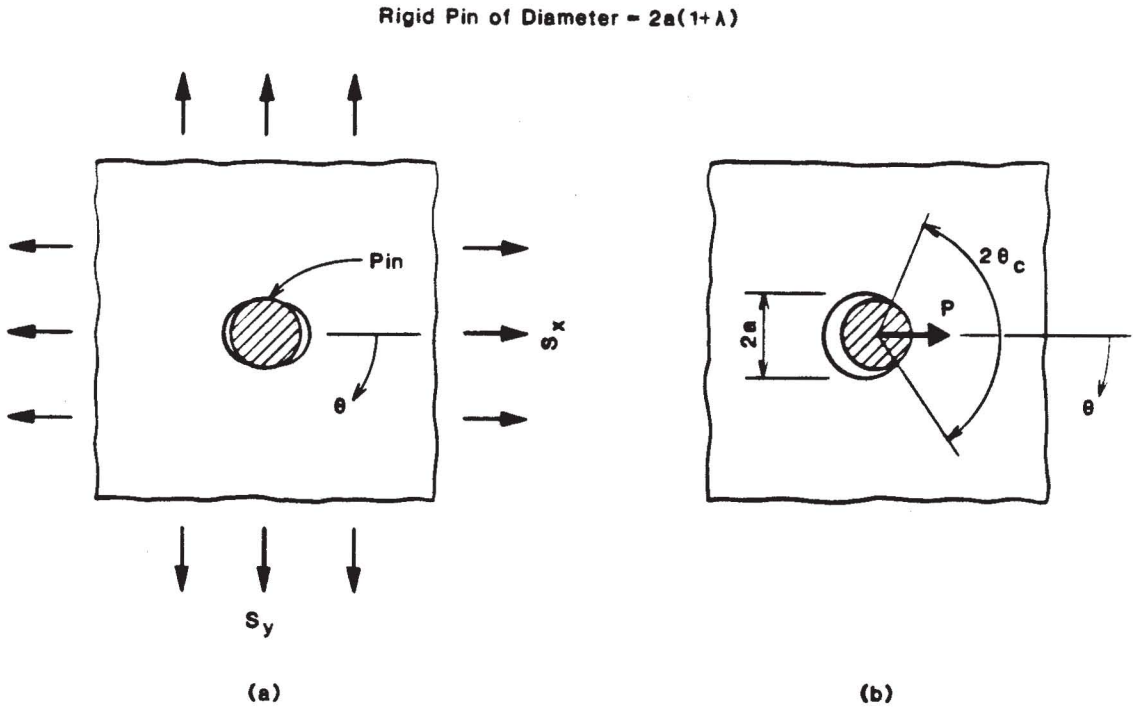

Fig. 1 - Pin Plate Loading Conditions Investigated by Eshwar (1978)

The investigation of the loaded pin condition has as its results a set of curves relating pin load, plate elastic properties, hole radius, pin-to-hole clearance, arc of contact, and maximum radial stress in the plate. An expression for radial stress distribution is also presented. The analysis is approached as a mixed boundary problem with moving boundaries. Boundary conditions, an Airy stress function and its auxiliary displacement function were written for the problem. A computer program was then written, and numerous cases were solved. From the numerical data obtained, the curves presented in the paper were developed. In all cases, a plate thickness of unity is assumed.

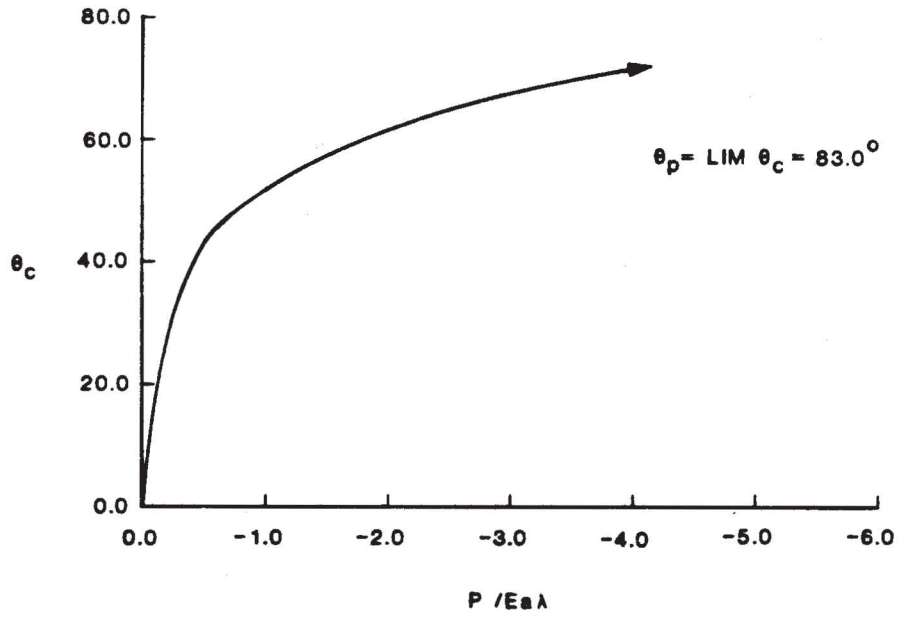

Fig. 2 - Load vs. Region of Contact from Eshwar (1978)

Figure 2 shows Eshwar's curve of load vs. region of contact for a material with Poisson's ratio equal to 0.3. In the figure, P is the pin load, E is the modulus of elasticity of the plate, a is the hole radius, λ is the proportional clearance as defined in Figure 1, and θ_c is one-half of the arc of contact.

Figure 3 presents Eshwar's curve of load vs. maximum radial stress, $\sigma_{r\ max}$. Notation is similar to that used in Figure 2. The maximum stress determined from the curve can then be used to determine the radial stress at any other point along the contact arc using the following expression:

$$\sigma_r = \sigma_{r\ max} \left[1 - \left(\theta^2/\theta_c^2\right)\right]^{\frac{1}{2}} \qquad (1)$$

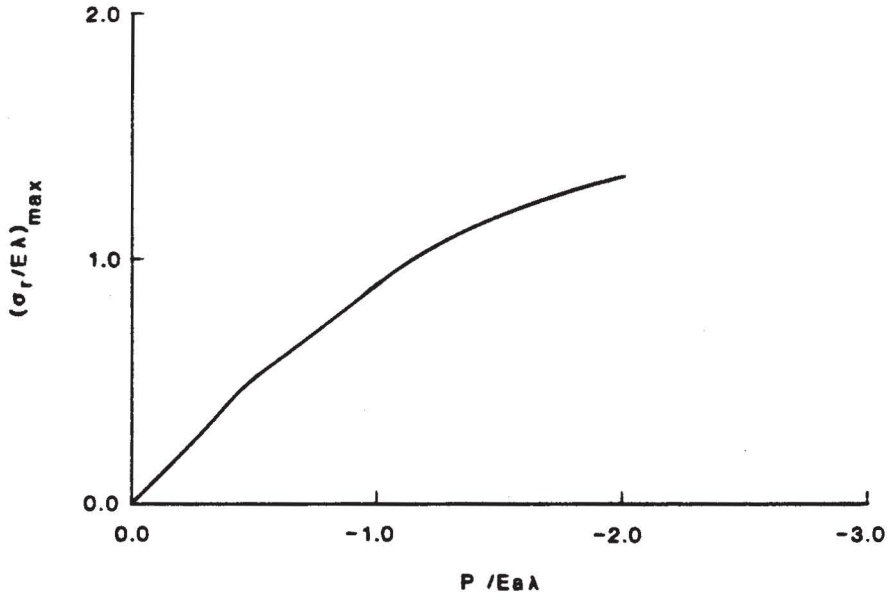

Fig. 3 - Load vs. Maximum Radial Stress from Eshwar (1978)

Finally, Figure 4 shows Eshwar's curve of load vs. pin displacement in the direction of the applied load. U is the pin displacement, and all other values are as previously defined.

These curves are strictly the product of a mathematical solution to the pin-in-hole problem. No attempt has been made by Eshwar to correlate these results to any test data. In the discussions that follow, these curves will be compared to both other theoretical studies of this problem and to the test data accumulated in this investigation, as appropriate.

Rao (1978) presents a broader discussion of the mathematical analysis of the pin-in-infinite-plate problem which was addressed by Eshwar (1978). Rao expands upon the problem by also addressing the effects of an elastic pin, interference fits, different levels of fric-

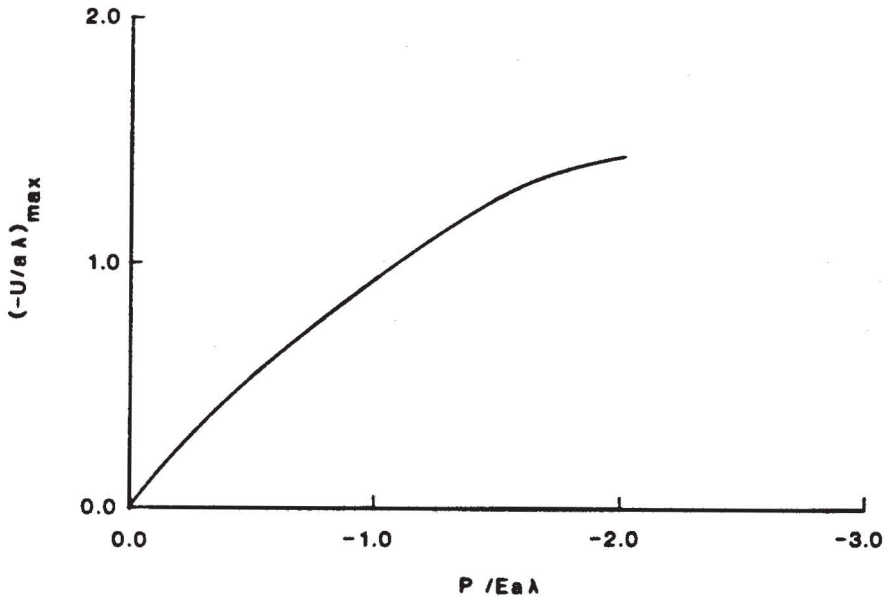

Fig. 4 - Load vs. Pin Displacement from Eshwar (1978)

tion between pin and plate, and a polarly varying interference or clearance. Obviously, not all of these considerations are important relative to pinned connections as used in civil engineering structures. Specifically, interference fits in pinned joints are generally not utilized in standard practice. Likewise, fabrication techniques in common use are not sophisticated enough to yield any knowledge about the magnitude of a polarly varying clearance; i.e., holes and pins are assumed to be round. Also, Rao only addresses the varying clearance aspect for the biaxially loaded plate and not for the loaded pin case.

Friction between pin and plate is only considered at the two extremes: $\mu = 0$ (as was assumed by Eshwar) and $\mu = \infty$. Infinite friction essentially implies a bonded joint. Machined surfaces of steel on steel exhibit a coefficient of friction of less than 1.0, so, of these

two extremes, $\mu = 0$ is closer to reality. Furthermore, Frocht and Hill (1940) experimentally addressed the question of pin friction by introducing lubrication in the joint and concluded that the reduction in coefficient of friction only slightly reduced the stress concentration in the plate. The Frocht and Hill paper will be discussed additionally at a later point.

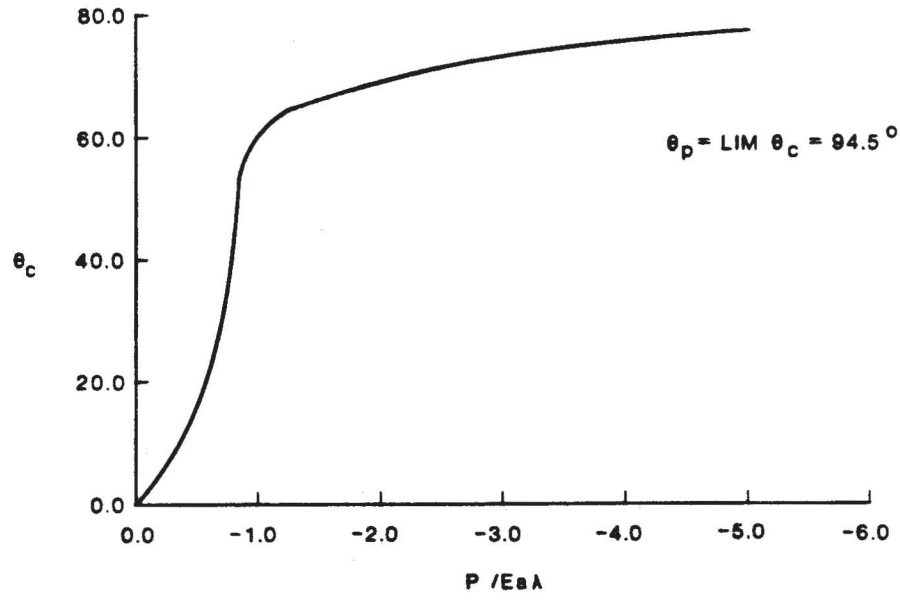

Fig. 5 - Load vs. Region of Contact from Rao (1978)

The effect of pin elasticity does have a significant effect on joint behavior, however. Rao presents an analysis similar to that of Eshwar, but accounts for elastic deformation in the pin. Two curves of results are presented here for the loaded pin case with $\upsilon = 0.3$ and $E_{pin} = E_{plate}$. Figure 5 shows Rao's curve of load vs. region of contact. Note that, at the limit, the plate starts to "wrap around" the pin slightly. This behavior was observed in the test program portion

of the current study. Figure 6 presents a curve of load vs. pin displacement. Rao did not provide curves of load vs. radial stress for the elastic pin cases. As with the curves from Eshwar (1978), these curves will also be further evaluated in the discussions that follow.

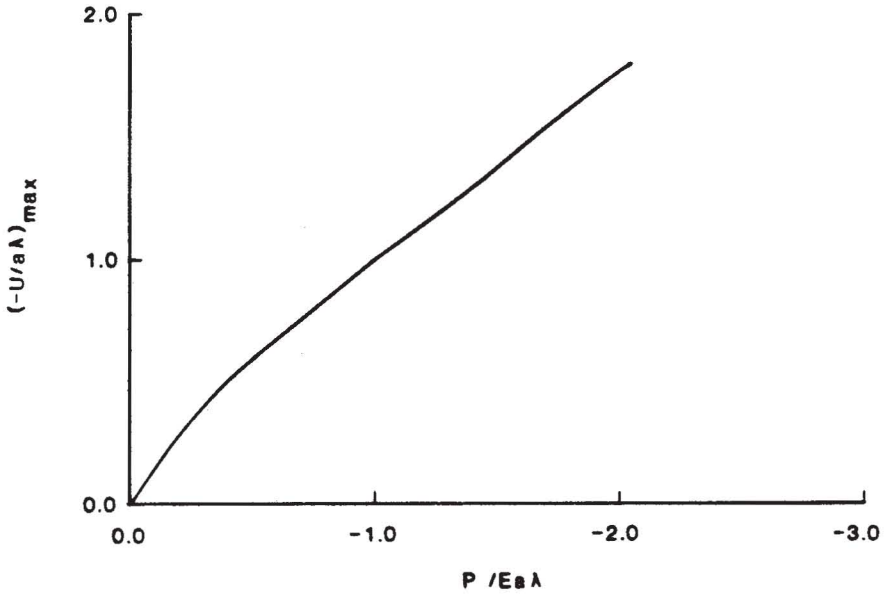

Fig. 6 - Load vs. Pin Displacement from Rao (1978)

Rao also presents an introductory attempt to address a pin plate of finite size. A round-ended link plate with a concentric hole (such as Specimen 1-A of this study) with a rigid interference fit pin is analyzed. As was stated above, the interference fit arrangement is outside of the scope of this investigation.

A classic treatment of elastic stresses in the head of an eyebar is presented by Timoshenko and Goodier (1970). Figure 7 shows the basic shape treated and defines the notation used.

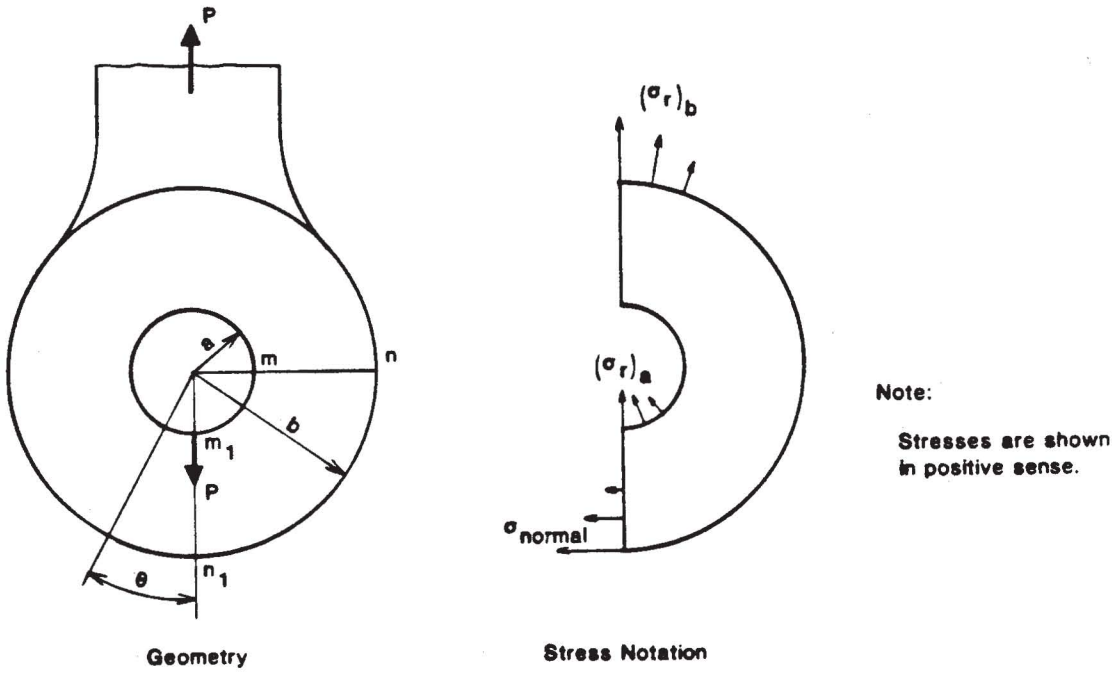

Fig. 7 - Eyebar Investigated by Timoshenko and Goodier (1970)

Two equations are presented which define the radial stresses acting on the inner and outer boundaries of the eyebar head. These equations are based on the assumptions of a neat fit pin, no friction between the pin and the hole, and a Poisson's ratio of 0.3.

$$\left(\sigma_r\right)_a = -\frac{2P}{\pi}\frac{\cos\theta}{a} \text{ for } -\frac{\pi}{2} \le \theta \le \frac{\pi}{2} \tag{2}$$

$$\left(\sigma_r\right)_b = -\frac{2P}{\pi}\frac{\cos\theta}{b} \text{ for } \frac{\pi}{2} \le \theta \le \frac{3\pi}{2} \tag{3}$$

Timoshenko has expanded these equations and solved for the normal stresses on sections mn and m_1n_1 for the proportions b/a = 2 and b/a = 4. Again, these calculations are based on a Poisson's ratio of 0.3. The curves defining these stress distributions are shown in Figure 8 for section mn and Figure 9 for section m_1n_1. The values presented assume a plate thickness of unity.

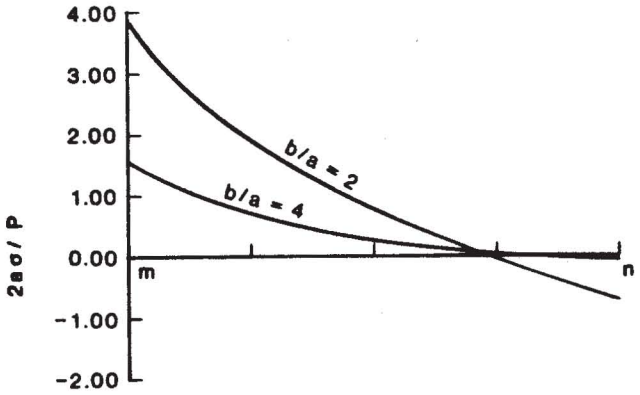

Fig. 8 – Normal Stresses on Section mn

This work on eyebar heads is an extension of Timoshenko's study of elastic stresses in a circular ring compressed by two equal and opposite forces acting along a diameter. Seely and Smith (1952) present a similar closed ring study, but expand the investigation to consider behavior up to the ultimate load. In this case, ultimate load is defined as the load at which a plastic hinge is formed at each of the four quarter points of the ring. Because this work is somewhat dis-

placed from the subject of this study, no discussion of the Seely and Smith investigation will be made here. The reference is made primarily because of its similarity to the basis of the Timoshenko eyebar work.

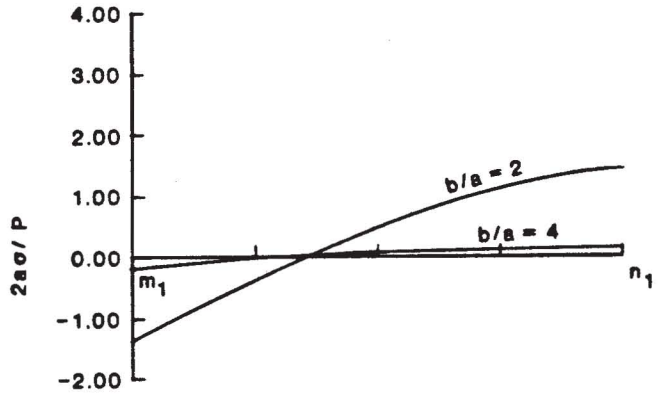

Fig. 9 - Normal Stresses on Section m_1n_1

In the discussion presented above, we have indicated that the mathematical investigations conducted by others will be of limited use in developing the results desired within the scope of this study. This should not be interpreted as meaning that this work is not significant. There is simply a difference of goals. The current research is investigating the ultimate load behavior of pin plates under static loading. Ultimate load is defined as that load which produces fracture or buckling failure. Studies which consider behavior principally in the elastic range are of particular value in the investigation of cyclically loaded connections. [It is noted that two of the authors whose work was discussed above (Eshwar and Rao) are associated with the De-

partment of Aeronautical Engineering of the Indian Institute of Science]. Under cyclic loading, large plastic strains could not be tolerated at working load levels.

In the following sections, experimental studies of pin plates performed by other investigators will be presented. These test results will be compared to the theoretical work and suitable conclusions will be drawn.

Experimental Work. The experimental investigations which have been carried out over the years have generally been relatively limited in scope. Often, a research project was initiated to explore pin plate behavior with respect to a specific purpose. This is in contrast to the theoretical studies discussed previously which considered general behavior. Regardless of purpose, however, the results of these tests are enlightening in the understanding of pin plate behavior and performance.

Johnston (1939) conducted a very extensive test program in which 106 pin plates were loaded to failure. This work was particularly interested in plate links used in bridge hanger details and, more specifically, in plate failure due to out-of-plane instability, referred to as "dishing." The ranges of dimensions of the test specimens were thus guided by the typical proportions of such bridge hangers in use at that time.

Figure 10 depicts the specimen configuration used by Johnston. Only Specimens 104, 105, and 106 had the corners clipped; all other specimens had plain rectangular ends. Figure 10 also shows the notation established by Johnston. This notation has been adopted by other

experimental researchers and will be used in this work when discussing the current tests.

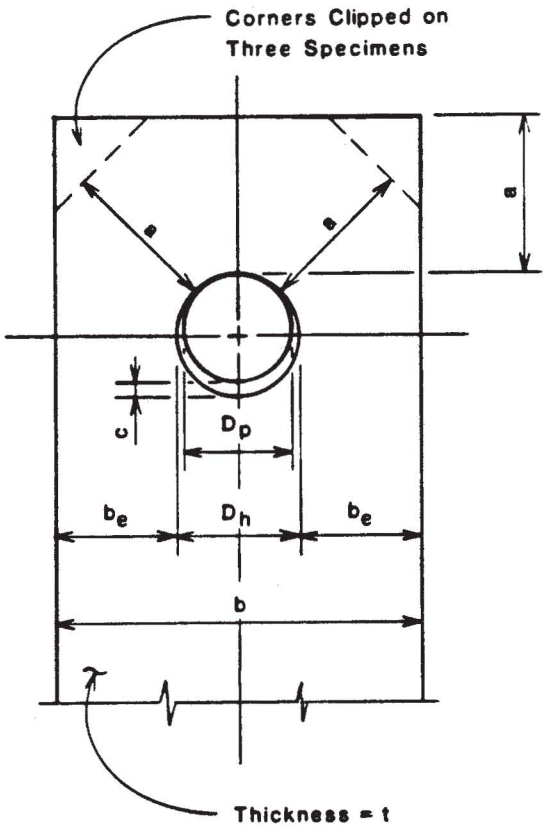

Fig. 10 - Specimen Configuration Tested by Johnston (1939)

The phenomenon of dishing will not be actively considered in this paper. This is for two reasons. First, as stated in the introduction, we have a particular interest in the application of pin plate behavior knowledge to the design of lifting eyes. Lifting eyes are most commonly of stout proportions that preclude dishing. Second, a future effort will study application of finite element analysis to pin plates.

ANSYS, the program to be used for this study, does not have the capability to solve a dishing problem. A buckling solution is available, but only in an elastic structure (Kohnke, 1983, pg. 1.7.1). Test observations indicate a great deal of plastic deformation prior to the onset of dishing, so a linear solution with the buckling option would be quite meaningless. Resultantly, the Johnston specimens which failed by dishing will not be considered in this investigation.

A total of 28 of the Johnston specimens failed by fracture. The as-built dimensions, material properties, ultimate load, and location of failure for these tests are assembled in Table 1. All dimensional notation is defined in Figure 10. The "location of failure" terminology is defined as follows. A failure beyond the pin hole is a fracture due to tensile "hoop" stress on a line parallel to the applied load. A side failure is a simple tensile failure in the net section to the side of the hole. Representations of both types of failures are shown in Figure 11.

Table 1

Pin Plate Test Results Reported by Johnston (1939)

Test Number	D_h, in inches	D_p, in inches	t, in inches	b_e, in inches	a, in inches	F_y, in kips per square inch	F_u, in kips per square inch	P_{ult}, in kips	Location of Failure
25	3.017	3.000	0.254	2.485	1.016	41.6	63.7	38.0	Beyond
31	3.072	3.000	0.256	2.458	0.998	41.6	63.7	36.9	Beyond
32	3.069	3.000	0.258	2.460	1.685	41.6	63.7	49.0	Beyond
37	3.016	3.000	0.373	2.493	0.997	39.4	63.4	53.7	Beyond
38	3.016	3.000	0.372	2.495	1.709	39.4	63.4	72.0	Beyond
43	3.066	3.000	0.373	2.466	0.959	39.4	63.4	58.9	Beyond

Table 1 (con't.)

Pin Plate Test Results Reported by Johnston (1939)

Test Number	D_h, in inches	D_p, in inches	t, in inches	b_e, in inches	a, in inches	F_y, in kips per square inch	F_u, in kips per square inch	P_{ult}, in kips	Location of Failure
44	3.066	3.000	0.371	2.474	1.681	39.4	63.4	78.0	Beyond
56	3.067	3.000	0.494	2.471	1.685	38.5	63.4	101.5	Beyond
57	3.066	3.000	0.494	2.480	2.174	38.5	63.4	118.9	Beyond
58	3.066	3.000	0.495	2.475	2.601	38.5	63.4	138.2	Beyond
61	3.015	3.000	0.745	2.494	0.988	31.3	60.2	108.4	Beyond
62	3.016	3.000	0.747	2.505	1.702	31.3	60.2	150.6	Beyond
63	3.016	3.000	0.746	2.491	2.176	31.3	60.2	162.0	Beyond
64	3.016	3.000	0.745	2.492	2.579	31.3	60.2	185.9	Beyond
67	3.067	3.000	0.745	2.465	1.010	31.3	60.2	111.6	Beyond
68	3.067	3.000	0.742	2.459	1.679	31.3	60.2	147.2	Beyond
69	3.067	3.000	0.745	2.465	2.215	31.3	60.2	172.8	Beyond
79	3.018	3.000	0.514	1.510	0.978	39.6	62.6	64.6	Beyond
80	3.016	3.000	0.512	1.509	1.674	39.6	62.6	98.6	Side
81	3.017	3.000	0.515	1.504	2.201	39.6	62.6	100.5	Side
82	3.016	3.000	0.512	1.506	2.571	39.6	62.6	99.8	Side
83	3.015	3.000	0.513	1.508	2.905	39.6	62.6	100.9	Side
84	3.015	3.000	0.513	1.506	3.210	39.6	62.6	100.5	Side
91	3.016	3.000	0.508	3.485	1.008	36.5	63.1	83.8	Beyond
92	3.015	3.000	0.507	3.487	1.731	36.5	63.1	113.3	Beyond
93	3.015	3.000	0.509	3.485	2.191	36.5	63.1	129.2	Beyond
94	3.020	3.000	0.507	3.481	2.573	36.5	63.1	139.8	Beyond
106	3.200	3.000	0.492	2.402	2.897	41.0	65.5	151.2	Beyond

Note: 1 in. = 25.4 mm; 1 kip = 4.45 kN; 1 ksi = 6.89 MPa

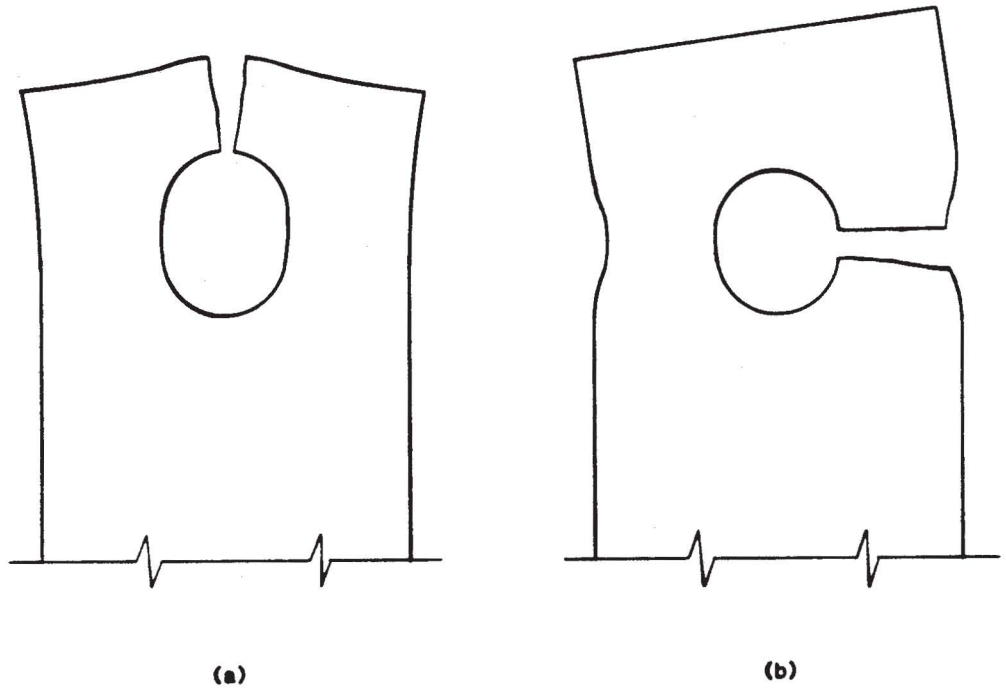

Fig. 11 - (a) Fracture Beyond the Hole, (b) Fracture to the Side

In addition to ultimate load by one of three modes of failure (side, beyond, or dishing), Johnston also defined the general yield load of the specimen. During each test, gross pin movement with respect to a point on the plate 8.5 inches from the center of the hole was measured with a dial indicator. This deflection was plotted against load. The point at which the slope of the curve had changed by a factor of three was defined as the general yield point.

The data accumulated in the tests were reduced to a set of empirical equations which can be used to predict the strength and behavior of plate links. Each of these equations is written in terms of the average bearing stress on the projected area of the pin. Thus, if we let f_{py} = average bearing stress at the general yield load, f_{pt} = average

bearing stress at the ultimate load, and use other previously defined notation, we can write the Johnston equations as follows.

$$f_{py} = \frac{F_y}{2}\left[3\left(\frac{a}{D_h}\right)-\left(\frac{a}{D_h}\right)^2 - 2\left(\frac{c}{D_h}\right)\right] \tag{4}$$

for failure by fracture at the side:

$$f_{pt} = 2\,F_u\left(\frac{b_e}{D_h}\right) \tag{5}$$

for failure by fracture beyond:

$$f_{pt} = F_u\left[1.13\left(\frac{a}{D_h}\right)+\frac{0.92\left(\frac{b_e}{D_h}\right)}{1+\left(\frac{b_e}{D_h}\right)}\right] \tag{6}$$

for failure by dishing:

$$f_{pt} = 20 + 315\left(\frac{t}{D_h}\right)+ 75\left(\frac{t\,b_e}{D_h^2}\right) + 20\left(\frac{a}{D_h}\right)- 20\left(\frac{a}{D_h}\right)^2 \tag{7}$$

The applicability of these equations is limited to the following dimensional ranges: a/D_h between 0.3 and 1.2; and, c/D_h between 0.0 and 0.07. The following limits also apply only to Equation 4: b_e/D_h greater than 0.5; and, t/D_h greater than 0.05. Applied to a particular pin plate, the lowest value calculated by Equations 5, 6, and 7 indicates both the expected ultimate strength of the plate and the type of failure.

In this paper, Johnston also introduced the concept of balanced design, i.e., those proportions for which fracture beyond the hole and

to the side would be imminent simultaneously. The following equation gives a ratio of edge distances which produces an approximately balanced design:

$$\frac{a}{b_e} = \frac{1 + 1.75\left(\frac{b_e}{D_h}\right)}{1 + \left(\frac{b_e}{D_h}\right)} \tag{8}$$

Equation 8 is based on the assumption that the plate is laterally restrained or is thick enough that dishing will not occur. If the proportions established by Equation 8 are used, the minimum thickness required to prevent dishing can be determined using Equation 9.

$$\frac{t}{D_h} = \frac{-20 + 123\left(\frac{b_e}{D_h}\right) - 20\left(\frac{a}{D_h}\right) + 20\left(\frac{a}{D_h}\right)^2}{315 + 75\left(\frac{b_e}{D_h}\right)} \tag{9}$$

The information in Table 1 shows that, in most cases, the pin fit relatively closely in the hole. All specimens had a pin clearance of 0.072 inch or less except Specimen 106, which had 0.20 inch clear. For these small clearances, Johnston noted a slight change in the general yield point but no change in ultimate strength. Lastly, the clipping of the corners beyond the pin was found to have only a very minor effect on ultimate strength.

Frocht and Hill (1940) performed two series of tests on pin plate specimens. One series consisted of a set of aluminum plates loaded through either steel or aluminum pins. Pin clearance varied from a neat fit to a clearance of 0.015 inch. Tensometers with a 1/2 inch

gage length were used to measure strain. The second set was a group of bakelite models from which strains were read photoelastically. Pin clearance was varied as with the aluminum specimens. The general configuration of the specimens is identical to that used by Johnston (1939). The notation defined in Figure 10 will be used here for consistency.

The goal of the Frocht and Hill paper, as stated in the title, is to develop a record of stress concentration factors as a function of plate geometry and proportions. Only tensile stresses at the sides of the hole were considered in this investigation. The peak tensile stresses, noted as S_t, were determined from the photoelastic patterns or from the measured strains. This peak stress was then divided by the average tensile stress on the net section or by the average bearing stress on the projected area of the pin to arrive at the stress concentration factor, k.

Individual test results for each specimen were not published in the paper. The interpreted results were presented as curves. The two most significant curves are reproduced here. Figure 12 shows a plot of stress concentration factor vs. the ratio of hole diameter to plate width for aluminum specimens loaded through a neat fit aluminum pin. Figure 13 shows a plot of stress concentration factor based on average bearing stress vs. the same ratio for the photoelastic tests.

As would be expected, clearance between pin and hole resulted in an increase in the stress concentration factor. The photoelastic tests indicated an increase on the order of 10% for a clearance of 0.018

inch. The aluminum tests yielded an increase of only about 2.5% for a clearance of 0.015 inch.

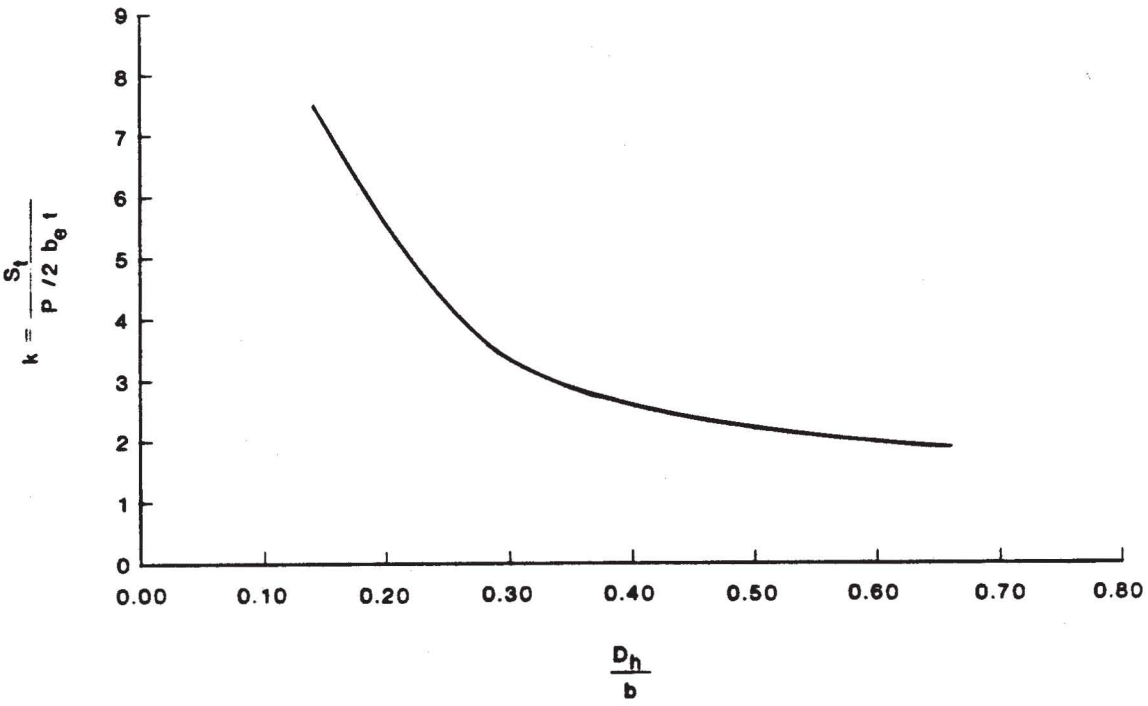

Fig. 12 - Stress Concentration Factors with a Neat Fit Pin from Frocht and Hill (1940)

Frocht and Hill also investigated the effect of lubrication on the stress concentration factor by introducing grease in the connection. It was found that the reduction of friction between pin and plate reduced the stress concentration factor by about 3.4%. Similarly, the change from an aluminum pin to a steel pin increased the factor by about the same amount.

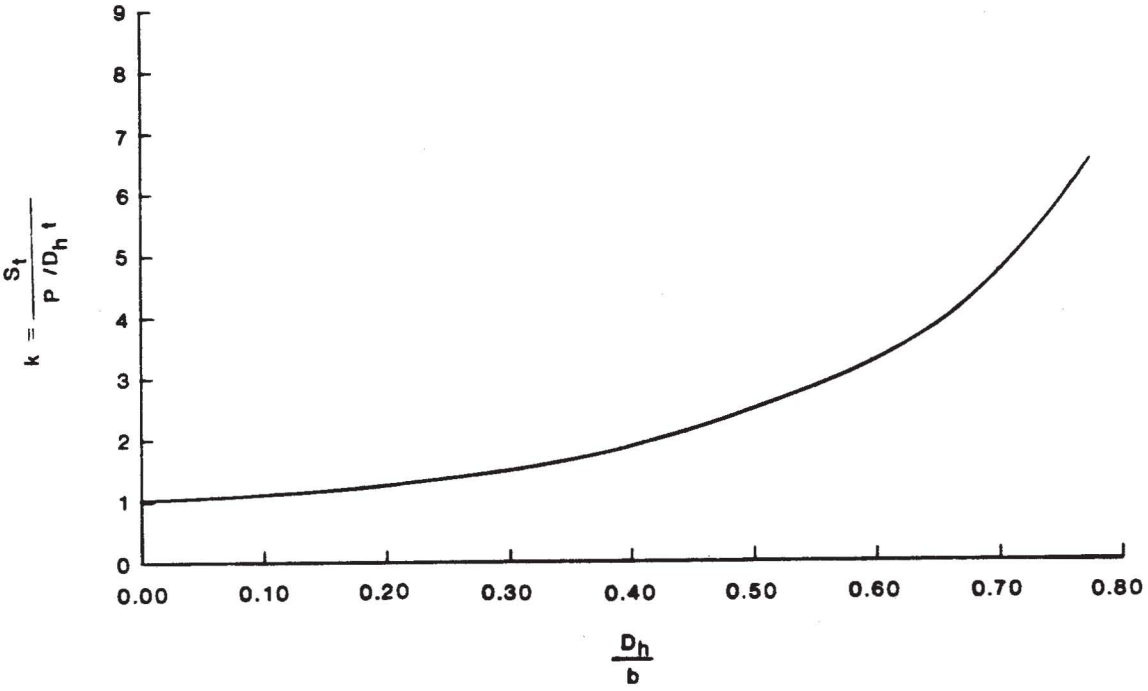

Fig. 13 - Stress Concentration Factors Based on Average Bearing Stress from Frocht and Hill (1940)

This work investigated stresses only in the elastic range. This is particularly valuable when considering a pinned connection subject to cyclic loading where fatigue resistance is important. However, when considering the ultimate strength of a statically loaded connection, these stress concentration factors can be used only to predict the onset of yielding in the plate. Beyond that point, these values are no longer valid.

Tolbert (1970) performed an investigation of pin plate behavior using steel specimens coated with a birefringent material. The most significant aspect of Tolbert's work is his study of behavior with large pin-to-hole clearances. A total of 13 specimens comprised this

study. All were of the rectangular configuration illustrated in Figure 10. The dimensions, material properties, and failure loads of the specimens are shown in Table 2.

Table 2

Pin Plate Test Results Reported by Tolbert (1970)

Test Number	D_h, in inches	D_p, in inches	t, in inches	b_e, in inches	a, in inches	F_y, in kips per square inch	F_u, in kips per square inch	P_{ult}, in kips	Location of Failure
1	1.000	0.500	0.10	0.970	0.396	35.0	53.7	3.640	Beyond
2	1.000	0.625	0.10	0.970	0.396	35.0	53.7	3.765	Beyond
3	1.000	0.750	0.10	0.970	0.396	35.0	53.7	4.235	Beyond
4	1.000	0.875	0.10	0.970	0.396	35.0	53.7	4.810	Beyond
5	1.000	1.000	0.10	0.970	0.396	35.0	53.7	5.250	Beyond
6	1.000	1.000	0.10	1.763	0.370	35.0	53.7	5.120	Beyond
7	1.000	1.000	0.10	1.500	0.370	35.0	53.7	5.090	Beyond
8	1.000	1.000	0.10	1.239	0.370	35.0	53.7	4.970	Beyond
9	1.000	1.000	0.10	1.000	0.370	35.0	53.7	4.800	Beyond
10	1.000	1.000	0.10	0.750	0.370	35.0	53.7	4.570	Beyond
11	1.000	1.000	0.10	0.970	0.509	35.0	53.7	N/R	Beyond
12	1.000	1.000	0.10	0.970	0.750	35.0	53.7	N/R	Dishing
13	1.000	1.000	0.10	0.970	0.845	35.0	53.7	N/R	Dishing

Note: 1 in. = 25.4 mm; 1 kip = 4.45 kN; 1 ksi = 6.89 MPa; N/R = not reported

During each test, strains were measured photoelastically along a straight transverse line 1/4 inch beyond the hole and along a half-circle with a radius of 0.75 inch, also beyond the hole. A large volume of data was assembled and, for obvious reasons, will not be repro-

duced herein. Specific pieces of data will be presented in later sections where needed. (The original reference may be obtained through the Interlibrary Loan Office if access to all data is desired by the reader.)

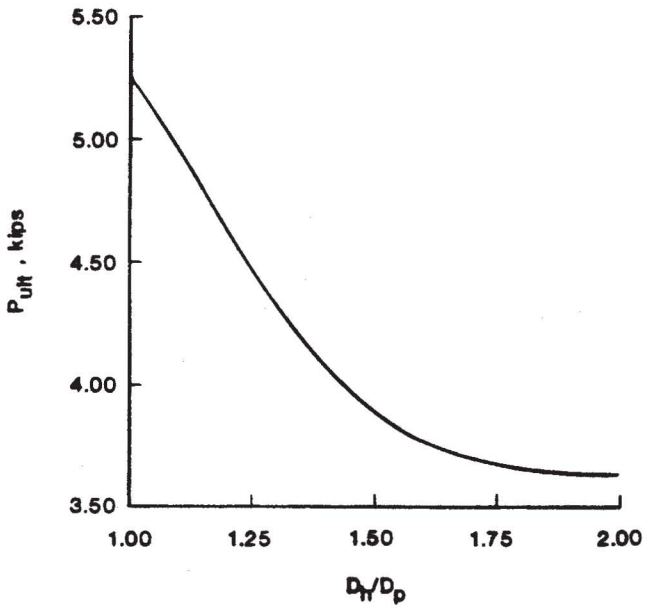

Fig. 14 – Ultimate Load vs. D_h/D_p from Tolbert (1970)

Previous investigators, discussed above, stated that increased pin clearance resulted in somewhat higher stresses around the hole. Tolbert demonstrated the effect when very large clearances were introduced. Tests 1 through 5 are identical plates loaded through different size pins. As would be expected, smaller pin diameters resulted in higher stress concentrations and, ultimately, lower failure loads. To show the trend, a curve of failure load vs. the ratio of hole diameter

to pin diameter is plotted in Figure 14. From these tests, it appears that the curve flattens beyond $D_h/D_p = 2.0$ and that further clearance will have minimal effect on ultimate strength. This behavior will be discussed additionally at a later point.

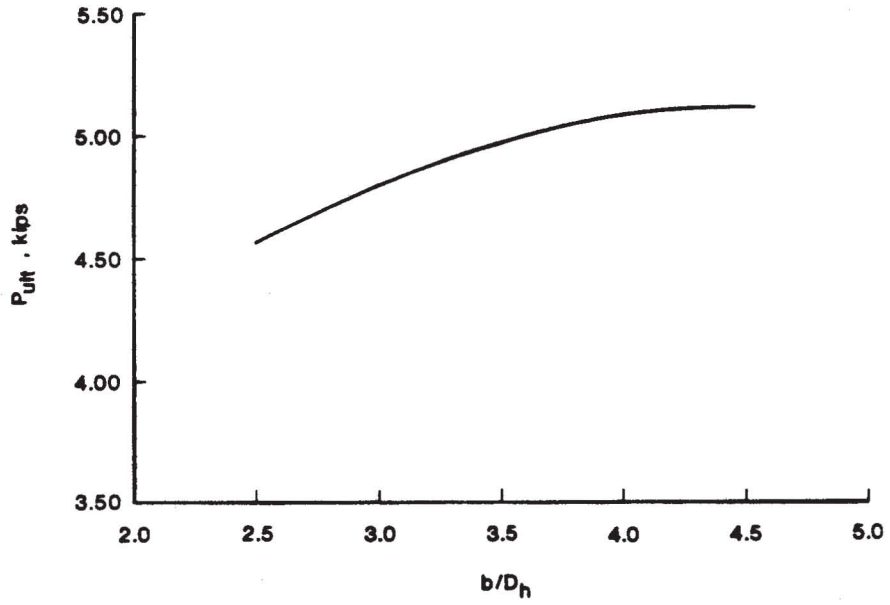

Fig. 15 – Ultimate Load vs. b/D_h from Tolbert (1970)

Tests 6 through 10 investigate the effect of increasing the side distance, b_e, on plate behavior. As was shown earlier by Johnston, an increase in b_e results in an increase in the ultimate load. A curve of failure load vs. the ratio of plate width to hole diameter is plotted in Figure 15. Again, a trend is noted. The curve appears to be flattening beyond $b/D_h = 4.5$, thus indicating the behavior of a plate of

infinite width. These results will be compared to the Johnston equations in the next section.

Tests 11 through 13, combined with Test 5, examined the effect of increased area beyond the pin hole. Strain readings were made at loads of 1.0 kip and 2.0 kips, but no ultimate loads were reported. Thus, further discussion of these tests is not possible at this time.

An important point must be stated here. Tolbert did not load the specimens to the point of fracture. Rather, the specimens were loaded until the load began to drop off. This indicated the ultimate load. All specimens were proportioned to fail beyond the hole. A pronounced arching of the plate material over the hole, as shown in Figure 11(a), was observed in all of the specimens. Tolbert interpreted this as a simple shear failure. However, the trend of increasing ultimate load with increasing side distance indicates a "hoop" behavior, as was noted by Johnston (1939). Thus, it is felt by this writer that, had the specimens been allowed to fracture, a failure of the type depicted in Figure 11(a) would have resulted.

U.S. Steel Research conducted a test program in which 23 specimens of the configuration shown in Figure 10 were loaded to failure. This work is reported by Blake (1981). The as-build dimensions, material properties, failure loads, and types of failure are assembled in Table 3. Note that an additional type of failure is referenced in Table 3. Figure 16 illustrates a shear failure of a pin plate.

The report written by Blake simply presents a description of the test program and raw test results. No interpretation of the data was made. U.S. Steel retained Dr. Theodore Higgins to evaluate the test

Table 3

Pin Plate Test Results Reported by Blake (1981)

Test Number	D_h, in inches	D_p, in inches	t, in inches	b_e, in inches	a, in inches	F_y, in kips per square inch	F_u, in kips per square inch	P_{ult}, in kips	Location of Failure
1-A	3.125	3.000	0.256	1.438	1.563	45.4	74.4	53.1	Side
1-B	3.125	3.000	0.256	2.188	1.375	45.4	74.4	57.9	Shear
1-C	2.125	2.000	0.256	1.438	1.313	45.4	74.4	47.5	Shear
1-D	2.125	2.000	0.256	2.188	1.375	45.4	74.4	50.1	Beyond
2-A	3.125	3.000	0.388	1.813	1.875	37.3	62.4	79.8	Side
2-C	2.125	2.000	0.388	1.813	1.750	37.3	62.4	71.5	Shear
2-D	2.125	2.000	0.388	2.813	1.875	37.3	62.4	75.8	Shear
3-A	3.125	3.000	0.488	2.188	2.250	37.5	68.1	150.0	Shear
3-B	3.125	3.000	0.488	3.313	2.250	37.5	68.1	147.0	Shear
3-C	2.125	2.000	0.488	2.188	2.250	37.5	68.1	121.0	Beyond
3-D	2.125	2.000	0.488	3.313	2.250	37.5	68.1	123.0	Beyond
4-A	3.125	3.000	0.722	2.906	2.938	38.0	69.4	245.0	Beyond
4-B	3.125	3.000	0.722	4.406	2.813	38.0	69.4	240.0	Beyond
4-C	2.125	2.000	0.722	2.969	2.938	38.0	69.4	216.0	Beyond
4-D	2.125	2.000	0.722	4.500	2.875	38.0	69.4	220.0	Beyond
4-E	3.625	3.500	0.722	3.031	3.000	38.0	69.4	255.0	Beyond
4-F	3.625	3.500	0.722	4.500	3.000	38.0	69.4	242.0	Beyond
5-C	3.625	3.500	1.256	4.406	4.250	33.3	67.6	510.0	Beyond
5-D	3.625	3.500	1.256	6.656	4.438	33.3	67.6	550.0	Beyond
6-C	3.625	3.500	1.766	5.875	6.000	40.9	72.0	950.0	Beyond
6-D	3.625	3.500	1.766	8.875	5.875	40.9	72.0	990.0	Beyond
7-C	3.625	3.500	2.018	6.688	6.625	30.8	60.8	1100.0	Shear
7-D	3.625	3.500	2.018	10.063	6.750	30.8	60.8	1185.0	Shear

Note: 1 in. = 25.4 mm; 1 kip = 4.45 kN; 1 ksi = 6.89 MPa

results and to reduce the data into a set of design equations suitable for use in the new Load and Resistance Factor Design (LRFD) version of the AISC Specification currently under development. A group of letters, referenced herein as Higgins (1982), contains the results of Higgins' study.

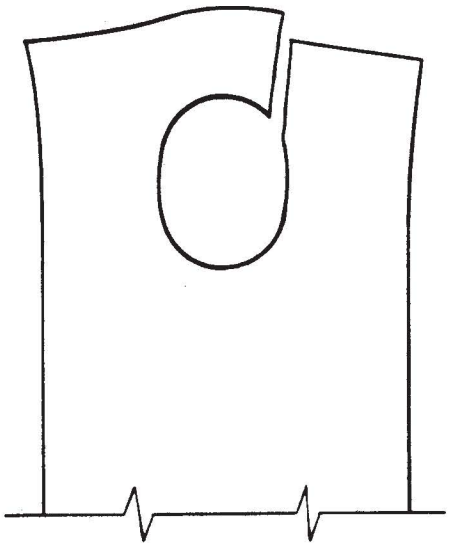

Fig. 16 - Pin Plate Fracture by Shear

The final result of Higgins' work is a set of equations which can be used to predict the ultimate strength of pin link plates:

for failure by fracture at the side:

$$P_{ult} = 2\ t\ b_{eff}\ F_u \qquad (10)$$

in which

$$b_{eff} = 2t + 0.625 \text{ but not more than } b_e \text{ actual}$$

For failure by shear beyond:

$$P_{ult} = 2\ t\left(a + D_h/2\right) F_{us} \qquad (11)$$

in which

F_{us} = ultimate shear stress of the steel = $0.58\ F_u$

For the purpose of the specification section, a provision requiring $a \geq b_{eff}$ was also included.

Blake (1981) states that strain gages were applied to the first specimen to verify the test operation. However, no strain data is included in the report. Load vs. pin deflection plots were drawn for each test. These were used by Higgins to arrive at a recommended allowable stress for the specification being written, but did not figure in any other part of the analysis.

This particular study is of great significance professionally because of its potential impact on the AISC Specification. Resultantly, the proposed design equations will be held up to detailed scrutiny in the following section. Also to be considered is the assumption made as to the value for F_{us}.

The last study to be discussed herein is that reported by Scott and Stone (1982). In this work, photoelastic models of link plates were tested to evaluate stress concentration factors. The configuration tested was similar to that shown in Figure 10 with the corners clipped. In all cases, the hole diameter was 1.75 inches and pin clearance was small, with a maximum clearance of 0.18 inch. The initial purpose for this study was to verify the adequacy of a design

equation in use at the time for lifting lug design. This equation was given as follows:

$$S_t = \frac{P\ \psi}{\lambda\, t\left(D_h/2\right)} \tag{12}$$

in which

S_t = maximum tensile stress

P = applied load

ψ = stress factor dependent upon pin clearance

$\lambda = b/D_h$

and the other terms are as previously defined.

By substituting the definition of λ, Equation 12 can be rewritten as

$$S_t = \frac{P\ \psi}{b\ t/2} \tag{13}$$

The photoelastic tests yielded a total of six (6) different curves of ψ plotted against the clearance ratio defined as c/D_h. At the small clearances considered, increasing pin clearance had a negligible effect, with most of the curves flattening out beyond $c = 0.05$. The variation in ψ was very great, however, for different values of λ. The reported extremes are $\psi \cong 3.0$ @ $\lambda = 3$ and $\psi \cong 5.0$ @ $\lambda = 1.6$.

One of the conclusions drawn in the paper is that these equations based on ψ are not optimum methods of evaluating the maximum tensile stress in a pin plate. The stress concentration factor, k, investigated by Frocht and Hill (1940) was then applied to this study. Curves of k vs. c/D_h were then developed for the various tests. Figure 17

shows three of the resulting curves. This data will be compared to the Frocht and Hill curve of Figure 12 in the next section.

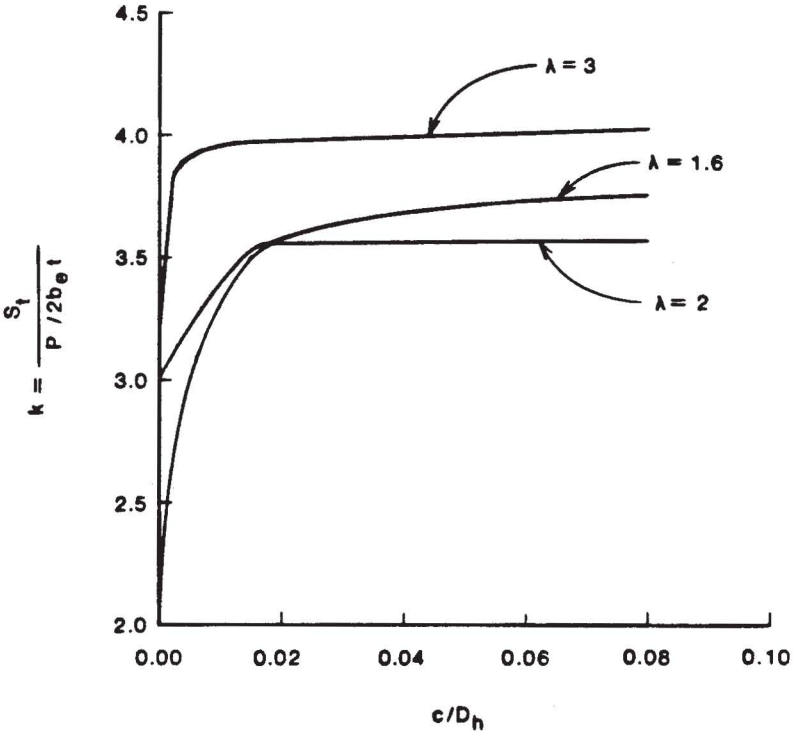

Fig. 17 - Stress Concentration Factors from Scott and Stone (1982)

Scott and Stone also addressed two other pin plate configurations in this study. Link plates of the type discussed above were assembled and loaded with a bushing between pin and plate. In this arrangement, the bushing had a neat fit in the hole, and varying clearance existed between the pin and the bushing. This is a very atypical configuration and is considered to be outside of the scope of the present investigation.

The second configuration considered was the standard eyebar, as shown in Figure 7. Only one curve of stress concentration factor vs. clearance ratio was presented for the eyebar; it is shown in Figure 18. Since the present study is not particularly interested in eyebar behavior, this information is presented primarily for reference.

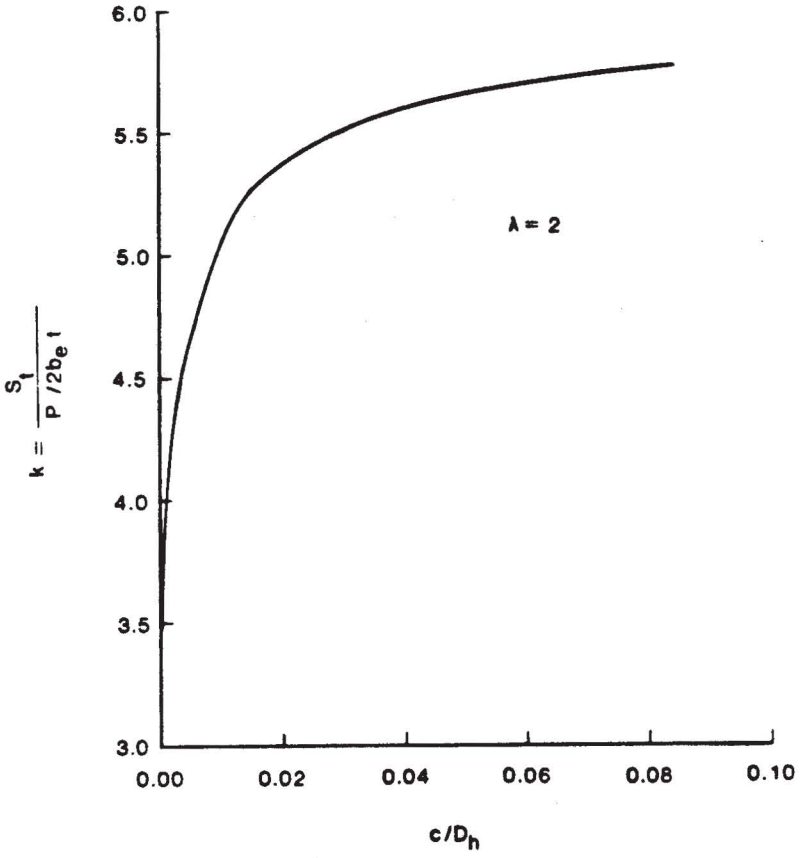

Fig. 18 - Eyebar Stress Concentration Factors from Scott and Stone (1982)

The Scott and Stone models were constructed of photoelastic plastic, so the only data accumulated in their tests were stress

values. No deflection or ultimate strength numbers were developed in this work. As was the case with some of the other investigations discussed above, the equations and quantities presented only apply to plates at load levels below first yield.

This completes our review of previous investigations conducted on the behavior of pin plates and pinned connections. Both theoretical and experimental studies have been addressed. The information and conclusions presented by the various investigators will be comparatively examined in the following section. The shortcomings of, and questions raised by, these works will then be used to develop the parameters of the present experimental project. This will be discussed in the section "Experimental Program."

Analysis of Previous Work. The papers by Eshwar and Rao present studies of simply the bearing stress between a pin and a plate. One of the most common methods of contact stress analysis in use today is that of Hertz as presented in Roark and Young (1975). The Hertz formulas provide methods for calculating maximum bearing stress, width of contact area, and gross body displacement. A comparison of the classic Hertz formulations and the results reported by Eshwar and Rao is thus recommended.

The Hertz formulas pertain to infinite solids; the Eshwar and Rao studies considered plates of unit thickness. This difference immediately suggests that a certain lack of agreement will be found. A reasonable difference could be resolved by comparison to experimental results. However, the results of this comparison, as shown below, are somewhat less than reasonable.

Consider the relationship of load vs. region of contact as predicted by Eshwar (Fig. 2) and Rao (Fig. 3). Rao accounts for pin elasticity and Eshwar does not, so the two curves are not identical; this is quite understandable. Hertz presents the following equation with which the width of the contact area can be calculated for the case of $E_{pin} = E_{plate}$ and $\upsilon = 0.3$:

$$b_c = 2.15\sqrt{\frac{P\ K_D}{E}} \tag{14}$$

in which b_c is the width of the contact area and K_D is defined as

$$K_D = \frac{D_h\ D_p}{D_h - D_p} \tag{15}$$

It can be seen that $\sin \theta_c = b/D_p$, so Equation 14 can be rewritten as follows:

$$\theta_c = \arcsin \ \ 2.15\sqrt{\frac{P\ K_D}{D_p^2\ E}} \tag{16}$$

From Eshwar and Rao, we can write the following relationships:

$$a = \frac{D_h}{2} \tag{17}$$

$$D_p = D_h\left(1 + \lambda\right) \tag{18a}$$

or

$$\lambda = \frac{D_p}{D_h} - 1 \tag{18b}$$

From this, we can write the Hertz formula of Equation 16 in terms of the Eshwar/Rao variables.

$$K_D = \frac{2a\ [2a\ (1 + \lambda)]}{2a - 2a\ (1 + \lambda)} \tag{19}$$

$$K_D = \frac{2a\ (1 + \lambda)}{-\lambda} \tag{20}$$

$$\frac{K_D}{D_p^2} = \frac{2a\ (1 + \lambda)/-\lambda}{[2a\ (1 + \lambda)]^2} \tag{21}$$

$$\frac{K_D}{D_p^2} = \frac{1}{-2a\lambda\ (1 + \lambda)} \tag{22}$$

$$\theta_c = \arcsin 2.15\sqrt{\frac{P}{Ea\lambda}\left[\frac{1}{-2\ (1 + \lambda)}\right]} \tag{23}$$

An interesting observation can be made from Equation 23: for a given value of $P/Ea\lambda$, an infinite number of values of θ_c can be calculated by varying λ. A numerical sample problem not only demonstrates this, but also shows a radical lack of agreement between the Rao curve of Figure 5 and the values calculated by the Hertz formula.

Consider a pin plate arrangement for which P = 6480 kips, D_h = 4.000 inches, and D_p = 2.000 inches. From the above equations, we find that λ = -0.500 and $P/Ea\lambda$ = -0.216 (let E = 30,000 ksi). From Figure 5, we read a value of $\theta_c = 5.5°$. However, using Equation 23, we calculate $\theta_c = 87.8°$. Now, consider a second set of values defining the pin plate: P = 129.5 kips, D_h = 4.000 inches, and D_p = 3.96 inches. From this, we find λ = -0.010 and $P/Ea\lambda$ = -0.216. For this same value of $P/Ea\lambda$, Figure 5 again yields a value of $\theta_c = 5.5°$. Equation 23 now gives a value of $\theta_c = 45.22°$. This is not only quite different than the Rao value, but also much less than was calculated from Equation 23 in the first example.

The first thought that comes to mind is to question the validity of the sample proportions. P = 6480 kips and D_p = 2.000 inches indicates an average bearing stress of 3240 ksi. This is radically unrealistic for steel (using E = 30,000 ksi implies that we are considering some type of steel). P = 129.5 kips and D_p = 3.96 inches equates to an average bearing stress of 32.7 ksi, a much more realistic figure. Numerous sample calculations were made to determine the results when the average bearing stress was kept at or below a level corresponding to that which could be sustained by real structural steels. A very liberal value of 200 ksi was adopted as the cut-off point.

This brief study indicated that, for realistic bearing stress levels, the maximum permissible variation in λ for a set value of $P/Ea\lambda$ results in a variation of θ_c of only about 4°. Thus, it is possible to plot θ_c vs. $P/Ea\lambda$ for the Hertz theory as expressed in Equation 23. Figure 19 presents plots of θ_c from Rao (1978) and as calculated by Equation 23. As can be seen, there is no agreement between the two theories.

It is obvious that the study of bearing stress in a pin plate arrangement requires much additional work. The discussion above presents a major discrepancy in the literature. However, further pursuit of this topic is somewhat beyond the scope of the present investigation. Bearing stress in the elastic range will affect joint deflection and, therefore, the yield load of a pin plate, but this local stress concentration has been found to have little effect on the ultimate strength of a statically loaded pin plate (Johnston, 1939).

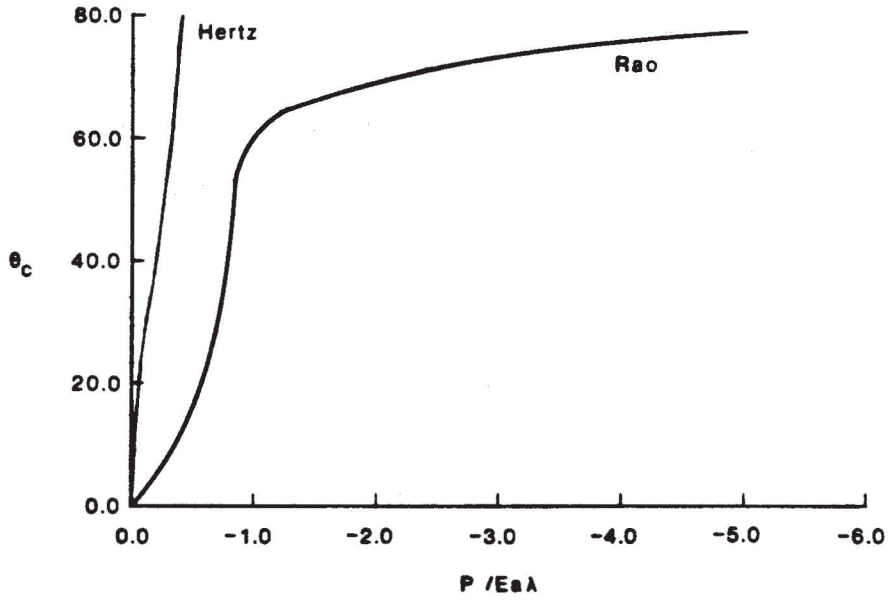

Fig. 19 - Comparison of Rao (1978) and Hertz Theory

There have been three major sets of expressions reported in the literature which can be used to calculate the ultimate load of a pin plate. Johnston (1939) presented three equations which were previously discussed (Eq. 5, 6, and 7). Higgins (1982) developed two equations (Eq. 10 and 11) which consider fracture only; Higgins' study did not address dishing failures. Lastly, Tolbert and Hackett (1974), using the information reported in Tolbert (1970), presented the following equation for failure beyond the hole:

$$P_{ult} = \left(2a + 0.293\ D_h\right) t\ F_{us}\ C_r \qquad (24)$$

in which C_r = reduction factor for pin clearance, as developed from the information shown in Figure 14. All other terms are as previously defined. Equation 24 is based on the assumption of a shear type of failure and is only applicable for plates with $b_e \geqslant a$.

The Johnston equations are clearly empirical and are restricted to use on plates that fall within certain dimensional ranges. The Higgins and Tolbert and Hackett equations are both based on a simplistic stress analysis. An immediately obvious course of action is that of comparison. The specimens tabulated in Tables 1, 2, and 3 will be analyzed using the three equation sets. The calculated results will be compared to the test results, and conclusions as to the accuracy of each method will be drawn.

A note must be made here about the ultimate shear strength of steel. As was stated above, Higgins (1982) suggests that $F_{us} = 0.58\ F_u$. Tolbert and Hackett suggested $F_{us} = 0.60\ F_u$. Both of these works referred to the Huber - von Mises energy of distortion theory (Seely and Smith, 1952) as the basis of these values. This is found to be in error; the energy of distortion theory applies to elastic stresses and is commonly used to define the shear yield stress (e.g., in the AISC Commentary). Tolbert (1970) measured the ultimate shear strength of the material used in his tests and found $F_{us} = 0.80\ F_u$. This writer checked various common references, such as Brockenbrough and Johnston (1981), and found different values suggested for F_{us}. For the purposes of this comparison, the following values have been adopted:

> for Tolbert (1970) specimens, use $F_{us} = 42.7$ ksi, as was reported;
>
> for Johnston and U.S. Steel specimens, average the factors suggested in the literature to obtain $F_{us} = 0.77\ F_u$. Measured values of F_u were reported for all specimens.

Of the 13 Tolbert tests, P_{ult} was reported only for Specimens 1 through 10. Pin-to-hole clearance was varied for Specimens 1 through 4. Since C_r of Equation 24 was developed from this series, it is obvious that we would find agreement. The Johnston and Higgins equations are for neat fit or low clearance pins only, so Tolbert Specimens 1 through 4 cannot be addressed. Therefore, only Specimens 5 through 10 will be used in this comparison. When examining the Johnston and U.S. Steel specimens, all will be addressed with the Johnston and Higgins equations. Only those specimens for which $b_e \geqslant a$ will be addressed with the Tolbert and Hackett equation. This gives us a total of 57 specimens checked using the Johnston and Higgins equations and 43 specimens checked using the Tolbert and Hackett equation.

The ratios of calculated P_{ult}/actual P_{ult} for all of the specimens by the three methods of calculation are plotted in Figure 20. A solid dot indicates the ratio for a case in which the correct mode of failure was predicted. A square indicates the ratio for a case in which the predicted failure mode was incorrect.

The Higgins equations are found to be very inaccurate. The predicted mode of failure was correct only 15 times out of 57 specimens, and very great scatter is seen, with a maximum error of 62.6%. The effective width concept appears to be the fault of this method.

The Johnston equations are relatively good in predicting both load and mode of failure, with the mode being correct 50 out of 57 times. Most of the mode errors incorrectly predicted dishing. The maximum error noted was 30% on Johnston Specimen 106. The next largest error was only 16.7%.

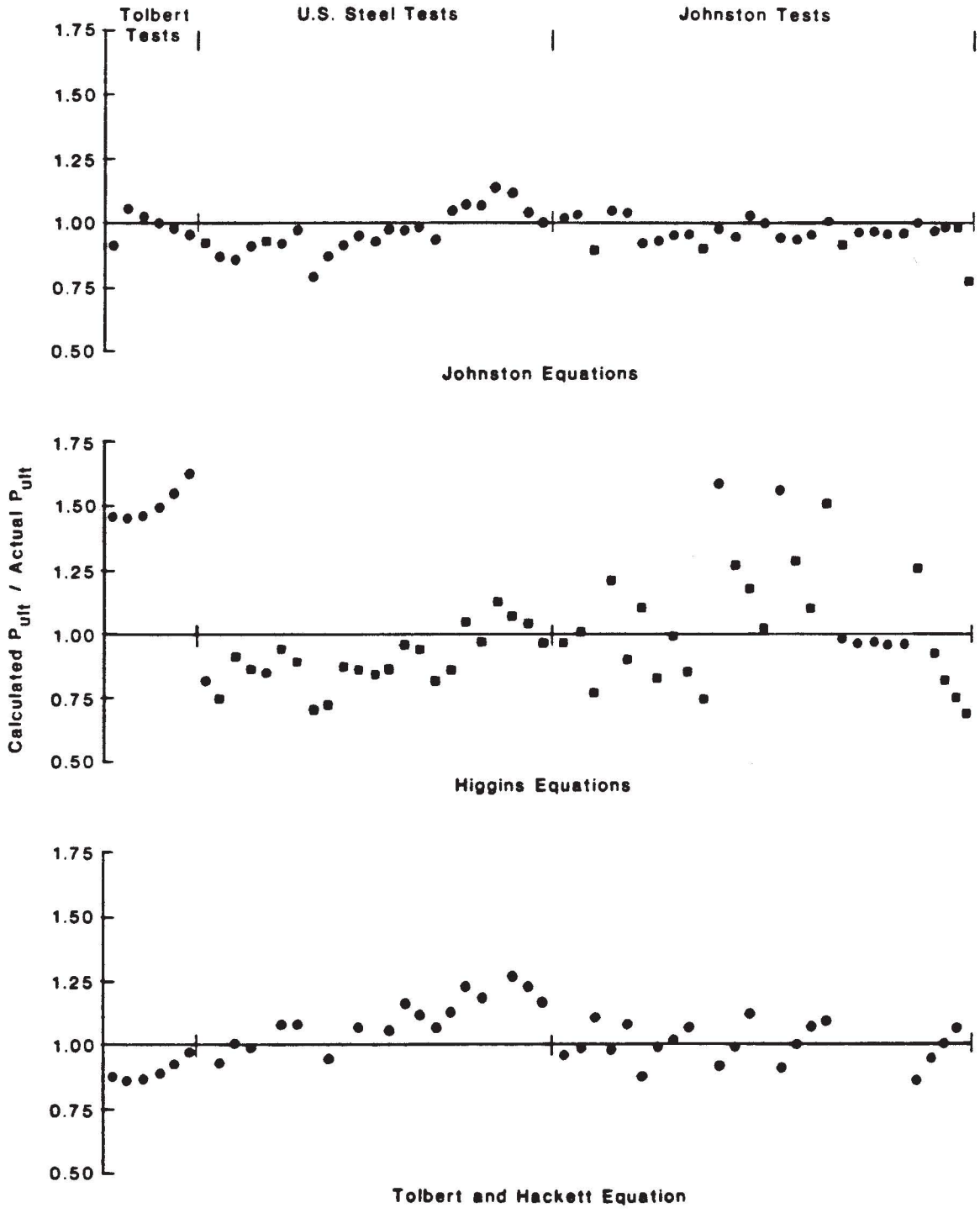

Fig. 20 – Comparative Performance of Ultimate Load Calculation Methods

The Tolbert and Hackett equation was also shown to provide fairly accurate results within its limitation of $b_e \geq a$. The maximum error found was 34.6%, but a trend toward increasing error was noted. The U.S. Steel Series 5, 6, and 7 specimens, which are the only plates over one inch thick considered here, showed consistently higher errors than did the thinner plates. Somewhat greater scatter was observed, as compared to the Johnston equations. Since Tolbert and Hackett only addresses one mode of failure, no mode errors occurred.

The Johnston equations seem to be the most useful and, generally, the most accurate for predicting failure behavior of pin plates. As this investigation progresses, examination of these equations outside of the dimensional ranges studied by Johnston will be conducted. The pin-to-hole clearance relationship discussed by Tolbert will also be introduced to the equations to further enhance their versatility.

The work reported by Scott and Stone (1982) lends itself to comparison to both that of Frocht and Hill (1940) and that of Timoshenko (1970).

Figure 12 presents a curve of stress concentration factors as a function of D_h/b from Frocht and Hill (1940). This curve applies only to a neat fit pin; i.e., $c = 0$. Figure 17 presents a set of curves of stress concentration factors as a function of c/D_h from Scott and Stone (1982). Each curve is for a different value of λ, where $\lambda = b/D_h$. Comparison of these two figures is quite direct for a value of $c = 0$. The appropriate values which could be read from Figures 12 and 17 are assembled in Table 4. As can be seen, although numerical agreement is

not exact, the order of magnitude is comparable, thus indicating fairly compatable analyses.

Table 4

Comparison of Scott and Stone (1982) to Frocht and Hill (1940)

$\frac{D_h}{b}$	k (S & S)	k (F & H)
0.333	3.25	3.00
0.500	3.00	2.20
0.625	2.00	1.95

Figure 12 is a plot of the stress concentration factors measured by Frocht and Hill on metal test specimens. As previously discussed, the tensometers used had a gage length of 1/2 inch. This is a relatively long gage length for accurately measuring tensile stress concentrations. It is very probable that the photoelastic technique used by Scott and Stone provided a more accurate assessment of the peak tensile stresses. This would account for the somewhat higher stress concentration factors reported in the more recent paper.

Scott and Stone also considered stress concentration factors in eyebars, as also addressed by Timoshenko and Goodier. For a neat fit pin and $\lambda = 2$, Figure 18 from Scott and Stone gives a value of $k = 3.5$. To compare to Timoshenko, we must consider both Figures 7 and 8. From the notation defined in Figure 7, we can see that $b/a = \lambda$ and that, for

$b/a = 2$, $a = b_e$. Thus, we can see that $2a\sigma/P = k$. From Figure 8, we can now read $k = 3.85$ for $\lambda = 2$. Again we have fairly good agreement, with a difference of only 10%. In this case, we are comparing Scott and Stone's photoelastic analysis results to Timoshenko's mathematical study.

We have now completed the comparisons of the work of previous investigators. A number of conclusions and statements can be made. The calculation of contact stresses appears to be an elusive problem. Mathematical studies performed by Eshwar, Rao, and Hertz were compared, and great disparity was found. The calculation of gross failure loads for pin plates of limited proportions were found to be generally good (Johnston), good for a certain case (Tolbert and Hackett), or poor (Higgins). Particular attention will be given to the Johnston equations in the next section. Lastly, the stress concentration factors reported by Scott and Stone show good agreement with previous work (Frocht and Hill, Timoshenko) and may be confidently used in calculating peak tensile stresses in the elastic range.

EXPERIMENTAL PROGRAM

Equipment and Procedures. In this segment of the investigation, a group of 13 pin plate specimens were loaded to failure in the laboratory. Strain and deflection measurements were taken to allow correlating these tests to previous studies and to the finite element analyses to be conducted as a part of the current work. The test equipment used and the procedures followed are discussed in this section.

The primary machine used to conduct the load tests was a Tinius Olsen Super L 400,000-pound universal testing machine. The machine used is equipped with a digital load and strain system, a load vs. strain graphic recorder, and servo control module. Load application can be maintained on the basis of either constant load rate or constant strain rate, with the latter being selected for this work. Tensile specimens are secured by serrated grips in the lower (fixed) and upper (moving) crossheads for load application.

A special set of test fixtures had to be fabricated to allow testing plates of the particular proportions studied here. Each specimen was provided with a 1" x 2-1/2" base plate. The lower test fixture consists of a C-shaped channel into which the specimen base plate could be inserted. A heavy bar extended from the bottom of the channel into the lower crosshead grip. The upper fixture consists of a pair of 3/4 inch plates suitably spaced to accept a specimen. Openings are cut in the plates to permit viewing the head of the test specimen. A front view of the test fixtures in use can be seen in most of the photographs

in Appendix A (e.g., Figure A2). A side view of the fixtures can be seen in Figure 21.

A number of strain gages were applied to the back surface of each specimen. The lead wires from the gages were collected on an acquisition board (Fig. 22, right), which was connected to a Hewlett Packard Model 3497A Data Acquisition/Control Unit (Fig. 22, center). The board was energized by a Power-Mate 0-18 VDC Regulated Power Supply. The acquisition system output was read by a Hewlett Packard HP-85 desktop computer (Fig. 22, left), which provided a hard copy output of load applied and strain at each gage. The HP-85 was programmed to execute a series of readings when the operator pressed a trigger switch.

The strain gages used were Micro-Measurements Model CEA-06-125UN-120 resistance gages. This is a general purpose strain gage for use on mild carbon steels. With optimum installation quality, strains of up to 5% can be measured when using gage lengths of 0.125 inch or more. These gages have a gage length of 0.125 inch and some did perform up to that level. The grid width of this model is only 0.100 inch. The narrow grid width is desirable for this work since measurement of stress (strain) concentrations is sought. The various accessories used in conjunction with the strain gages, such as adhesive, coatings, and the like, were all as recommended by the gage manufacturer.

The last piece of equipment used was a 2-inch travel 0.001-inch Ames dial indicator. The dial indicator mount was fixed to the lower crosshead and the plunger bore against the load pin. This arrangement permitted measurement of gross pin deflection with respect to the

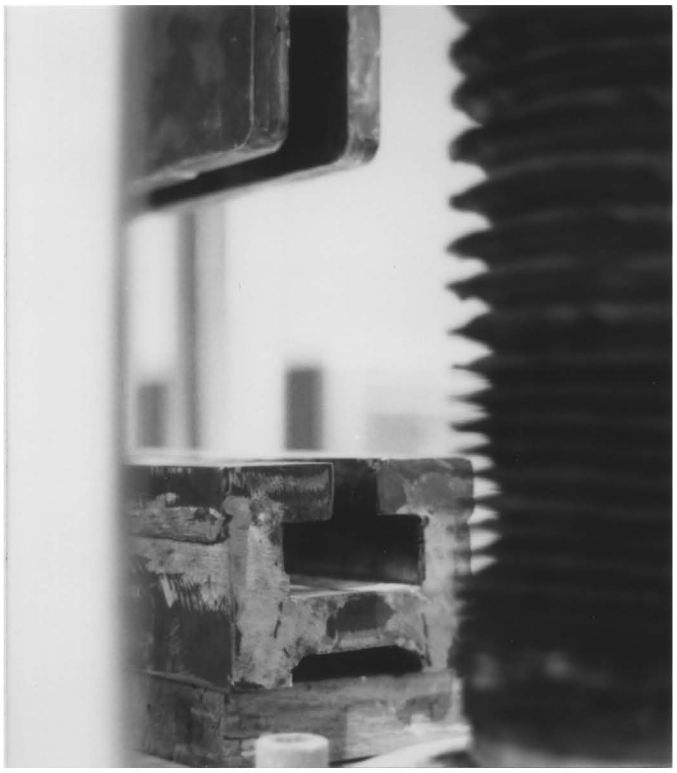

Fig. 21 - Side View of Test Fixtures

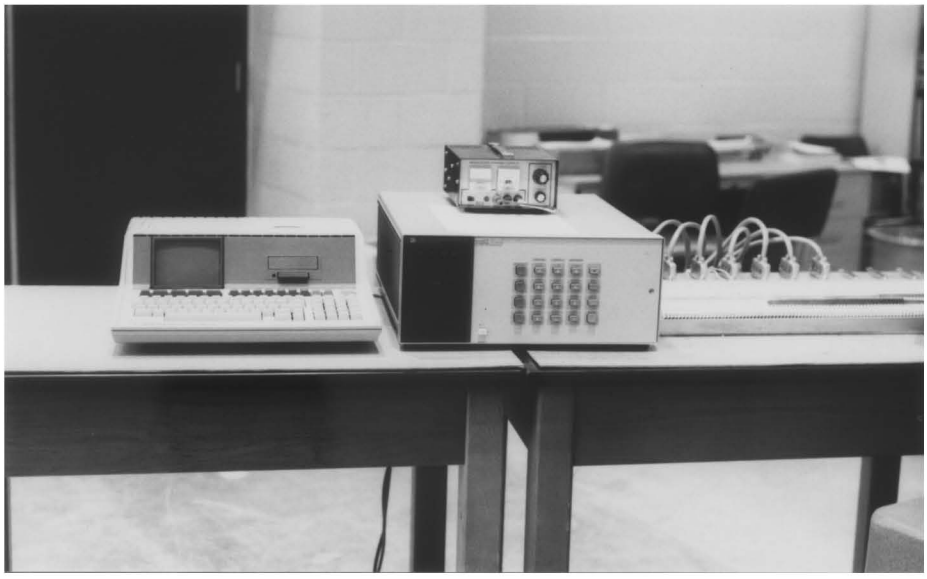

Fig. 22 - Data Acquisition System

specimen base. It is noted that deformation of the lower test fixture is a part of the pin deflection measurements made. However, the fixture is many times stiffer than the specimens and, of course, its deformation at a given load is essentially the same for all tests. Thus, this effect can be considered negligible for the purpose of this investigation.

Two primary sets of readings were taken during each test. First, strains were measured at six, seven, or eight points on each specimen using the previously described system. Readings were taken at load intervals of 2500 pounds. Second, pin deflection was read using the dial indicator. This measurement was also made every 2500 pounds. All of the readings taken for each specimen are assembled in a series of tables in Appendix A. The ultimate load reported for each specimen was read directly from the testing machine digital load indicator.

Test Specimens. A total of 13 specimens were fabricated for this investigation. The specimens were designed in five different groups, with differences among and within the groups selected in such a manner that specific areas of behavior could be studied. The fabricator was directed to prepare all of the specimens from ASTM A36 steel. As will be discussed below, this direction was not followed.

Detailed dimensions of all of the test specimens appear in Appendix A. A summary of the specimen dimensions, material properties, failure loads, and modes of failure are assembed in Table 5. Two notes of explanation are required. The value for b_e shown in the table is the average of the two sides. This method was previously used by Higgins (1982). Also, the left b_e dimension measured on the asym-

metrical specimens is the diagonal measurement indicated in the figures in Appendix A.

Table 5

Summary of Test Program Results

Test Number	D_h, in inches	D_p, in inches	t, in inches	b_e, in inches	a, in inches	F_y, in kips per square inch	F_u, in kips per square inch	P_{ult}, in kips	Location of Failure
1-A	1.992	1.986	0.412	1.368	1.414	97.6	109.4	98.3	Side
1-B	2.624	1.986	0.412	1.366	1.458	97.6	109.4	98.3	Side
1-C	3.384	1.986	0.415	1.371	1.382	97.6	109.4	93.3	Shear
1-D	4.006	1.986	0.415	1.369	1.387	97.6	109.4	86.1	Beyond
1-E	5.005	1.986	0.415	1.343	1.433	97.6	109.4	91.1	Side
2-A	2.755	2.744	0.503	1.520	2.258	54.1	78.6	123.6	Side
2-B	2.759	1.617	0.504	1.524	2.240	54.1	78.6	115.2	Dishing
2-C	2.753	1.362	0.509	1.516	2.254	54.1	78.6	113.3	Dishing
3-A	2.758	2.744	0.509	2.051	2.107	54.1	78.6	134.8	Beyond
3-B	3.004	1.617	0.508	1.905	1.908	54.1	78.6	104.5	Dishing
4-A	2.624	1.986	0.417	1.380	1.380	97.6	109.4	92.7	Shear
5-A	2.751	2.744	0.412	1.726	1.727	97.6	109.4	167.2	Side
			0.115	1.381	1.376	38.6	49.7		
5-B	2.753	1.617	0.412	1.745	1.739	97.6	109.4	123.6	Beyond
			0.115	1.411	1.395	38.6	49.7		

Note: 1 in. = 25.4 mm; 1 kip = 4.45 kN; 1 ksi = 6.89 MPa

First line of data for specimens 5-A and 5-B applies to the main plate; second line applies to the doubler plates

Photographs of each specimen before, during, and after the test are also contained in Appendix A. For convenience, photographs of the specimen groups after testing are presented here in Figures 23 through 27. Figure 28 shows the load pins after completion of the tests.

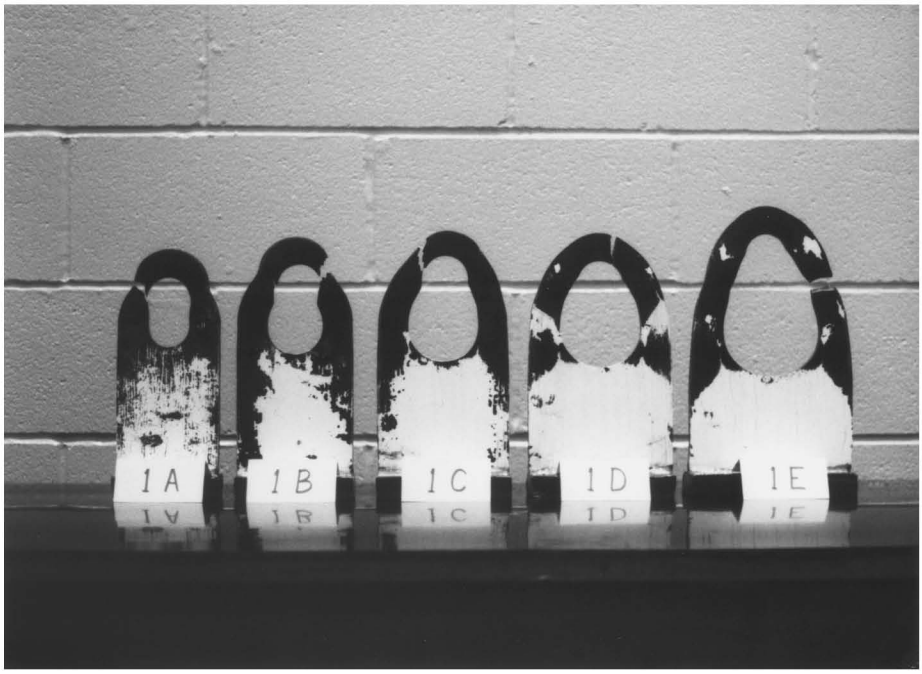

Fig. 23 - Series 1 Specimens

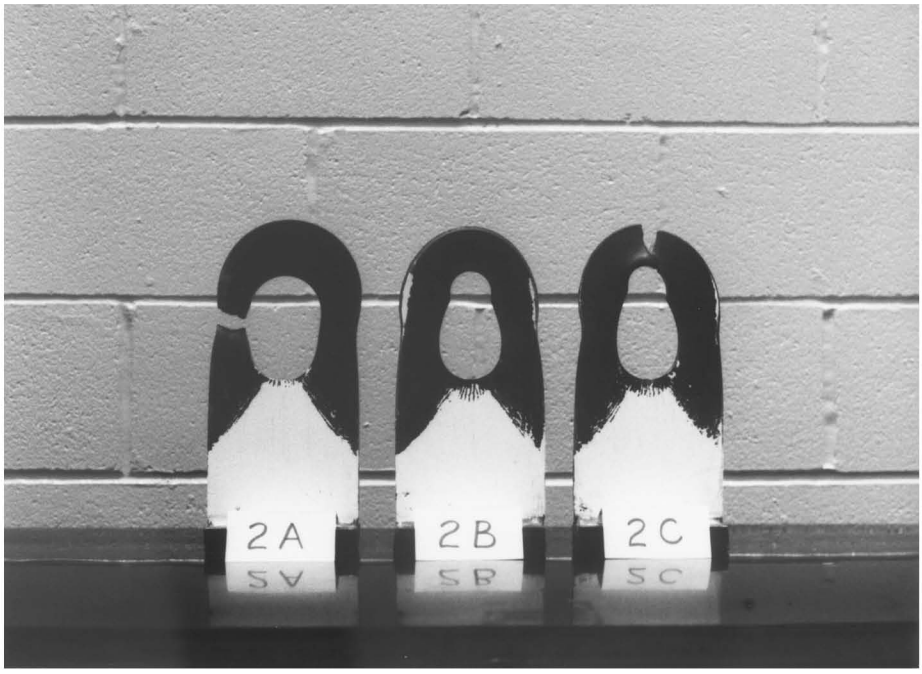

Fig. 24 - Series 2 Specimens

Fig. 25 - Series 3 Specimens

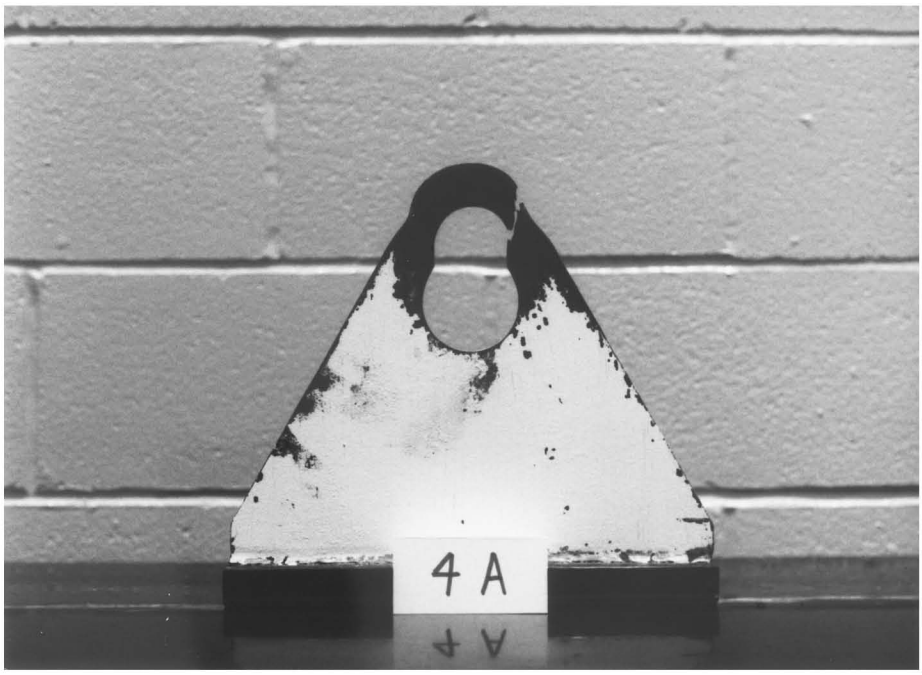

Fig. 26 - Series 4 Specimen

Fig. 27 - Series 5 Specimens

Fig. 28 - Load Pins After Tests

The five specimens of Series 1 were designed as an extension of Tolbert's work. In this case, however, the pin diameter was held constant, and the hole was increased. The net areas through and beyond the hole were also kept constant. This series is of particular professional interest because of the applicable provisions of the AISC Specification. AISC addresses pin plate strength in terms of net area, area beyond the hole, and projected bearing area of the pin. These three values are essentially the same for the five specimens of Series 1.

Series 2 also relates to the pin-to-hole clearance problem. In this case, three identical specimens are loaded to failure with different size pins. However, the area beyond the hole is substantial in order to cause a failure in the net section.

The five specimens in Series 3, 4, and 5 represent shapes commonly used in practice as lifting eyes. Series 3 was intended to be two identical plates loaded through different pins. A fabrication error resulted in an oversize hole in Specimen 3-B. A correction can be applied to the ultimate load, so the usefulness of the test is not lost. Series 4 is a single symmetrical triangular shape loaded through a loose fit pin. The two Series 5 specimens are of the same shape and general dimensions as Specimen 3-A. Here, however, the main plate is thinner, and the areas through and beyond the hole are built up by means of doubler plates. Unfortunately, this is the location of another fabrication error. As can be seen in Table 5, the strengths of the plates from which the Series 5 specimens were fabricated are radically different. Thus, the specimen behavior beyond first yield of the lower strength steel is of only limited use in the investigation.

Three tensile test coupons were cut from each piece of plate used to fabricate the test specimens. The coupons were loaded to failure and the results for each plate size averaged to establish the mechanical properties of each plate thickness. A summary of these test results is presented in Table 6. Stress-strain curves for each of the three plate thickness are shown in Figure 29.

Table 6

Mechanical Properties of Specimen Plates

Nominal Thickness, inches	F_y, in kips per square inch	F_u, in kips per square inch	Strain at F_u, in inches/inch	E, in kips per square inch	Elongation, %
1/8	38.6	49.7	0.2380	30,019.	32.15
3/8	97.6	109.4	0.0645	28,414.	18.55
1/2	54.1	78.6	0.1754	29,197.	33.92

Note: 1 in. = 25.4 mm; 1 ksi = 6.89 MPa

Test Results. The 13 test specimens, as previously discussed, were designed to investigate certain areas of pin plate behavior. This statement implies that certain results were expected in order to fill in some of the gaps in the existing knowledge. The actual results observed during the testing deviated in a number of instances from that which was expected. A narrative of the test program will be presented here, followed by a quantitative analysis of the results.

The Series 1 specimens were fabricated with nominally constant net areas through and beyond the hole. The same size pin was used to load

the specimens. The only variable was the hole diameter, which was increased progressively to give D_h/D_p ratios varying from 1.0 to 2.5. Considering the previous work on pin plates, a failure beyond the hole was expected for these specimens. As can be seen in Table 5, three of the five specimens failed to the side of the hole. It is noted that the steel from which the Series 1 specimens were fabricated is much less ductile than the steels used by previous investigators.

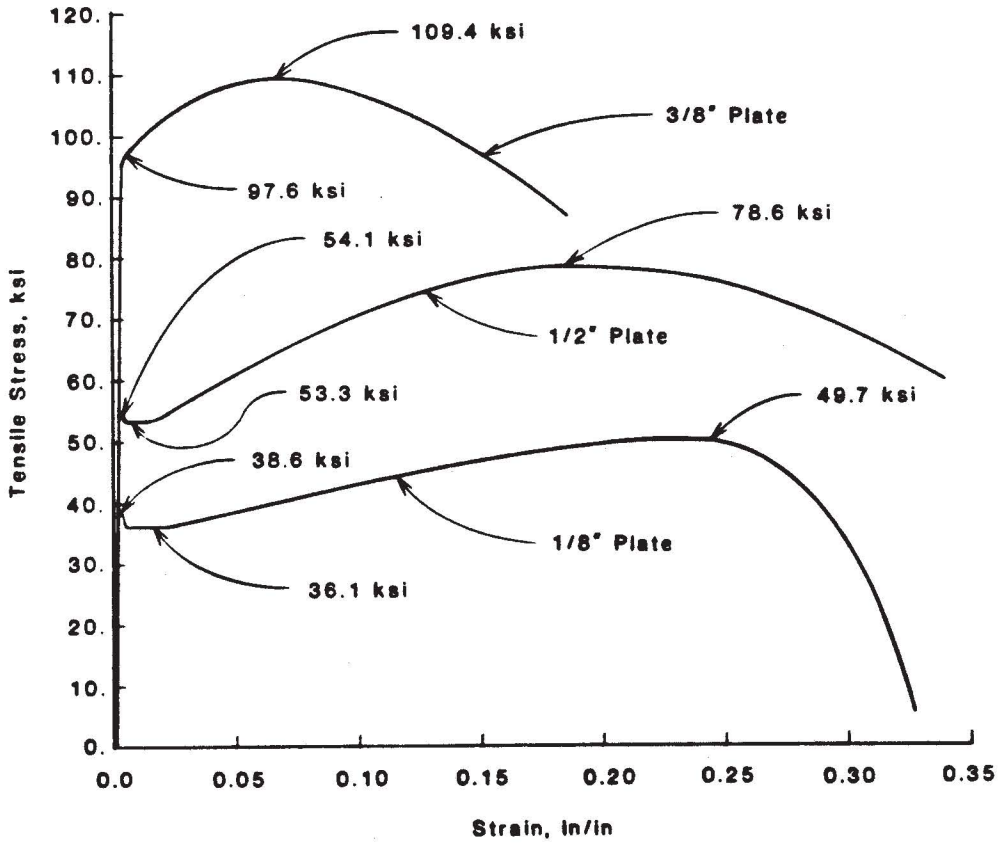

Fig. 29 - Stress-Strain Curves of Specimen Material

The Series 2 tests raised a serious question. Specimen 2-A failed as expected (in the net section) at a load only 3% off from that

predicted by the Johnston equations. Specimens 2-B and 2-C were essentially identical, but were loaded through smaller diameter pins. As was expected, the ultimate load dropped as the pin diameter was reduced, but the mode of failure changed, which was not expected. Both specimens failed by dishing. A particularly important point to note is that these specimens were dimensioned to meet the requirements of AISC § 1.14.5. These proportions are stated by the Specification to preclude dishing. It is not known at this point what load reduction, if any, would have been observed had the plates been blocked to prevent dishing.

Series 3 consists of two similar asymmetrical specimens of a typical "lifting eye" shape. As was previously mentioned, it was intended that these two specimens be identical, but a fabrication error occurred. Specimen 3-A behaved exactly as expected in terms of both ultimate load and mode of failure. Specimen 3-B failed by dishing. Again, these specimens were proportioned in accordance with AISC, so dishing was not expected. The change in failure mode cannot be attributed to the fabrication error (an oversized hole).

Series 4 was a single triangular plate loaded through a large clearance pin. The sloping sides of the plate appeared to buttress the sides of the hole, thereby preventing the spread necessary to permit a hoop tension failure. The result was a shear failure.

Series 5 consisted of two similar specimens of the same basic shape and size as Specimen 3-A. In this case, however, the areas through and beyond the hole were built up using doubler plates. As

compared to Specimen 3-A, the net area of 5-A was about 1.5% less and the area beyond the hole about 4.3% less. The differences between 3-A and 5-B were even less. Again, the change in pin-to-hole clearance was accompanied by a change in mode of failure. Noting the strength differences between the main plates and the doubler plates in Series 5, the ultimate load data cannot directly be related back to the ultimate loads of the Series 3 specimens.

As was done for the previous experimental information, these test results will first be compared to the three sets of failure equations discussed above. Initially, we will only consider the three specimens with very small pin clearances: 1-A, 2-A, and 3-A. Because of the material difference, 5-A will not be included.

Specimen 1-A showed poor comparison with all three calculation methods. Only the Higgins equations predicted the correct failure mode, and the error in magnitude varied from 20.2% (Johnston) to 25.4% (Higgins). The obvious conclusion that can be drawn here is that the less ductile, high strength steel of the Series 1 specimens exhibits a completely different behavior pattern than do the lower strength steels considered by the previous investigators. The inaccuracy is not only large, but in the cases of the Higgins and Tolbert and Hackett equations, the error was also unconservative.

Specimen 2-A could only be checked by the Johnston and Higgins equations, since $b_e < a$. The accuracy was found to be much better here, with both methods predicting the correct mode of failure, and the largest load error being only 3.3%. Both load calculations were on the conservative side. The strength and ductility of the Series 2 steel is

similar to that of the steels treated in the previous tests, so the good agreement between calculations and test was expected.

The calculated results for Specimen 3-A were scattered. The Johnston equations indicated failure by dishing at a load conservative by 4.9%. If the dishing equation is neglected, failure beyond the hole at a load 2.2% (3.0 kips) above the actual failure load is predicted. The Higgins equations indicated failure through the net section and were conservative by 2.5%. The Tolbert and Hackett equation was in error by 14.8% on the unconservative side.

It is concluded, once again, that the Johnston equations appear to provide the best method of calculating the ultimate load of a pin plate. We must now make two qualifications to this statement, however. The dishing equation appears to become increasingly inaccurate for higher strength steels, and the equation set as a whole becomes less accurate for high strength, low ductility steels. It is noted here for reference that the highest strength plate tested by Johnston had F_u = 65.5 ksi, and the least ductile had F_u/F_y = 1.402.

Tolbert and Hackett (1974) introduced the term C_r to deal with the reduction in pin plate strength due to pin-to-hole clearance. C_r for a given plate and pin combination is defined as the ultimate strength of that pin and plate arrangement divided by the ultimate strength of that plate with a neat fit pin. For example, P_{ult} = 98.3 kips for Specimen 1-A (the neat fit pin) and P_{ult} = 91.1 kips for Specimen 1-E. Thus C_r = 91.1/98.3 = 0.93 for Specimen 1-E. C_r will always be equal to or less than 1.0.

Tolbert and Hackett presented a curve of C_r vs. D_h/D_p based on one series of five tests in which failure occurred beyond the hole. The specimens of Series 1, 2, and 3 of the current investigation were designed to expand upon this data and either confirm the Tolbert and Hackett curve for C_r or modify it to account for the additional variables addressed by the present tests. Curves of C_r vs. D_h/D_p can be readily drawn for Series 1 and 2. Because of the aforementioned fabrication error of Specimen 3-B, an adjustment must be made to allow curving the Series 3 results.

Specimens 3-A and 3-B are not identical. In order to calculate C_r for Specimen 3-B, we need to know P_{ult} for 3-B with a neat fit pin. It was shown above that the Johnston equation for failure beyond the hole agreed very well with the test results of Specimen 3-A. Therefore, we will use this equation to calculate a neat fit pin ultimate load for Specimen 3-B. Specifically, we find P_{ult} = 128.9 kips for Specimen 3-B with D_h/D_p = 1.00.

Four curves of C_r vs. D_h/D_p can now be drawn, one each for Series 1, 2, and 3 and one for the Tolbert tests. These curves are shown in Figure 30. As can immediately be seen, the scatter is great.

The information shown in Figure 30 raises two major questions:

(1) Is the low reduction of strength of Series 1 a function, at least in part, of the low ductility of the material?

(2) If Specimens 2-B, 2-C, and 3-B were blocked to prevent dishing, what type of reductions in ultimate load would have occurred?

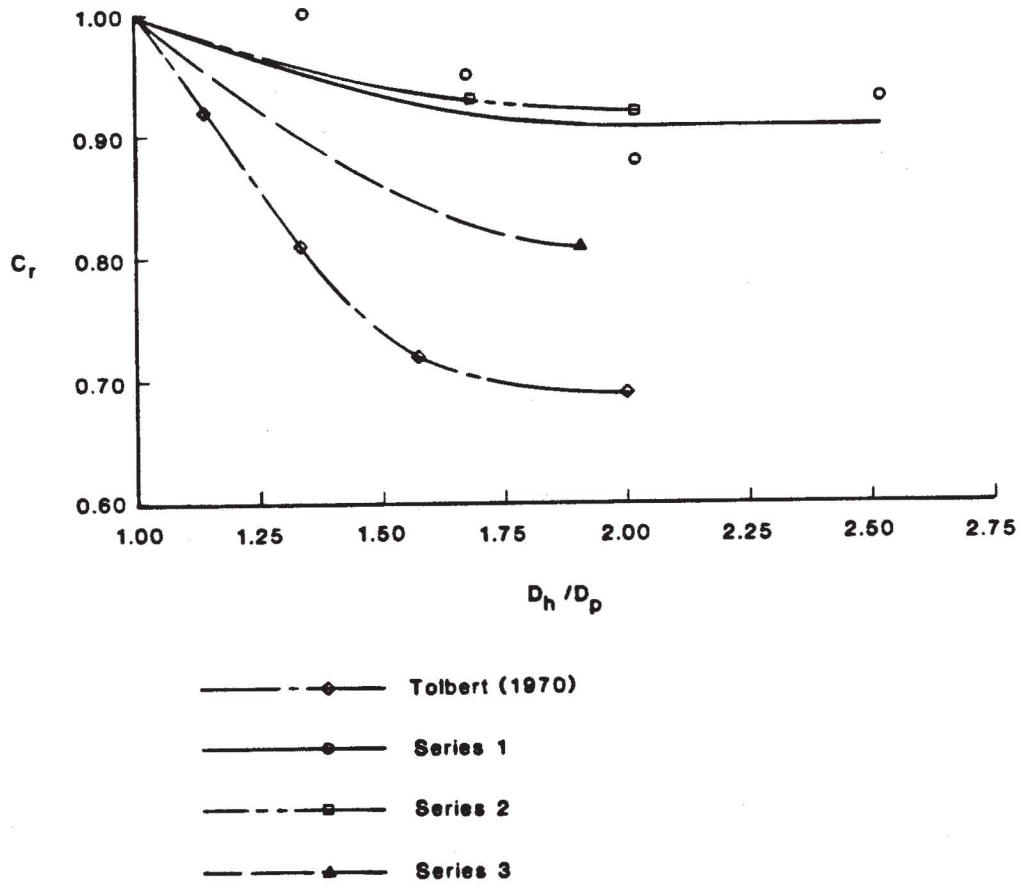

Fig. 30 - Summary of C_r vs. D_h/D_p Curves

One of two courses of action must be pursued to answer these questions. Either additional tests must be set up and run to expand the data base, or finite element failure analyses must be used to simulate additional tests. Because of the scatter of data points in Figure 30 and the changes of failure modes within specimen groups, any attempted evaluation or refinement of the data at this point is not warranted.

The last correlation to previous work which will be made in this paper shall consider the tensile stress concentration factor, k, as studied by Frocht and Hill (1940) and Scott and Stone (1982). Strains

were measured at the sides of the hole during the testing. From this data, the peak tensile stress, S_t, can be calculated. This allows a determination of the actual value of k.

Initially, let us consider only Specimens 1-A, 2-A, and 3-A, each of which had a close fitting pin. Specimen 1-A was found to have k = 2.6, as compared to a Frocht and Hill k value of 2.5. Specimen 2-A has k = 3.1 and a Frocht and Hill k of 2.3. Specimen 3-A has k = 2.3, as compared to k = 2.6 from Frocht and Hill. The actual k values of 1-A and 2-A are expected to be larger than predicted by Frocht and Hill because some pin clearance exists. For example, the Scott and Stone (1982) curves in Figure 17 indicate that k increases by 5.0% as c/D_h goes from 0.00 to 0.004 (Specimen 2-A had $c/D_h = 0.004$) for a plate with $b/D_h = 2.0$. A lower peak stress for Specimen 3-A is expected due to the greater area (and stiffness) of the net section to the left of the hole.

The remainder of the specimens in Series 1 through 4 are dimensionally outside of the bound of the work reported by Frocht and Hill (1940) and Scott and Stone (1982). For qualitative purposes only, k was calculated for each of these specimens and compared to the Frocht and Hill value read from Figure 12. As expected, all actual values were greater than those from the figure. The percentage increase with respect to change in c/D_h was generally of the same order of magnitude from one group to the next. However, it is felt that the data is too limited to permit any conclusions to be drawn from which the behavior of other plates could be predicted.

Neither of the earlier papers considered built up pin plates. Therefore, Specimens 5-A and 5-B cannot reasonably be compared to the previous work. Tensile stress concentrations in such built up members may be investigated further using finite element analysis or by conducting additional tests.

This completes the report of the experimental work conducted as a part of this investigation. A great deal of data was developed and a number of new questions raised. A summary of the major areas of study and recommendations for future research are presented in the Conclusions.

CONCLUSIONS

The literature search conducted as a part of this investigation has shown that the research of pin plate behavior, particularly in the inelastic range, is quite limited. Three general areas have been studied: contact stresses between pin and plate, elastic pin plate stresses, and ultimate capacities of pin plates. Significant discrepancies have been found among the contact stress calculation techniques reported in the literature. The various elastic stress equations and related stress concentration factors presented show fairly good agreement. Three ultimate load calculation methods were evaluated with respect to reported test date; the relative performance of each method is shown graphically in Figure 20.

The new tests conducted as a part of this study tended to raise more questions than they answered. It was shown that high strength, low ductility steel in a pin plate behaves differently than the lower strength steels studied by the previous investigators. Increasing pin-to-hole clearance not only resulted in reduced ultimate capacities, as expected, but also resulted in a change of failure mode (usually dishing). The behavior and performance of the asymmetrical specimens were essentially as expected. Because of the scatter of data, particularly with respect to the pin clearance study, final conclusions about plate behavior cannot be drawn here. A course of study for additional research of pin plates can be recommended, however.

Contact stresses are very local and do not appear to affect ultimate static capacity directly. For this reason, an extensive study of this problem was not presented in this report. A complete understanding of pin plate behavior requires a reasonable method of calculating these stresses, at least in the elastic range. The references cited, particularly Roark and Young (1975), note additional works which deal with this problem. It is felt that an improved understanding of contact stresses in pin plates can be developed using currently available information.

Out-of-plane instability, called dishing, was observed in a number of specimens with large pin clearance, but otherwise proportioned to prevent dishing. Additional tests must be conducted to expand the knowledge of dishing behavior. This is needed to more effectively proportion plates with large pin clearance to assure failure by fracture. This work is also necessary to complete the development of an expression relating pin clearance to reduction of ultimate capacity.

Lastly, the tests indicated that high strength, low ductility steel pin plates behave differently than the higher ductility steel plates tested in the past. More data must be developed about high strength plates in order to improve the accuracy of the ultimate strength equations for such steels. It is felt that it may be possible to accomplish much of this work using non-linear finite element analysis, as opposed to additional testing. The accuracy of a finite element model of one of the test specimens may be verified by comparing the analysis output to the measured strains tabulated in Appendix A.

Just how much can be accomplished using computer analysis will be a function of the level of sophistication of the program available for the work.

ACKNOWLEDGMENTS

The authors would like to thank David Menzies for his assistance in the preparation of the test equipment and guidance of the equipment operation. Thanks are also due to Todd Dunnavant for his help setting up and programming the data acquisition system.

The manuscript was typed by Roberta Apolant; her skill and patience are most appreciated.

REFERENCES

Blake, G.T. (1981). Structural Tests of Large Pin-Connected Links. Monroeville, PA: U.S. Steel Research.

Brockenbrough, R.L., and Johnston, B.G. (1981). Steel Design Manual. Pittsburgh: U.S. Steel Corp.

Eshwar, V.A. (1978). Analysis of Clearance Fit Pin Joints. International Journal of Mechanics and Science, Vol. 20, 477-484.

Frocht, M.M., and Hill, H.N. (1940). Stress-Concentration Factors Around a Central Circular Hole in a Plate Loaded Through Pin in the Hole. ASME Transactions, Vol. 62, March, A5 - A9.

Higgins, T.R. (1982). Unpublished Correspondence with N.W. Young, U.S. Steel Corporation, Coraopolis, PA.

Johnston, B.G. (1939). Pin-Connected Plate Links. ASCE Transactions, Paper No. 2023, 314-339.

Kohnke, P.C. (1983). ANSYS Engineering Analysis System Theoretical Manual (2nd ed.). Houston, Pennsylvania: Swanson Analysis Systems, Inc.

Rao, A.K. (1978). Elastic Analysis of Pin Joints. Computers and Structures, Vol. 9, No. 2, 125-144.

Roark, R.J., and Young, W.C. (1975). Formulas for Stress and Strain (5th ed.). New York: McGraw-Hill, Inc.

Scott, R.G., and Stone, J.C. (1982). The Effects of Design Variables on the Critical Stresses of Eye Bars Under Load: An Evaluation by Photoelastic Modeling. Livermore CA: Lawrence Livermore Laboratory.

Seely, F.B., and Smith, J.O. (1952). Advanced Mechanics of Materials (2nd ed.). New York: John Wiley & Sons, Inc.

Specification for the Design, Fabrication, and Erection of Structural Steel for Buildings (1978). Chicago: American Institute of Steel Construction.

Standard Specifications for Highway Bridges (1977). Washington, D.C.: American Association of State Highway and Transportation Officials.

Timoshenko, S.P., and Goodier, J.N. (1970). Theory of Elasticity (3rd ed.). New York: McGraw-Hill, Inc.

Tolbert, R.N. (1970). A Photoelastic Investigation of Lug Stresses and Failures. Unpublished master of science thesis, Vanderbilt University, Nashville, TN.

Tolbert, R.N., and Hackett, R.M. (1974). Experimental Investigation of Lug Stresses and Failures. AISC Engineering Journal, Vol. 11, No. 2, 34-37.

APPENDIX A

SPECIMEN PHOTOGRAPHS AND TEST RESULTS

Data accumulated in each test is assembled in Appendix A. The following information is presented for each test.

1. A drawing of the specimen showing as-built dimensions and strain gage locations appears first in each set. The view shown in the drawing is the same view as that appearing in the photographs. Note that the gages were bonded to the back face of the specimen.

2. A table summarizing primary values and test results is located below the as-built drawing.

3. The next page of each set contains a group of photographs of the specimen before, during, and after the test. The face of the specimen shown was coated with a lime/water whitewash. Progressive deterioration of the coating provided an easily photographed indication of the areas of high stress in the plate as the load was increased. This is not a calibrated brittle coating, so no quantitative results can be obtained from the whitewash cracks.

4. Following the photographs is a table which contains all of the dial indicator and strain gage readings made during the test. The dial indicator was set up to measure gross pin deflection relative to the rigid base which supported the

specimen during the test. Strain gage locations and orientations are shown on the as-built drawing of the specimen.

It will be noticed that strain gage readings are missing in a number of locations in the tables. A complete absence of readings for a gage indicates a faulty gage installation. A termination of readings in a column indicates delamination of the gage from the surface of the specimen during the test. Lastly, the random missing readings for Gage #1 of Specimen 1-B are due to an operational problem with the data acquisition system used to read the strain gages.

5. Next, a curve of load vs. pin deflection is shown. This data was plotted to allow a determination of the general yield point of the specimen. Johnston (1939) had defined the general yield point as that load at which the slope of the curve is three times the initial slope. These curves were plotted and the general yield point determined to allow comparison with Johnston's work as necessary.

6. The last item is a set of curves of load vs. strain for each gage. Also plotted on this drawing are a vertical line at the strain corresponding to the yield point of the material and a horizontal line corresponding to the general yield point of the specimen. The vertical line has been omitted for Specimens 5-A and 5-B due to the difference in yield points of the plates used to fabricate these specimens.

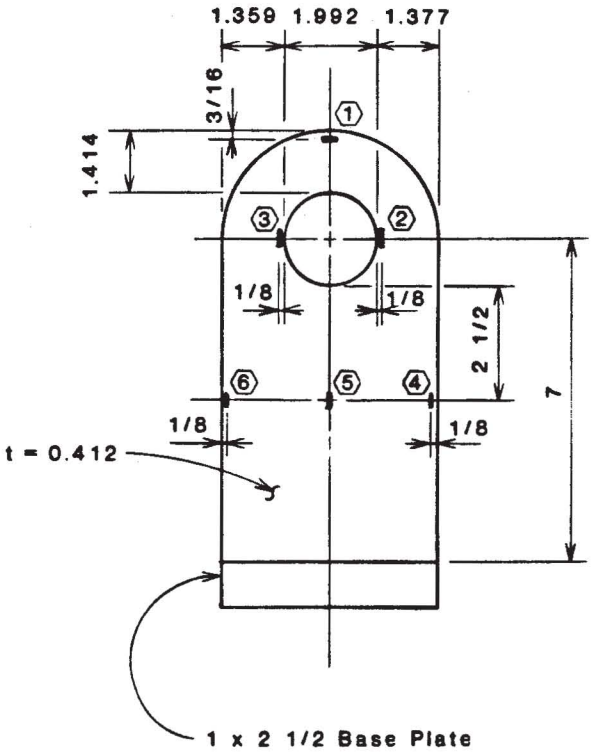

Notes:

▌ indicates strain gage

Dimensions are in inches. 1 in = 25.4 mm

Fig. A1 - As-built Dimensions of Specimen 1-A

Table A1

Summary of Results of Test 1-A

Item	Value
D_h/D_p	1.00
Yield Load, kips	87.3
Failure Load, kips	98.3
Location of Failure	Side

Note: 1 kip = 4.45 kN

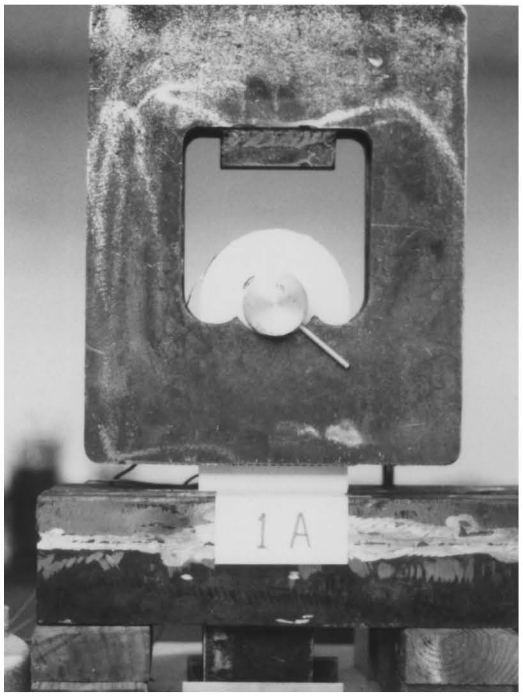

Fig. A2 - Specimen 1-A
at 0.0 kips

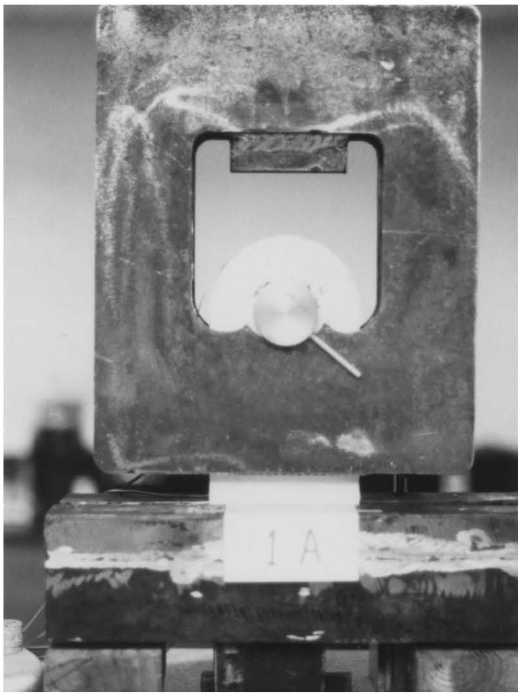

Fig. A3 - Specimen 1-A
at 87.5 kips

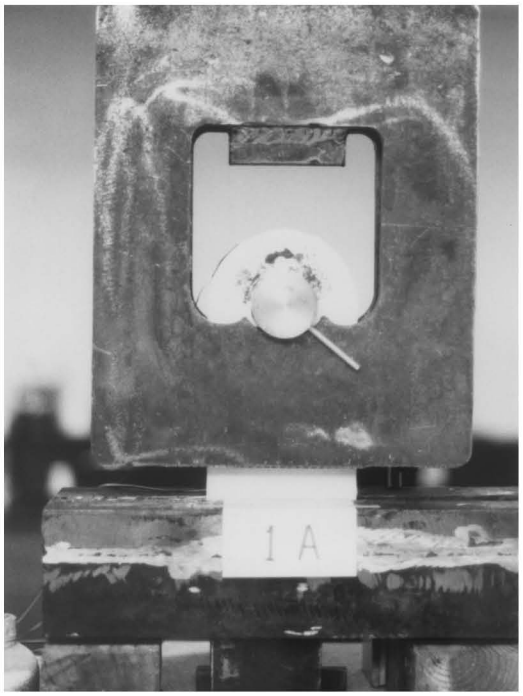

Fig. A4 - Specimen 1-A
at 94.0 kips

Fig. A5 - Specimen 1-A
After Failure

Table A2

Test Readings of Specimen 1-A

Load in Kips	Pin Deflection in Inches	Strain $(x10^{-3})$, inches/inch					
		Gage #1	Gage #2	Gage #3	Gage #4	Gage #5	Gage #6
2.0	0.168	0.0997	0.1975	0.1980	0.0406	0.0186	0.0352
3.0	0.179	0.1452	0.3139	0.3100	0.0885	0.0552	0.0850
5.0	0.193	0.2288	0.4973	0.4846	0.1623	0.1115	0.1638
7.0	0.203	0.3266	0.6833	0.6637	0.2405	0.1701	0.2488
9.0	0.209	0.4058	0.8272	0.8022	0.3041	0.2180	0.3168
10.0	0.212	0.4484	0.9050	0.8781	0.3408	0.2459	0.3559
12.5	0.221	0.5619	1.107	1.077	0.4357	0.3193	0.4582
15.0	0.299	0.6745	1.296	1.256	0.5218	0.3829	0.5472
17.5	0.236	0.7841	1.472	1.422	0.5971	0.4371	0.6270
20.0	0.243	0.8967	1.647	1.589	0.6676	0.4866	0.7014
22.5	0.249	1.015	1.819	1.753	0.7356	0.5345	0.7743
25.0	0.255	1.126	1.982	1.911	0.7988	0.5795	0.8443
27.5	0.259	1.254	2.144	2.065	0.8585	0.6241	0.9158
30.0	0.264	1.378	2.304	2.220	0.9168	0.6681	0.9888
32.5	0.268	1.503	2.462	2.376	0.9756	0.7127	1.064
35.0	0.273	1.631	2.620	2.534	1.032	0.7582	1.139
37.5	0.278	1.752	2.777	2.690	1.086	0.8018	1.215
40.0	0.282	1.880	2.931	2.844	1.143	0.8453	1.289
42.5	0.286	2.019	3.094	3.004	1.203	0.8894	1.366
45.0	0.290	2.146	3.248	3.153	1.260	0.9306	1.434
47.5	0.293	2.283	3.415	3.307	1.317	0.9722	1.503
50.0	0.296	2.424	3.594	3.466	1.375	1.014	1.572
52.5	0.299	2.556	3.780	3.632	1.432	1.056	1.639
55.0	0.303	2.703	3.978	3.813	1.490	1.097	1.705
57.5	0.306	2.853	4.179	4.008	1.547	1.140	1.772

Table A2 (con't.)

Test Readings of Specimen 1-A

Load in Kips	Pin Deflection in Inches	Strain $(x10^{-3})$, inches/inch					
		Gage #1	Gage #2	Gage #3	Gage #4	Gage #5	Gage #6
60.0	0.309	3.024	4.381	4.217	1.602	1.181	1.839
62.5	0.312	3.204	4.595	4.430	1.658	1.221	1.900
65.0	0.315	3.419	4.884	4.684	1.721	1.264	1.966
67.5	0.318	3.654	5.203	4.984	1.782	1.306	2.030
70.0	0.321	3.924	5.527	5.389	1.840	1.347	2.094
72.5	0.325	4.247	5.829	5.887	1.898	1.387	2.160
75.0	0.328	4.680	6.087	6.450	1.953	1.427	2.228
77.5	0.331	5.140	6.266	6.934	2.009	1.467	2.294
80.0	0.336	5.807	6.339	7.425	2.062	1.506	2.361
82.5	0.343	6.689	6.385	7.775	2.114	1.545	2.430
85.0	0.352	9.027	6.487	8.174	2.161	1.583	2.501
87.5	0.367	15.20	6.961	9.032	2.203	1.622	2.577
90.0	0.387	22.24	8.365	10.80	2.242	1.661	2.656
92.5	0.410	29.31	10.54	13.43	2.287	1.696	2.739
94.0	0.432	35.83	12.60	15.92	2.309	1.713	2.790
95.0	0.450	41.66	14.43	18.06	2.329	1.724	2.833
97.0	0.503	38.81	17.99	22.26	2.372	1.736	2.917

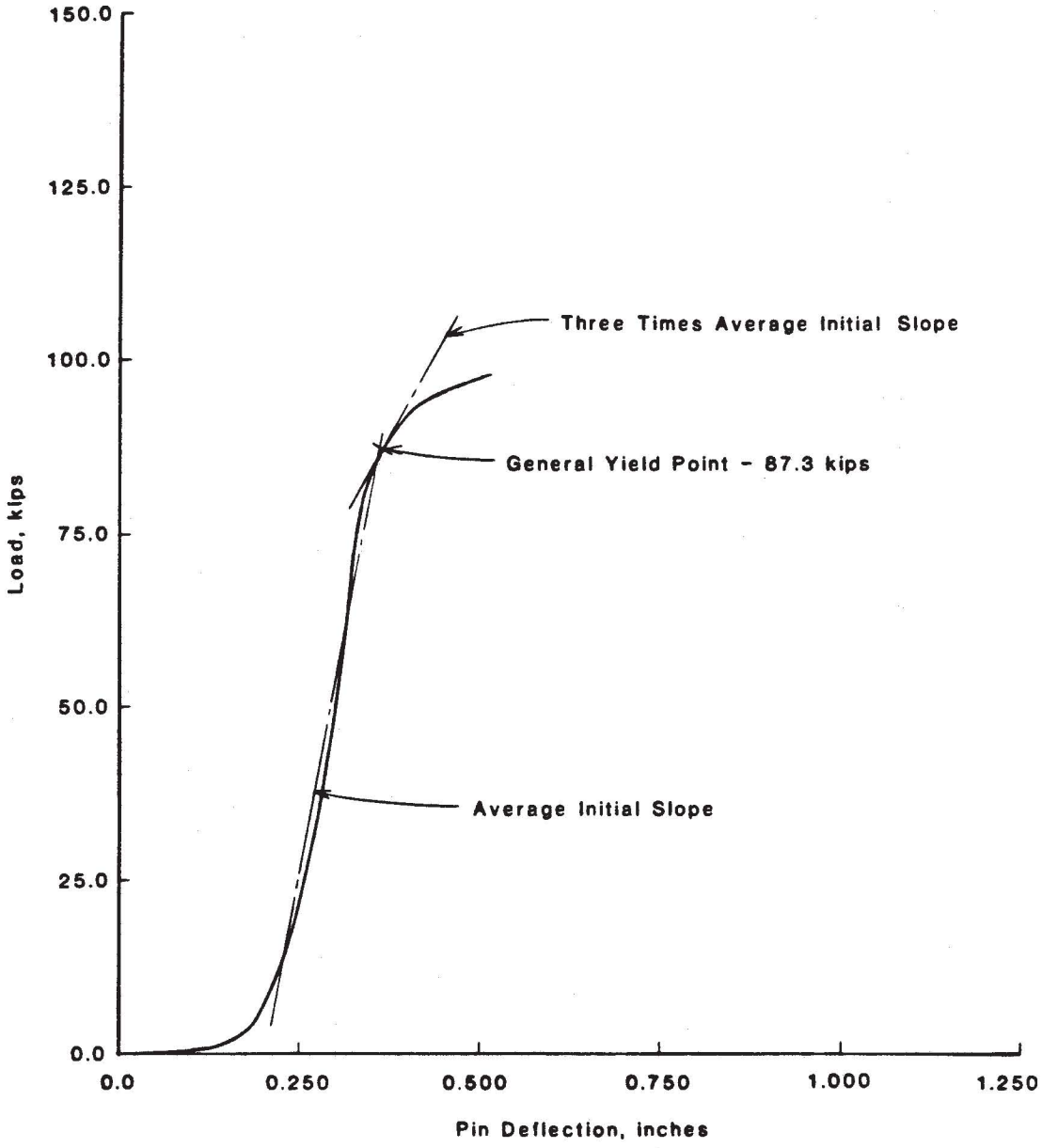

Fig. A6 - Load vs. Pin Deflection - Specimen 1-A

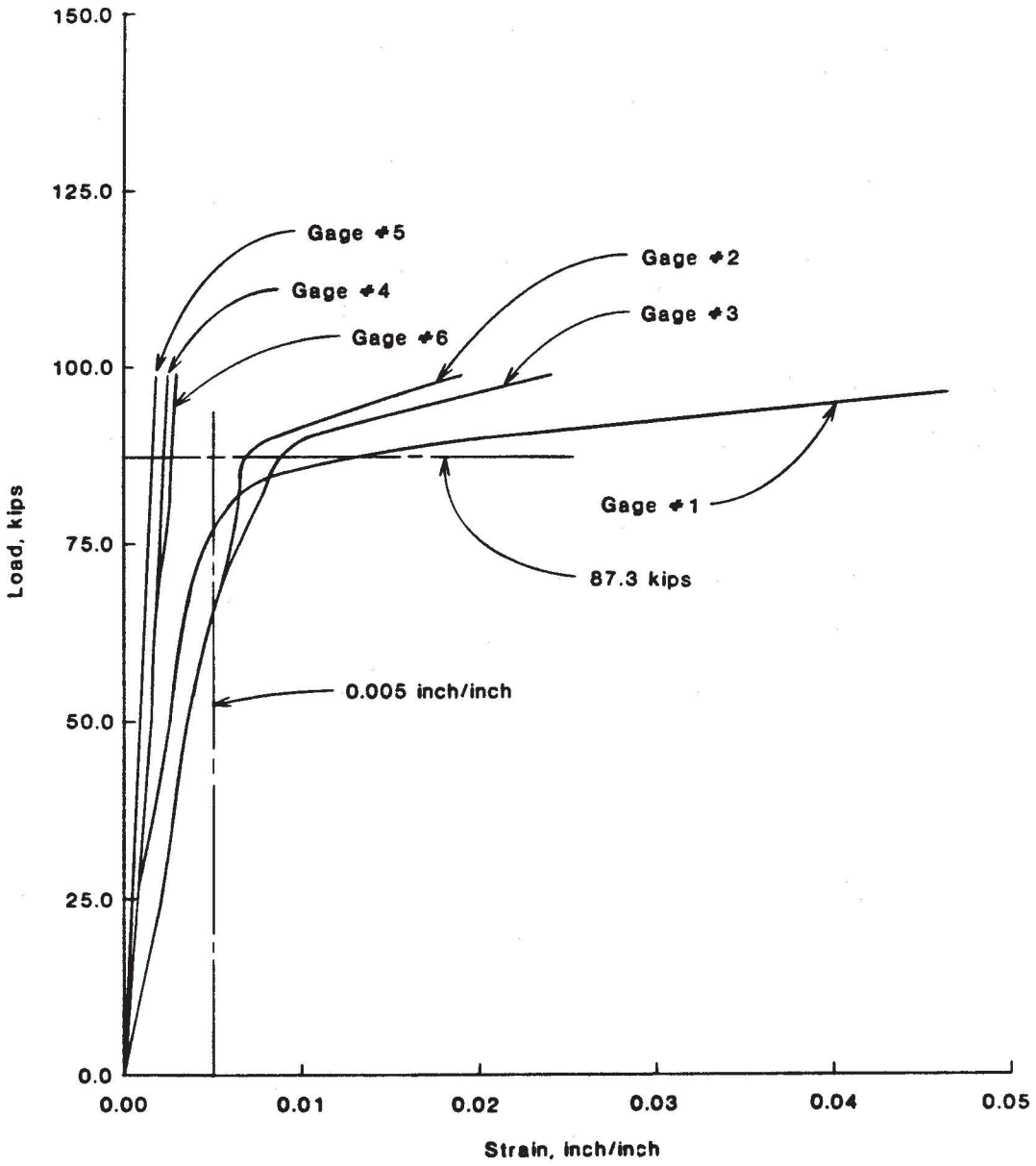

Fig. A7 - Load vs. Strain - Specimen 1-A

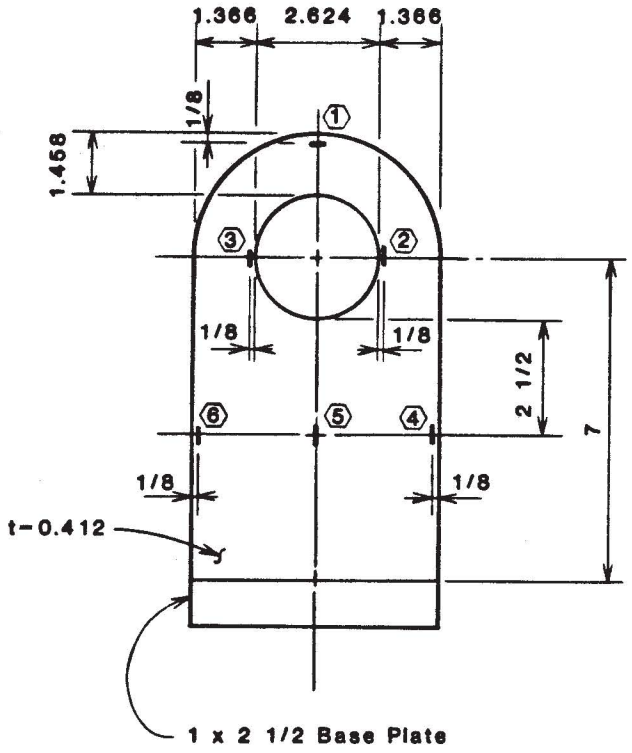

Notes:

| indicates strain gage

Dimensions are in inches. 1 in = 25.4 mm

Fig. A8 - As-built Dimensions of Specimen 1-B

Table A3

Summary of Results of Test 1-B

Item	Value
D_h/D_p	1.32
Yield Load, kips	76.8
Failure Load, kips	98.3
Location of Failure	Side

Note: 1 kip = 4.45 kN

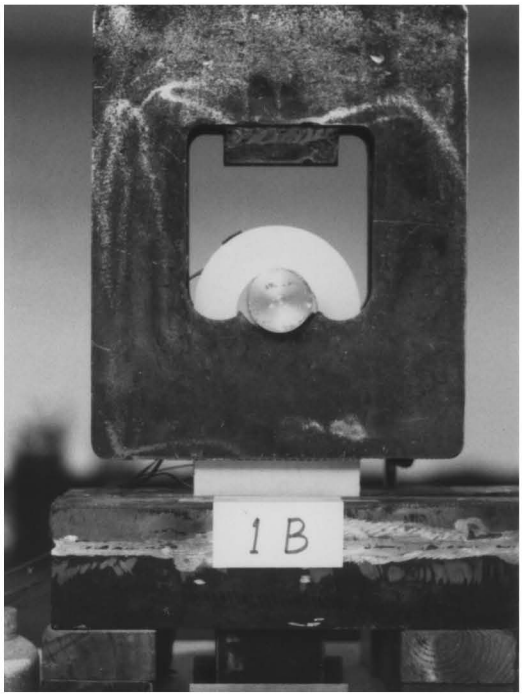

Fig. A9 - Specimen 1-B
at 0.0 kips

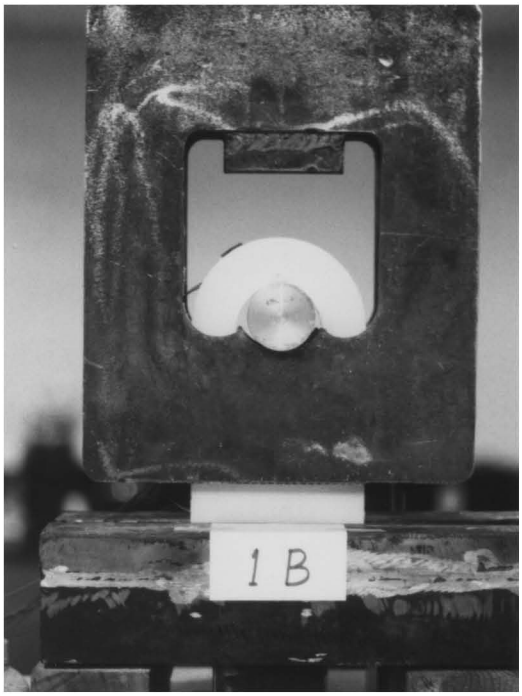

Fig. A10 - Specimen 1-B
at 40.0 kips

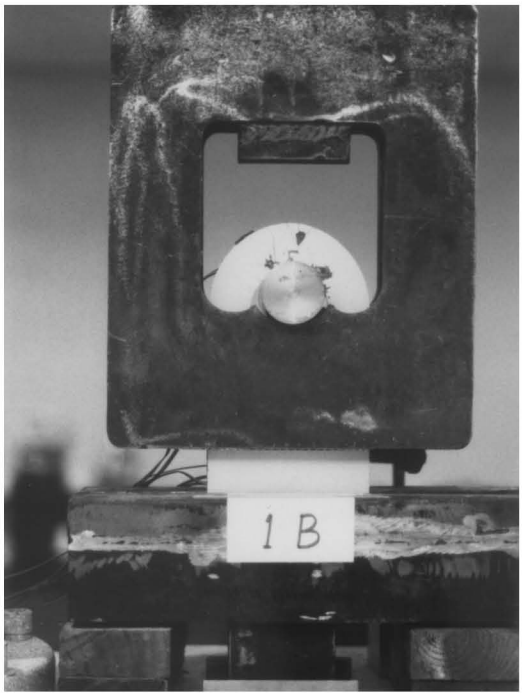

Fig. A11 - Specimen 1-B
at 80.0 kips

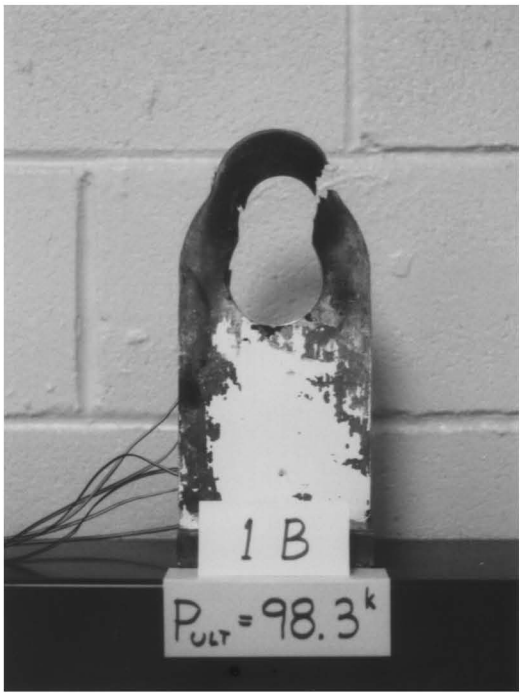

Fig. A12 - Specimen 1-B
After Failure

Table A4

Test Readings of Specimen 1-B

Load in Kips	Pin Deflection in Inches	Strain $(x10^{-3})$, inches/inch					
		Gage #1	Gage #2	Gage #3	Gage #4	Gage #5	Gage #6
1.5	0.083						
2.5		0.2585	0.1920	0.1846	0.0563	0.0132	0.0441
3.5	0.098						
5.0	0.108	0.5517	0.3656	0.3508	0.0950	0.0147	0.0769
7.5	0.120	0.8722	0.5382	0.5165	0.1322	0.0166	0.1132
10.0	0.130	0.9356	0.7109	0.6833	0.1764	0.0245	0.1578
12.5	0.137	1.051	0.8880	0.8550	0.2214	0.0328	0.2053
15.0	0.144	1.385	1.058	1.019	0.2616	0.0372	0.2470
17.5	0.151	2.247	1.250	1.205	0.3072	0.0431	0.2970
20.0	0.157	3.197	1.423	1.372	0.3484	0.0490	0.3421
22.5	0.164	3.679	1.608	1.547	0.3906	0.0558	0.3906
25.0	0.170	4.665	1.815	1.744	0.4381	0.0656	0.4465
27.5	0.175	6.206	2.014	1.934	0.4823	0.0749	0.4990
30.0	0.182	12.02	2.236	2.144	0.5318	0.0872	0.5583
32.5	0.188	26.91	2.465	2.360	0.5823	0.1019	0.6221
35.0	0.194		2.695	2.578	0.6314	0.1156	0.6869
37.5	0.200		2.982	2.802	0.6823	0.1298	0.7511
40.0	0.205	27.16	3.161	3.014	0.7305	0.1426	0.8287
42.5	0.211	28.80	3.393	3.227	0.7816	0.1563	0.9019
45.0	0.217		3.631	3.445	0.8361	0.1700	0.9864
47.5	0.223	36.53	3.871	3.661	0.8934	0.1837	1.075
50.0	0.229		4.113	3.879	0.9566	0.1959	1.153
52.5	0.235	52.55	4.352	4.098	1.027	0.2057	1.241
55.0	0.243	53.13	4.566	4.301	1.101	0.2150	1.353
57.5	0.251		4.795	4.513	1.179	0.2224	1.461

Table A4 (con't.)

Test Readings of Specimen 1-B

Load in Kips	Pin Deflection in Inches	Strain $(x10^{-3})$, inches/inch					
		Gage #1	Gage #2	Gage #3	Gage #4	Gage #5	Gage #6
60.0	0.261		5.141	4.809	1.261	0.2277	1.510
62.5	0.271		5.663	5.286	1.345	0.2326	1.603
65.0	0.283		6.411	5.987	1.434	0.2356	1.676
67.5	0.295		7.355	6.934	1.526	0.2365	1.812
70.0	0.310		8.497	8.108	1.620	0.2380	2.129
72.5	0.325		9.796	9.265	1.714	0.2399	2.700
75.0	0.343		10.90	10.73	1.806	0.2463	2.289
77.5	0.362				1.889	0.2605	2.995
80.0	0.385				1.960	0.2859	3.365
82.5					2.017	0.3196	3.202
85.0					2.060	0.3578	3.354
87.5					2.098	0.3995	4.928
90.0					2.133	0.4426	5.575
92.5					2.158	0.4892	4.279
95.0					2.167	0.5399	5.325

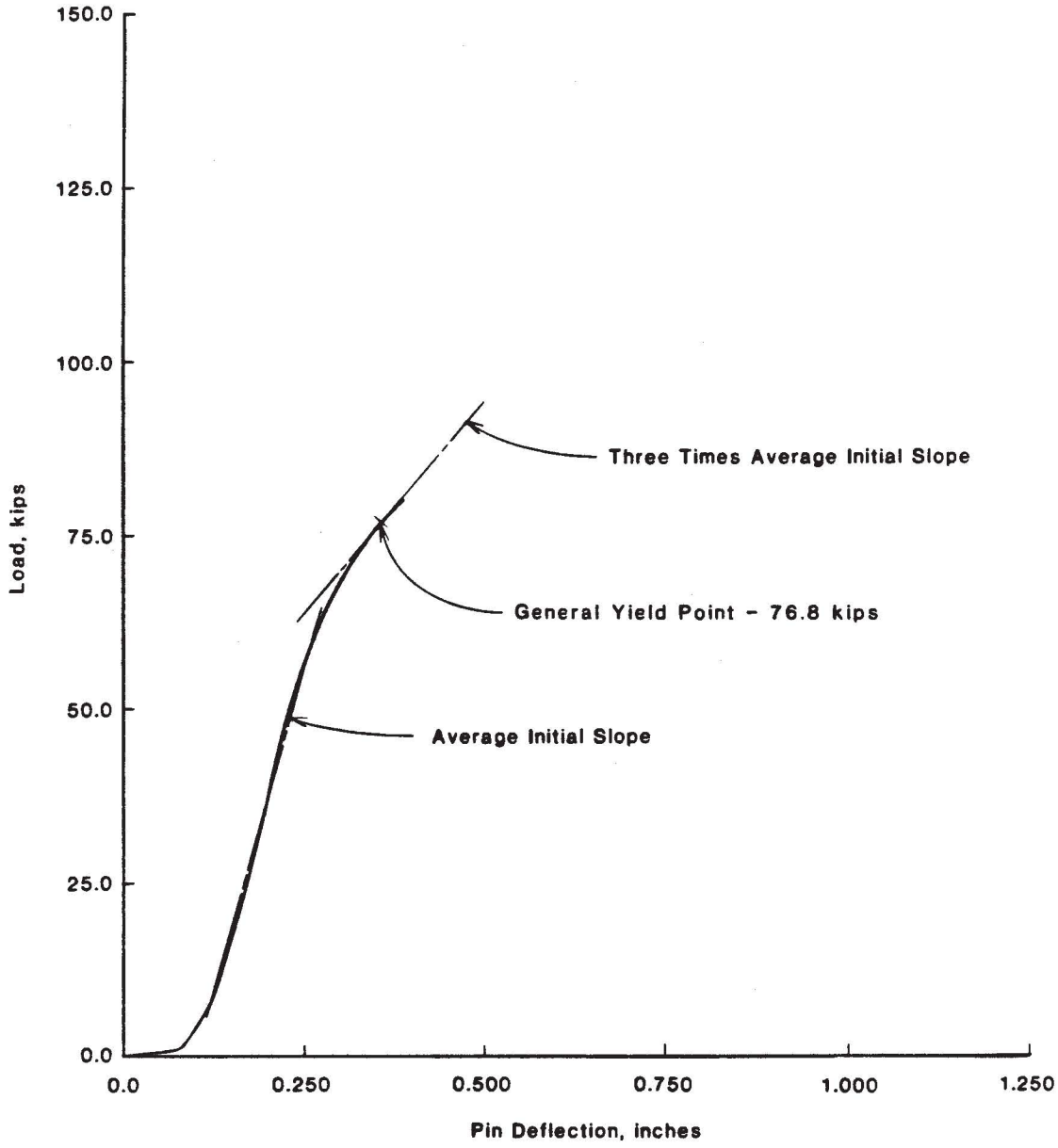

Fig. A13 - Load vs. Pin Deflection - Specimen 1-B

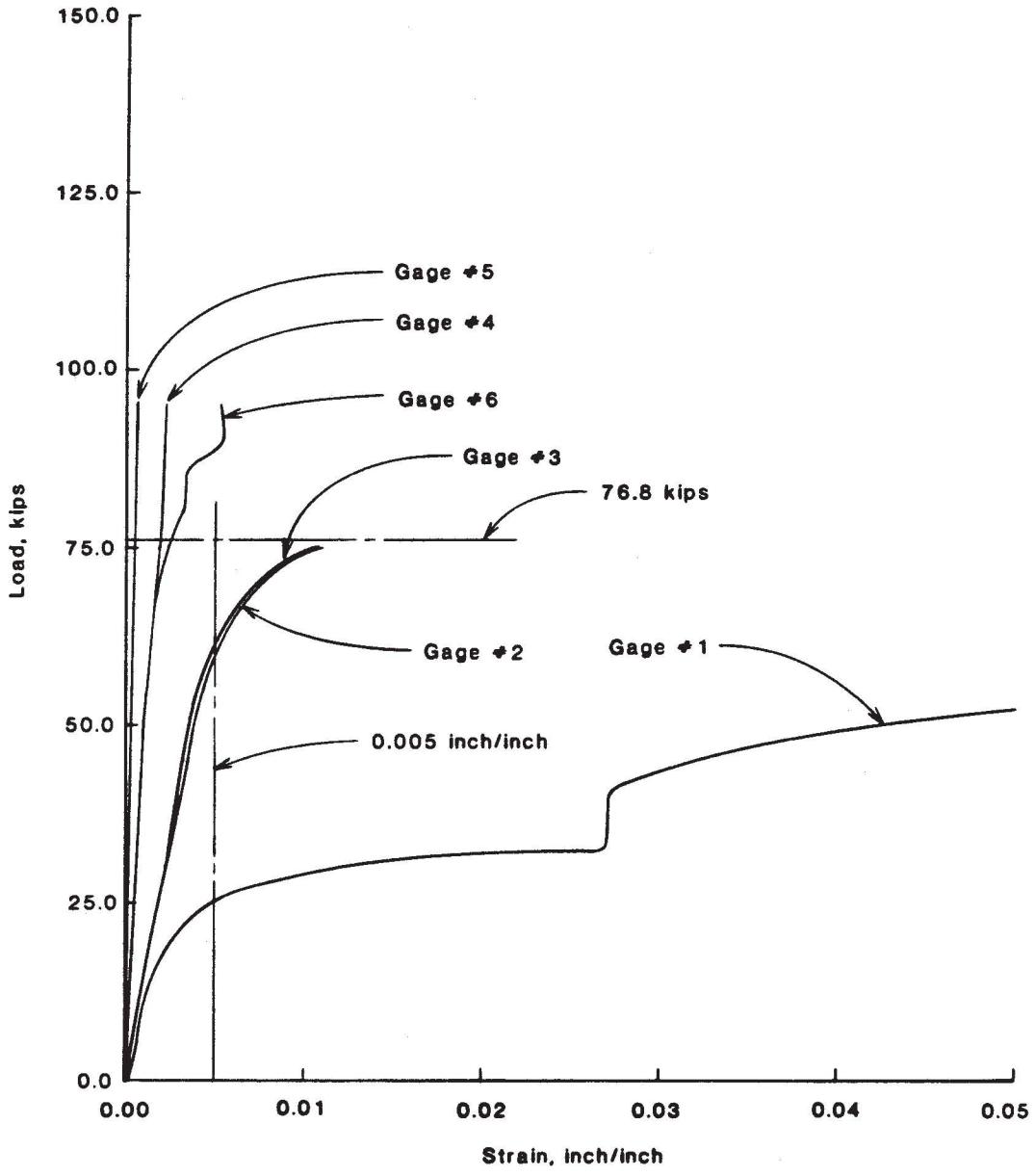

Fig. A14 - Load vs. Strain - Specimen 1-B

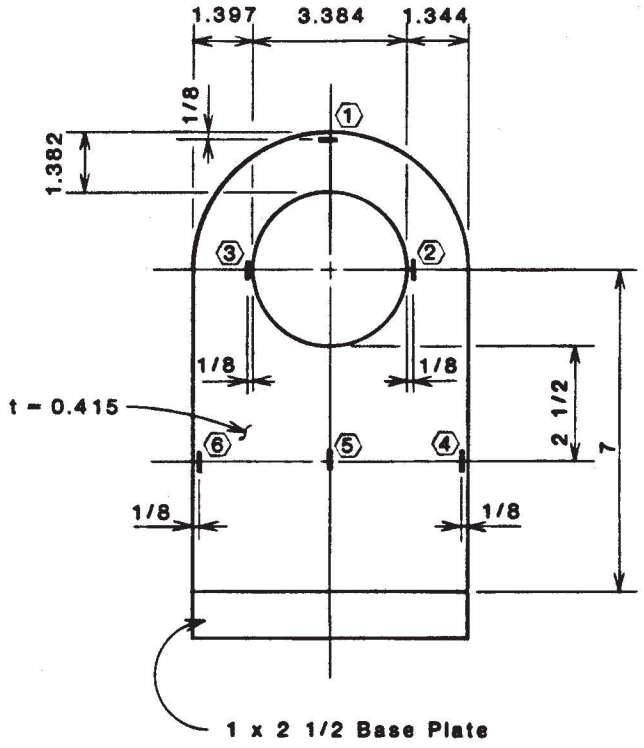

Notes:

| indicates strain gage

Dimensions are in inches. 1 in = 25.4 mm

Fig. A15 - As-built Dimensions of Specimen 1-C

Table A5

Summary of Results of Test 1-C

Item	Value
D_h/D_p	1.70
Yield Load, kips	60.3
Failure Load, kips	93.3
Location of Failure	Shear

Note: 1 kip = 4.45 kN

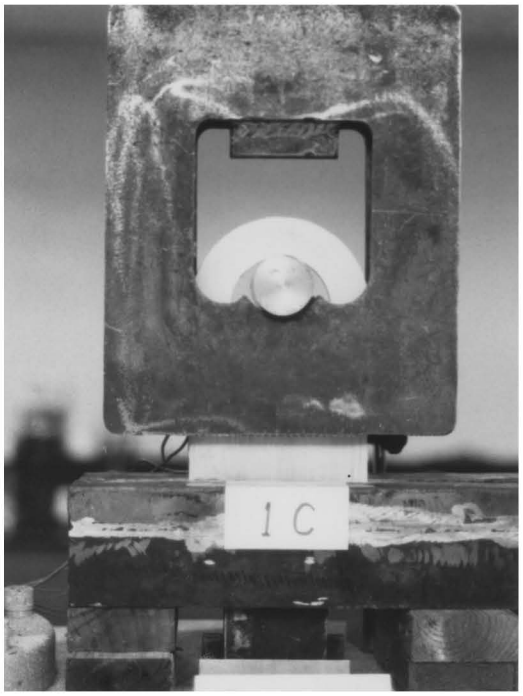

Fig. A16 - Specimen 1-C
at 0.0 kips

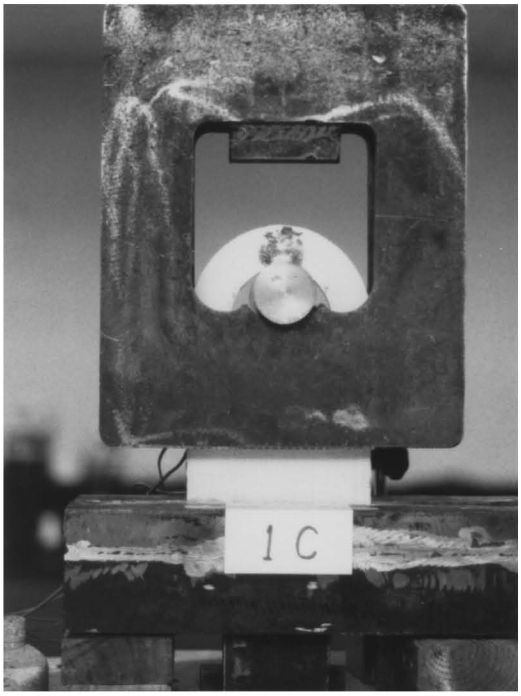

Fig. A17 - Specimen 1-C
at 62.5 kips

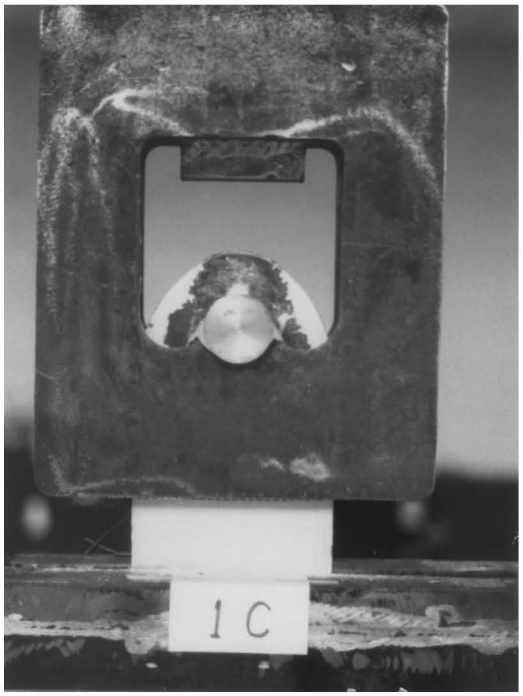

Fig. A18 - Specimen 1-C
at 90.0 kips

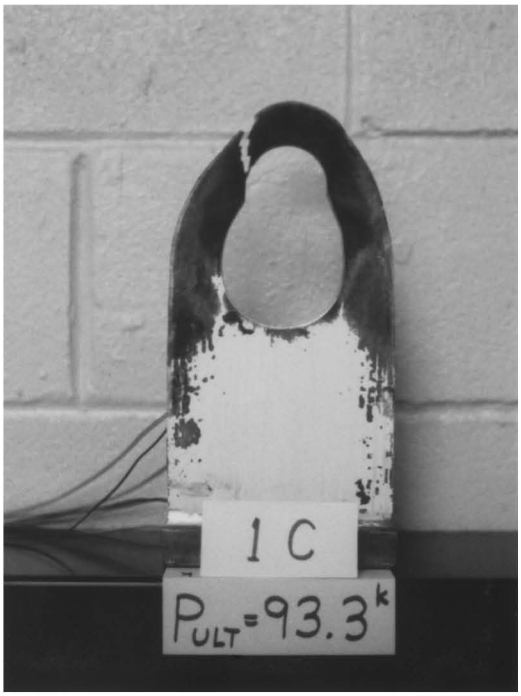

Fig. A19 - Specimen 1-C
After Failure

Table A6

Test Readings of Specimen 1-C

Load in Kips	Pin Deflection in Inches	Strain $(x10^{-3})$, inches/inch				
		Gage #1	Gage #2	Gage #3	Gage #4	Gage #6
0.5	0.016					
2.5	0.052	0.3008	0.0138	0.0265		
5.0	0.078	0.5661	0.1645	0.1924		
7.5	0.095	0.8209	0.3457	0.3894		
10.0	0.108	1.115	0.5393	0.5978	0.0618	0.0697
12.5	0.118	1.502	0.7375	0.8123	0.1290	0.1469
15.0	0.127	1.884	0.9290	1.019	0.1919	0.2196
17.5	0.134	2.320	1.129	1.236	0.2572	0.2954
20.0	0.142	2.811	1.338	1.463	0.3246	0.3706
22.5	0.148	3.366	1.555	1.695	0.3920	0.4446
25.0	0.155	3.976	1.771	1.928	0.4540	0.5122
27.5	0.161	4.660	1.994	2.171	0.5160	0.5802
30.0	0.167	5.410	2.220	2.414	0.5737	0.6438
32.5	0.174	6.238	2.452	2.664	0.6292	0.7048
35.0	0.180	7.174	2.695	2.915	0.6854	0.7654
37.5	0.186	8.225	2.935	3.158	0.7396	0.8242
40.0	0.193	9.515	3.175	3.396	0.7954	0.8849
42.5	0.200	11.82	3.430	3.633	0.8551	0.9507
45.0	0.208	15.50	3.658	3.840	0.9145	1.017
47.5	0.217	20.47	3.869	4.026	0.9812	1.094
50.0	0.228	26.57	4.046	4.185	1.056	1.186
52.5	0.240	32.81	4.190	4.318	1.146	1.295
55.0	0.253		4.301	4.443	1.248	1.406
57.5	0.270		4.384	4.601	1.363	1.508
60.0	0.289		4.448	4.861	1.489	1.610

Table A6 (con't.)

Test Readings of Specimen 1-C

Load in Kips	Pin Deflection in Inches	Strain $(x10^{-3})$, inches/inch				
		Gage #1	Gage #2	Gage #3	Gage #4	Gage #6
62.5	0.311		4.509	5.257	1.622	1.715
65.0	0.335		4.617	5.815	1.750	1.823
67.5	0.363		4.889	6.651	1.869	1.927
70.0	0.394		5.538	8.027	1.972	2.020
72.5	0.429		6.938	10.29	2.058	2.101
75.0	0.466		9.468	12.78	2.126	2.166
77.5	0.507		12.65	15.60	2.185	2.222
80.0	0.550		12.76	18.27	2.240	2.271
82.5			13.91	19.10	2.299	2.319
85.0				19.59	2.352	2.360
87.5					2.403	2.396
90.0					2.458	2.432
92.5					2.513	2.452

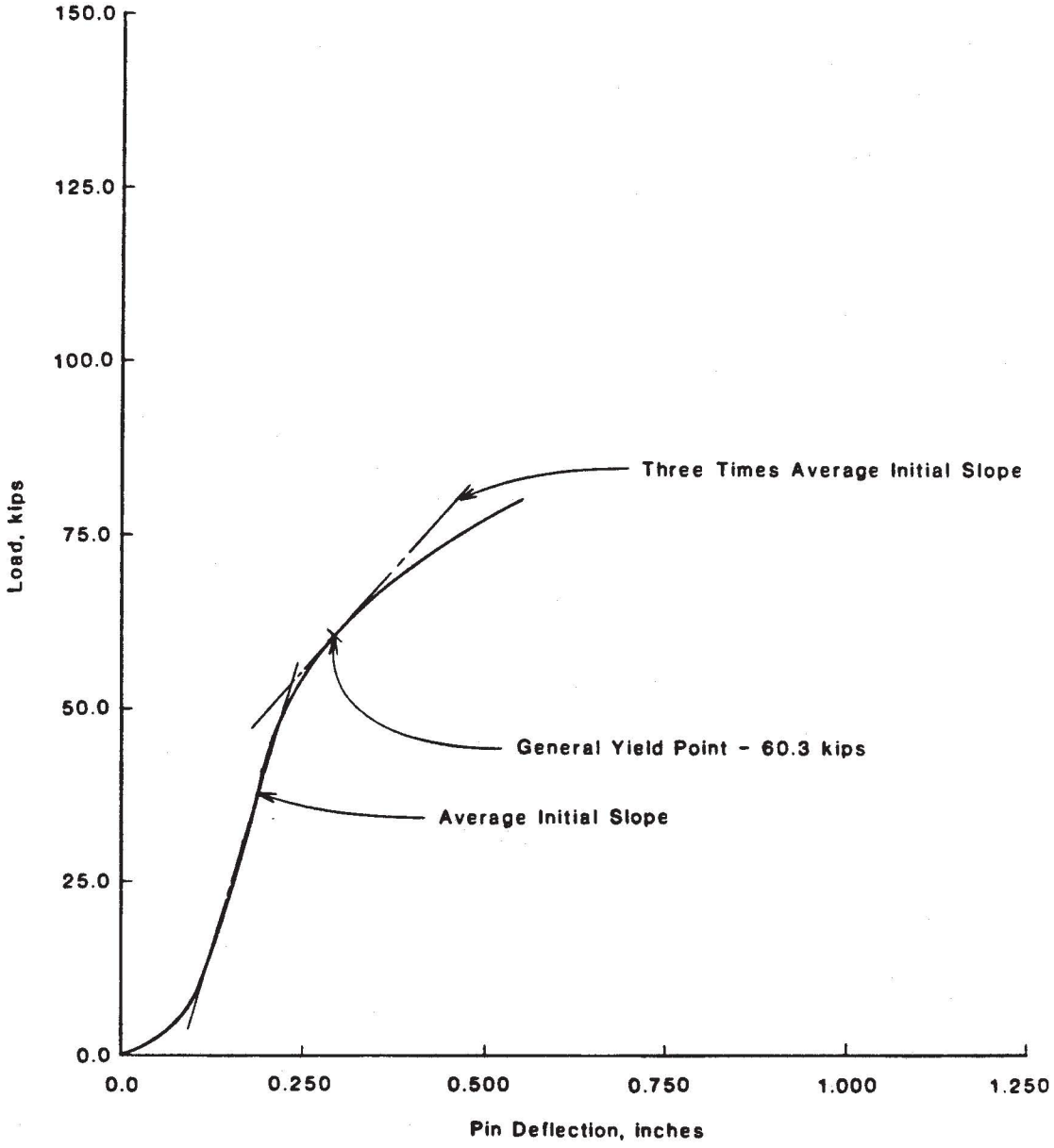

Fig. A20 - Load vs. Pin Deflection - Specimen 1-C

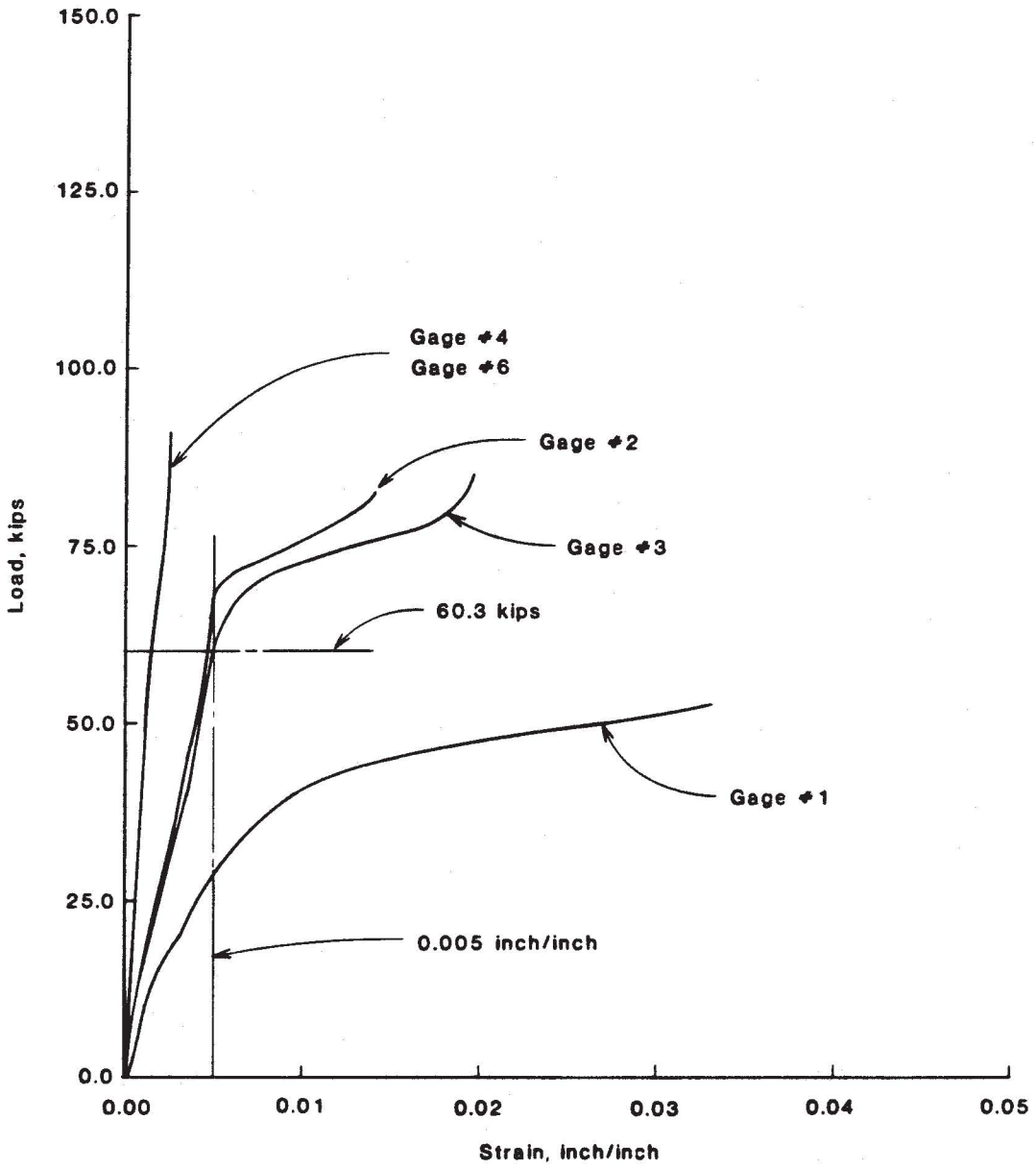

Fig. A21 - Load vs. Strain - Specimen 1-C

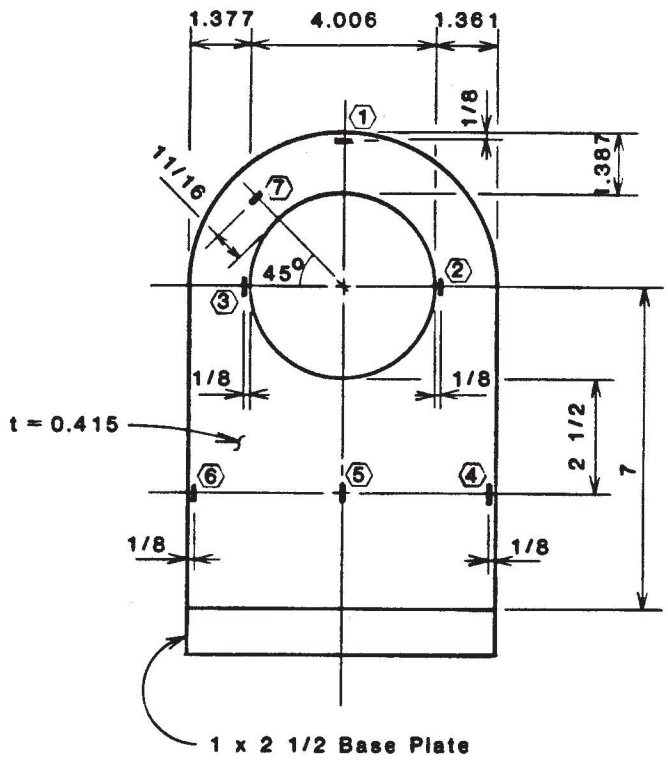

Notes:

▌ indicates strain gage

Dimensions are in inches. 1 in = 25.4 mm

Fig. A22 - As-built Dimensions of Specimen 1-D

Table A7

Summary of Results of Test 1-D

Item	Value
D_h/D_p	2.02
Yield Load, kips	55.5
Failure Load, kips	86.1
Location of Failure	Beyond

Note: 1 kip = 4.45 kN

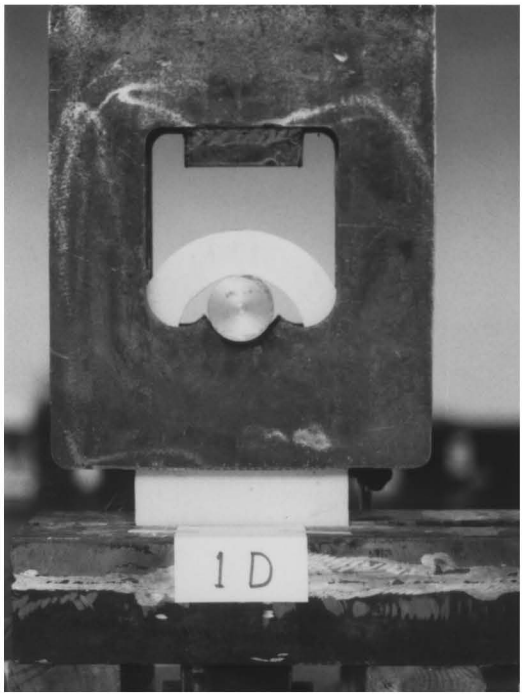

Fig. A23 - Specimen 1-D
at 0.0 kips

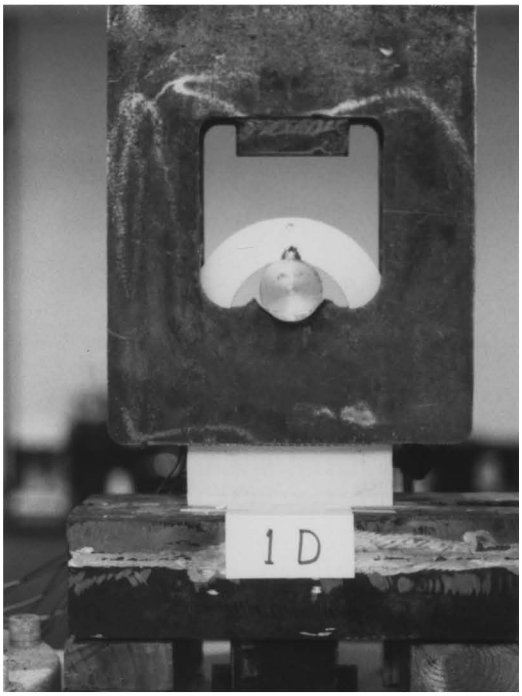

Fig. A24 - Specimen 1-D
at 35.0 kips

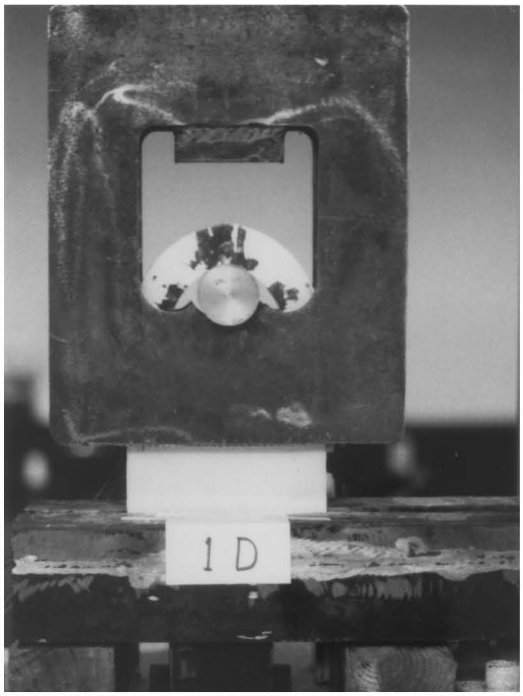

Fig. A25 - Specimen 1-D
at 67.5 kips

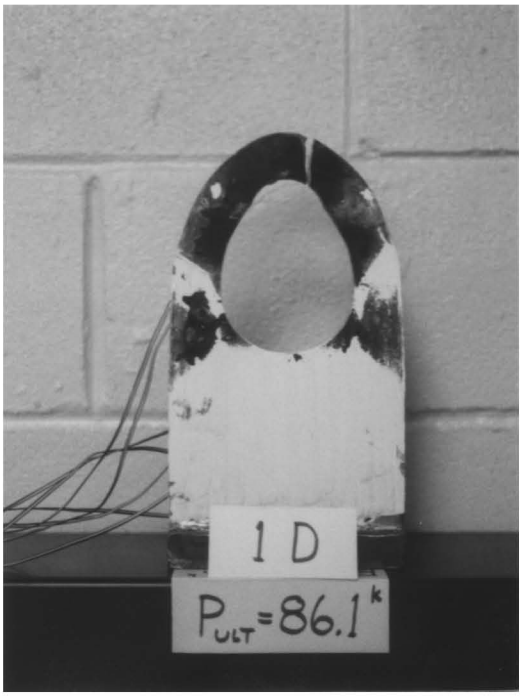

Fig. A26 - Specimen 1-D
After Failure

Table A8

Test Readings of Specimen 1-D

Load in Kips	Pin Deflection in Inches	Strain $(x10^{-3})$, inches/inch						
		Gage #1	Gage #2	Gage #3	Gage #4	Gage #5	Gage #6	Gage #7
0.5	0.186							
2.5	0.225	0.2118	0.2222	0.2218	0.2350	0.1573	0.2379	
5.0	0.247	0.4528	0.3899	0.3900	0.3742	0.2311	0.3870	
7.5	0.261	0.7082	0.6138	0.6153	0.5134	0.2990	0.5385	
10.0	0.273	0.9824	0.8392	0.8417	0.6300	0.3457	0.6684	0.0251
12.5	0.282	1.331	1.079	1.084	0.7442	0.3865	0.7994	0.0796
15.0	0.291	1.757	1.338	1.345	0.8654	0.4332	0.9387	0.1445
17.5	0.300	2.280	1.611	1.621	0.9895	0.4820	1.077	0.2144
20.0	0.310	2.920	1.887	1.900	1.107	0.5257	1.206	0.2837
22.5	0.319	3.697	2.168	2.184	1.222	0.5710	1.341	0.3521
25.0	0.327	4.628	2.438	2.458	1.318	0.5996	1.462	0.4145
27.5	0.335	5.737	2.713	2.739	1.407	0.6232	1.581	0.4746
30.0	0.343	6.997	2.993	3.026	1.490	0.6409	1.695	0.5336
32.5	0.352	8.406	3.270	3.312	1.567	0.6517	1.802	0.5931
35.0	0.360	10.12	3.539	3.592	1.645	0.6576	1.910	0.6675
37.5	0.369	12.23	3.765	3.828	1.716	0.6552	2.009	0.7556
40.0	0.379	15.68	3.970	4.045	1.791	0.6458	2.112	0.8767
42.5	0.390	20.58	4.140	4.226	1.869	0.6296	2.217	1.045
45.0	0.403	26.66	4.270	4.368	1.951	0.6103	2.325	1.275
47.5	0.417		4.349	4.462	2.036	0.5852	2.438	1.593
50.0	0.434		4.384	4.516	2.128	0.5557	2.557	2.010
52.5	0.455		4.384	4.536	2.227	0.5202	2.683	2.525
55.0	0.481		4.360	4.531	2.327	0.4794	2.812	3.094
57.5	0.511		4.337	4.527	2.426	0.4361	2.940	3.717
60.0	0.539		4.336	4.549	2.517	0.3943	3.063	4.565

Table A8 (con't.)

Test Readings of Specimen 1-D

Load in Kips	Pin Deflection in Inches	Strain $(x10^{-3})$, inches/inch						
		Gage #1	Gage #2	Gage #3	Gage #4	Gage #5	Gage #6	Gage #7
62.5	0.583		4.394	4.653	2.594	0.3579	3.172	5.562
65.0	0.627		4.569	4.988	2.655	0.3304	3.267	6.428
67.5	0.674		4.994	5.674	2.695	0.3142	3.334	6.915
70.0	0.727		5.942	6.967	2.728	0.3068	3.394	7.152
72.5	0.783		7.382	8.806	2.759	0.3038	3.447	7.295
75.0	0.840		9.185	10.94	2.791	0.3048	3.499	7.582
77.5	0.905		11.31	12.45	2.818	0.3083	3.547	8.183
80.0	0.971		13.50	14.15	2.846	0.3142	3.594	9.034
82.5			15.66	14.77	2.873	0.3210	3.640	10.02
85.0			17.95		2.895	0.3313	3.680	11.15

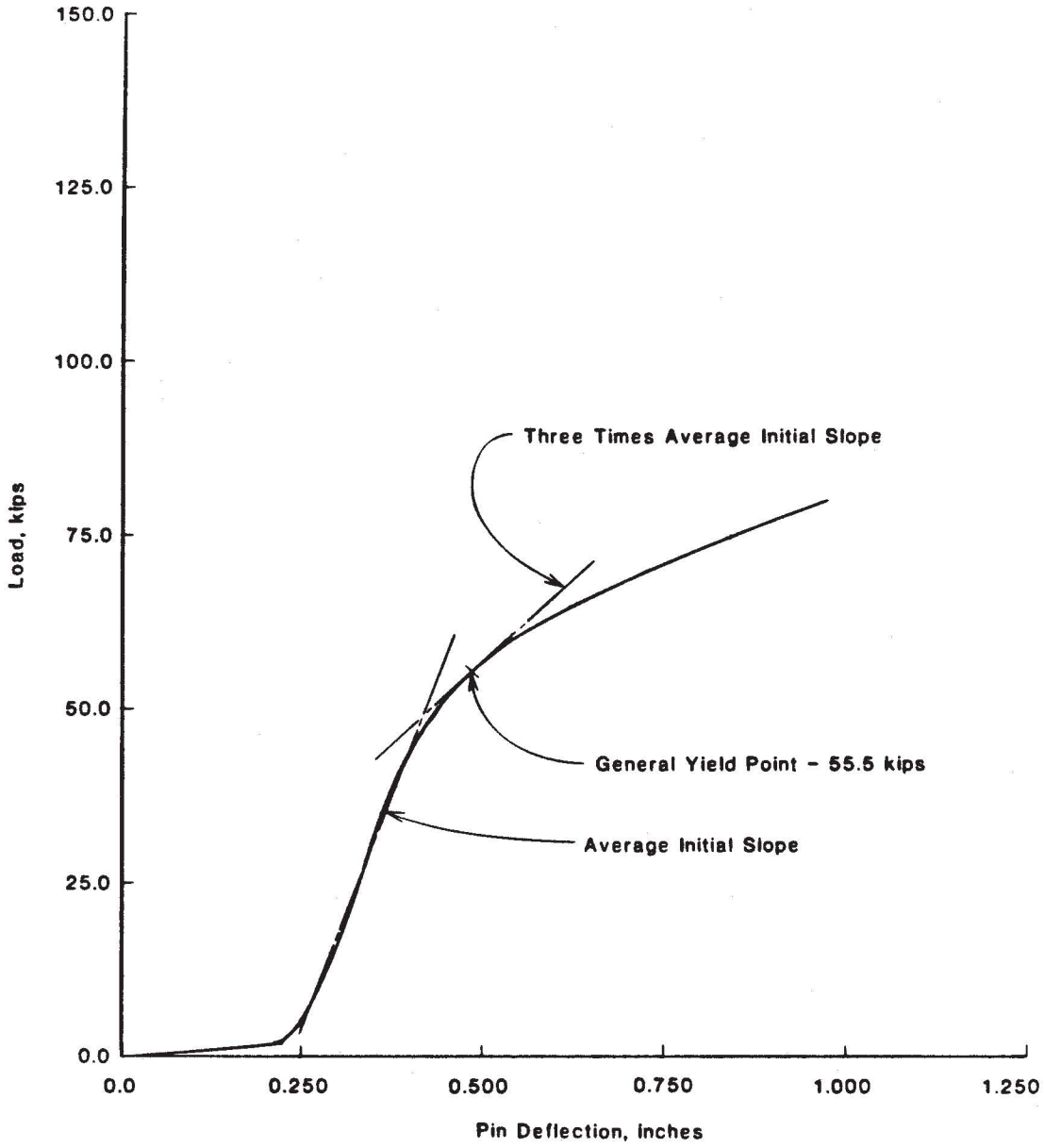

Fig. A27 - Load vs. Pin Deflection - Specimen 1-D

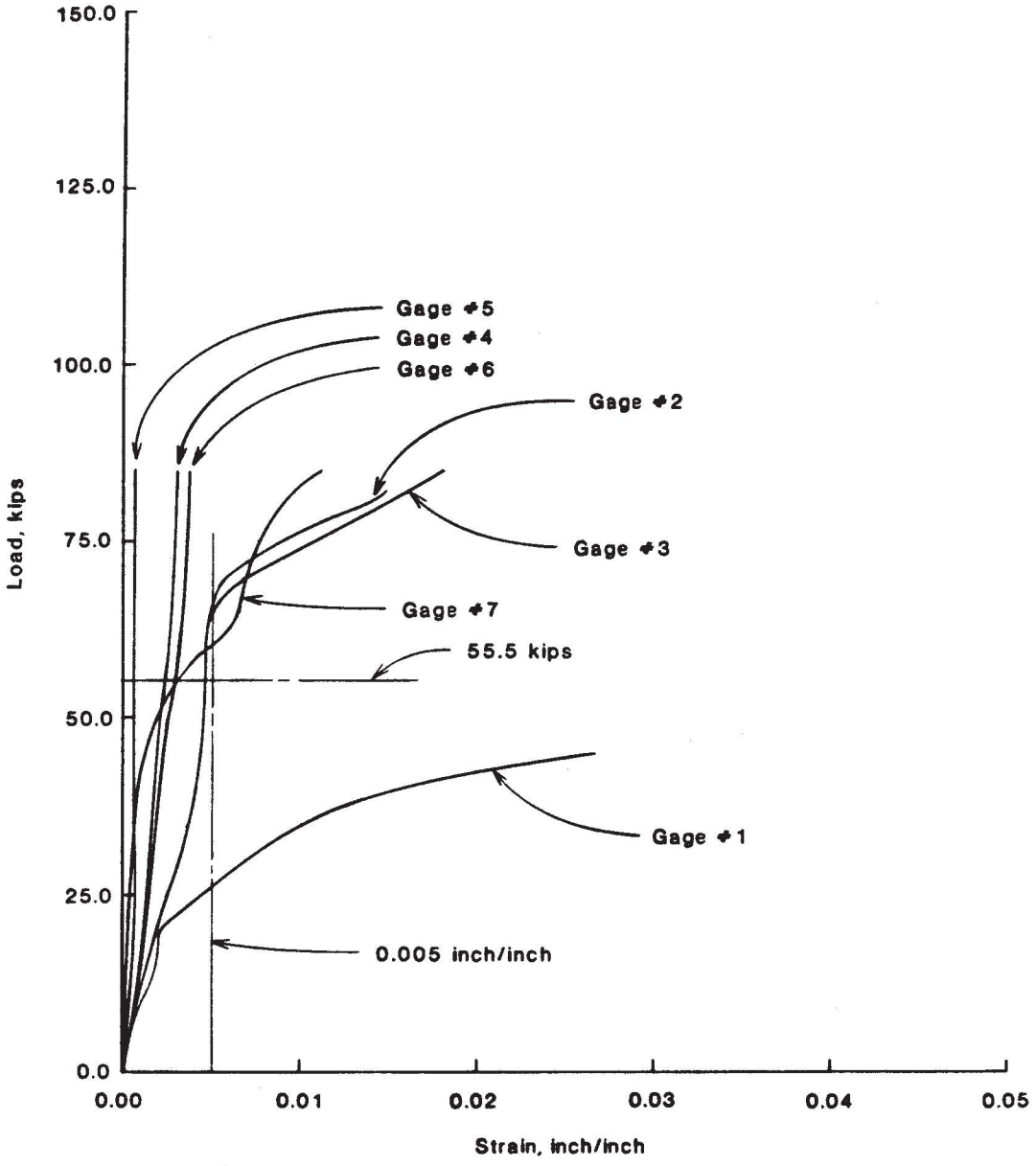

Fig. A28 - Load vs. Strain - Specimen 1-D

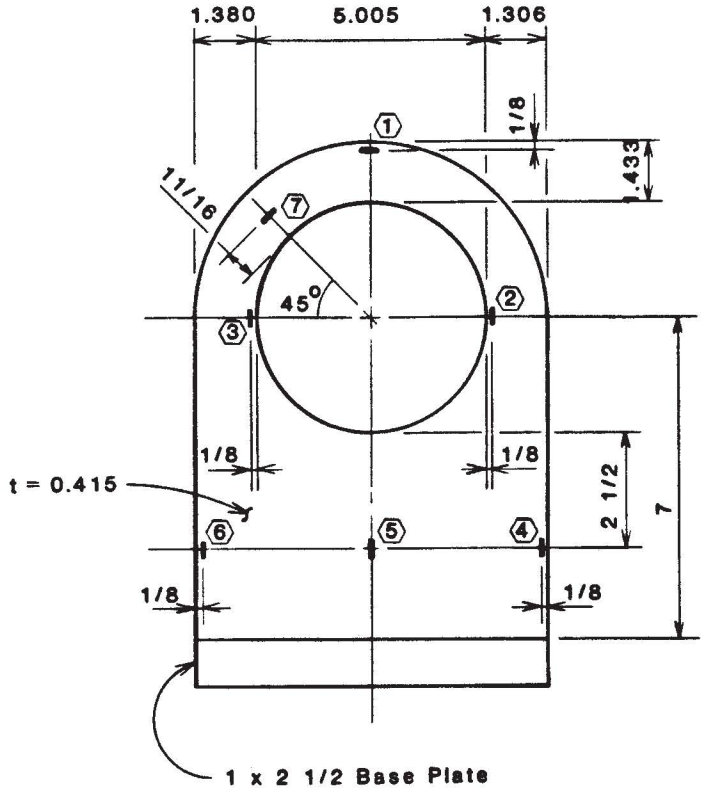

Notes:

| indicates strain gage

Dimensions are in inches. 1 in = 25.4 mm

Fig. A29 – As-built Dimensions of Specimen 1-E

Table A9

Summary of Results of Test 1-E

Item	Value
D_h/D_p	2.52
Yield Load, kips	48.5
Failure Load, kips	91.1
Location of Failure	Side

Note: 1 kip = 4.45 kN

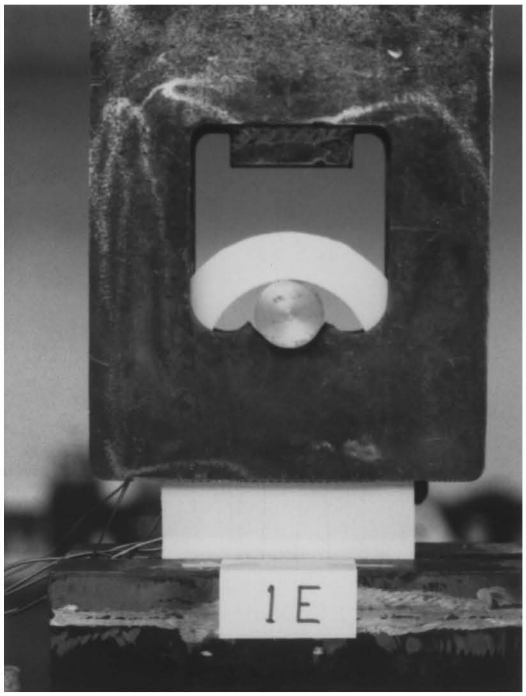

Fig. A30 - Specimen 1-E
at 0.0 kips

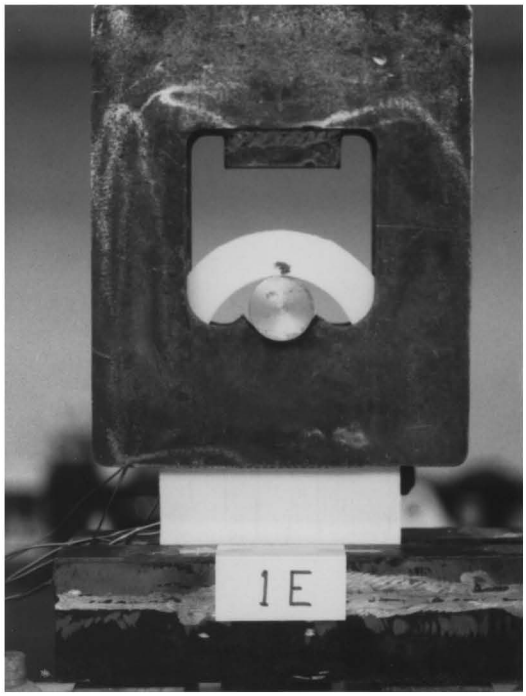

Fig. A31 - Specimen 1-E
at 30.0 kips

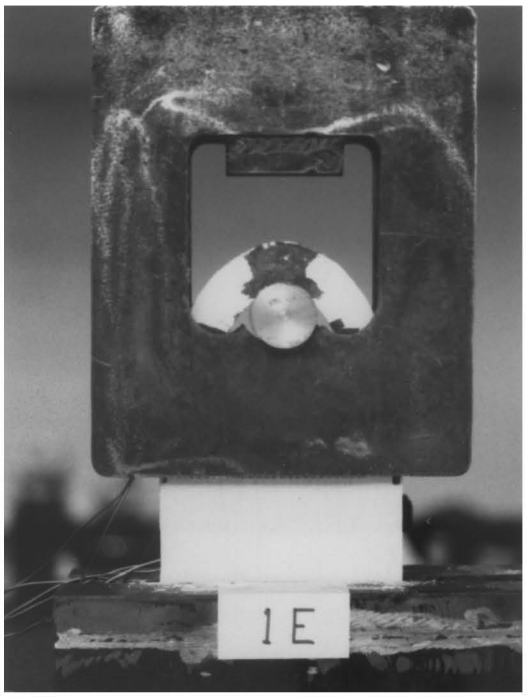

Fig. A32 - Specimen 1-E
at 80.0 kips

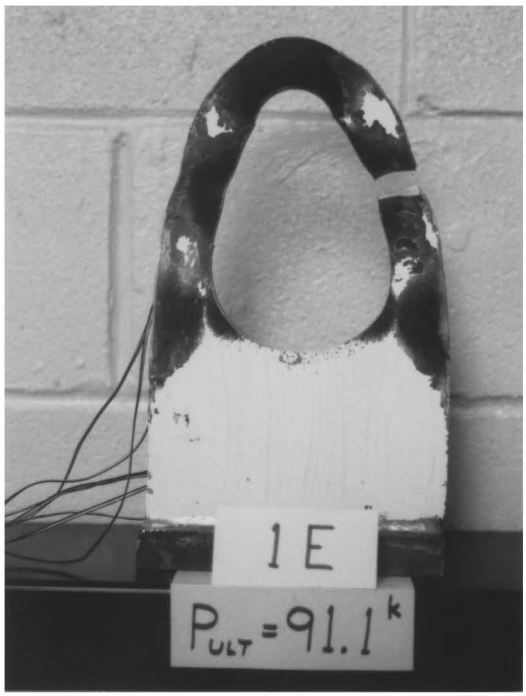

Fig. A33 - Specimen 1-E
After Failure

Table A10

Test Readings of Specimen 1-E

Load in Kips	Pin Deflection in Inches	Strain $(x10^{-3})$, inches/inch					
		Gage #1	Gage #2	Gage #3	Gage #4	Gage #6	Gage #7
0.5	0.122						
2.5	0.170	0.3542	0.0476	0.0554			0.0102
5.0	0.184	0.6904	0.2202	0.2290	0.0319	0.0706	0.0637
7.5	0.193	1.076	0.4155	0.4248	0.0942	0.1584	0.1241
10.0	0.201	1.586	0.6251	0.6344	0.1687	0.2590	0.1854
12.5	0.208	2.157	0.8392	0.8491	0.2467	0.3630	0.2462
15.0	0.216	2.807	1.059	1.067	0.3257	0.4661	0.3080
17.5	0.223	3.572	1.291	1.296	0.4078	0.5702	0.3709
20.0	0.231	4.484	1.532	1.536	0.4875	0.6711	0.4313
22.5	0.238	5.579	1.780	1.785	0.5657	0.7679	0.4887
25.0	0.246	6.850	2.034	2.039	0.6413	0.8607	0.5429
27.5	0.255	8.312	2.297	2.304	0.7159	0.9516	0.5972
30.0	0.263	9.999	2.572	2.588	0.7912	1.049	0.6512
32.5	0.272	11.88	2.831	2.868	0.8621	1.145	0.7116
35.0	0.282	14.22	3.076	3.144	0.9349	1.250	0.7971
37.5	0.293	17.46	3.297	3.401	1.008	1.359	0.9184
40.0	0.306	22.22	3.485	3.632	1.082	1.483	1.097
42.5	0.320	28.44	3.633	3.826	1.159	1.612	1.349
45.0	0.338	36.00	3.734	3.977	1.237	1.746	1.717
47.5	0.359		3.785	4.074	1.316	1.884	2.215
50.0	0.386		3.793	4.121	1.396	2.028	2.859
52.5	0.416		3.785	4.138	1.483	2.168	3.617
55.0	0.455		3.786	4.143	1.566	2.302	4.630
57.5	0.502		3.846	4.176	1.639	2.423	5.973
60.0	0.557		3.967	4.254	1.691	2.529	7.381

Table A10 (con't.)

Test Readings of Specimen 1-E

Load in Kips	Pin Deflection in Inches	Strain $(x10^{-3})$, inches/inch					
		Gage #1	Gage #2	Gage #3	Gage #4	Gage #6	Gage #7
62.5	0.617		4.116	4.377	1.734	2.616	8.617
65.0	0.683		4.270	4.547	1.773	2.688	9.522
67.5	0.748		4.428	4.783	1.811	2.749	10.03
70.0	0.818		4.627	5.150	1.846	2.803	10.27
72.5	0.892		4.910	5.653	1.879	2.856	10.34
75.0	0.968		5.293	6.266	1.907	2.907	10.32
77.5	1.042		5.742	6.930	1.937	2.956	10.27
80.0	1.120		6.299	7.702	1.965	3.000	10.20
82.5			6.883	8.478	1.992	3.042	10.11
85.0			7.443	9.224	2.016	3.081	10.01
87.5			7.883	9.901	2.039	3.120	9.905
90.0			8.132	10.45	2.060	3.155	9.808
91.0			8.101	10.59	2.062	3.166	9.766

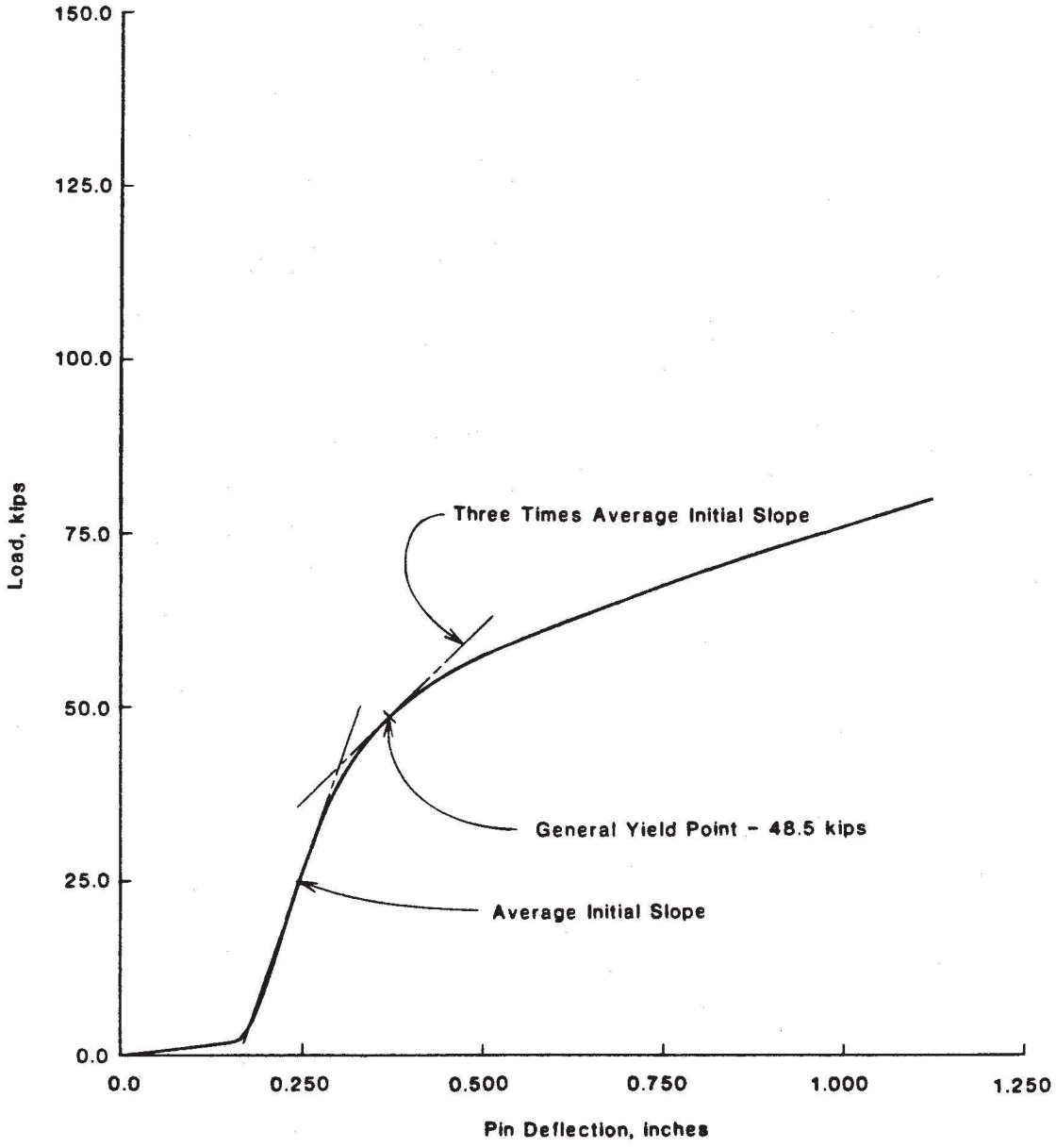

Fig. A34 - Load vs. Pin Deflection - Specimen 1-E

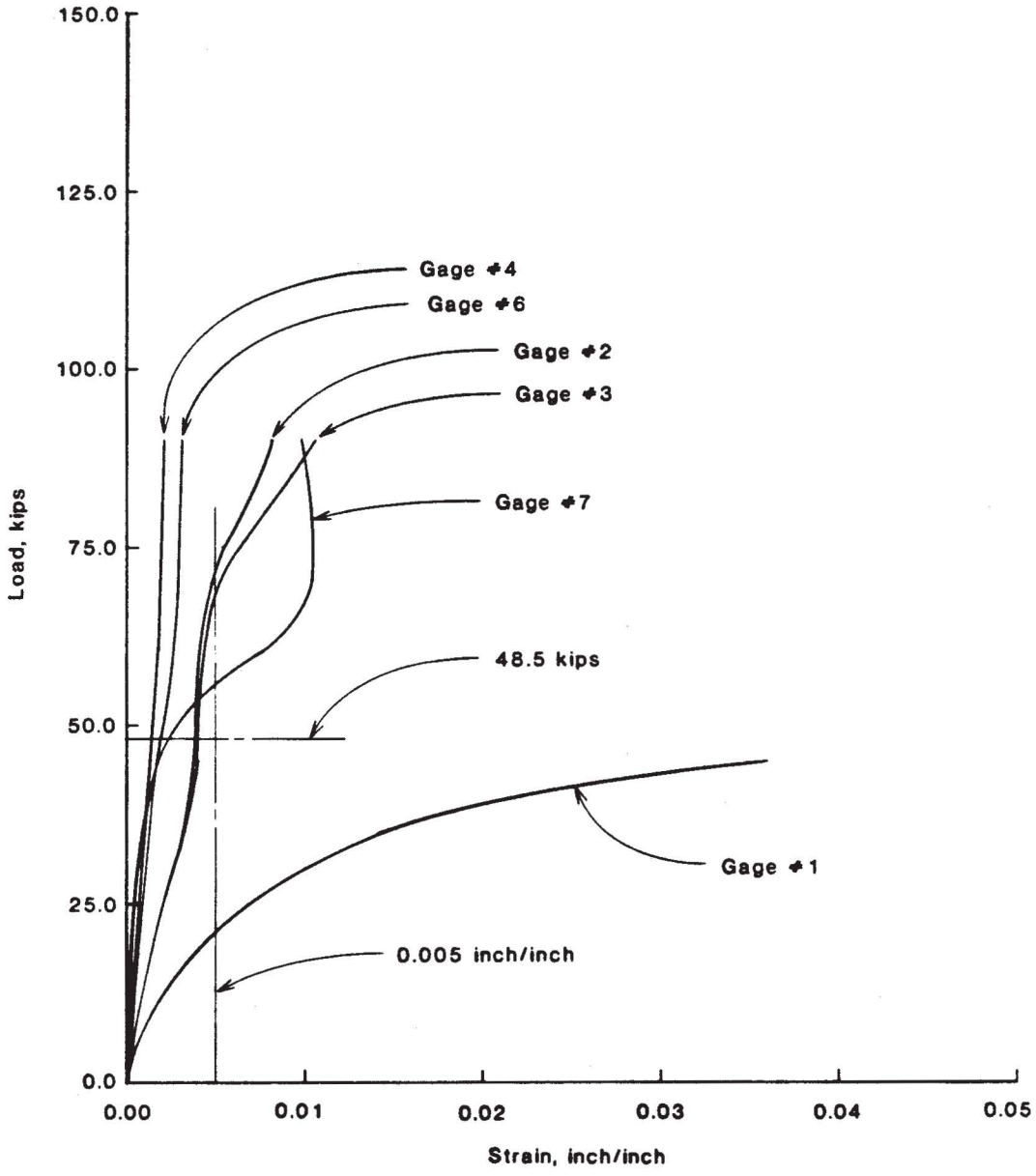

Fig. A35 - Load vs. Strain - Specimen 1-E

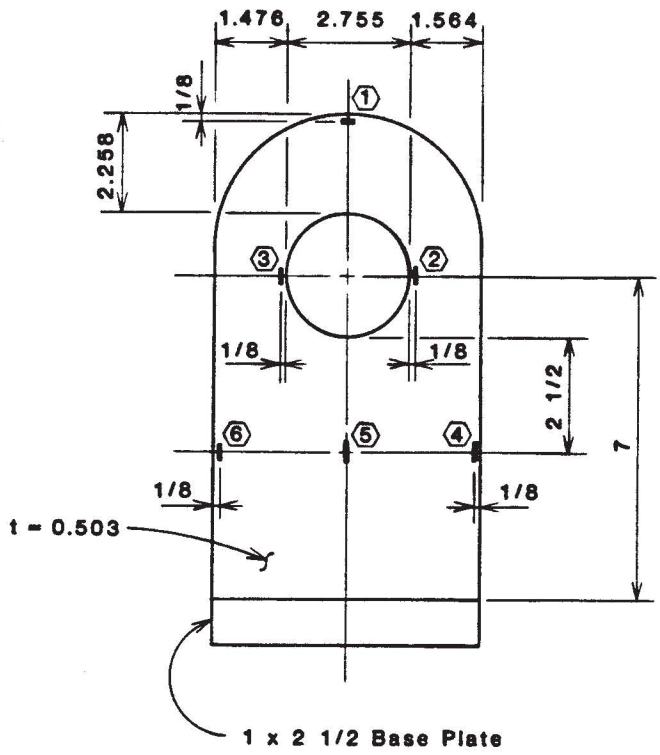

Notes:

▮ indicates strain gage

Dimensions are in inches. 1 in = 25.4 mm

Fig. A36 - As-built Dimensions of Specimen 2-A

Table A11

Summary of Results of Test 2-A

Item	Value
D_h/D_p	1.00
Yield Load, kips	74.6
Failure Load, kips	123.6
Location of Failure	Side

Note: 1 kip = 4.45 kN

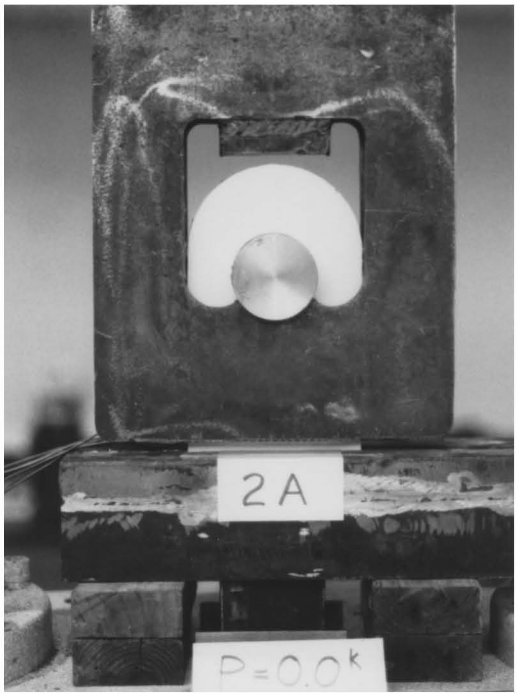

Fig. A37 - Specimen 2-A
at 0.0 kips

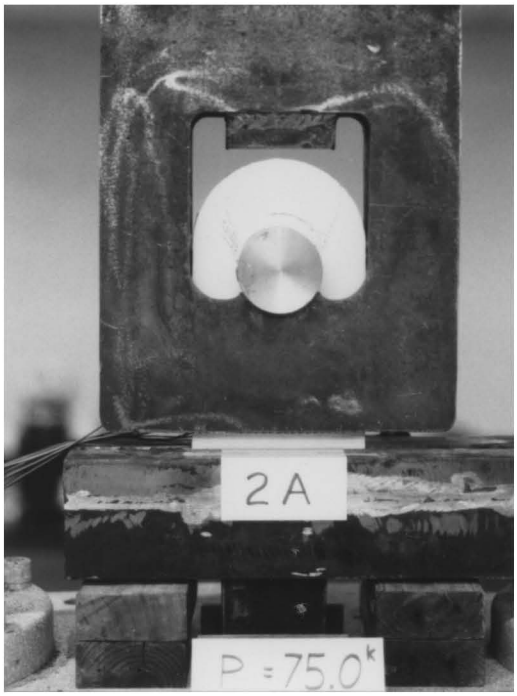

Fig. A38 - Specimen 2-A
at 75.0 kips

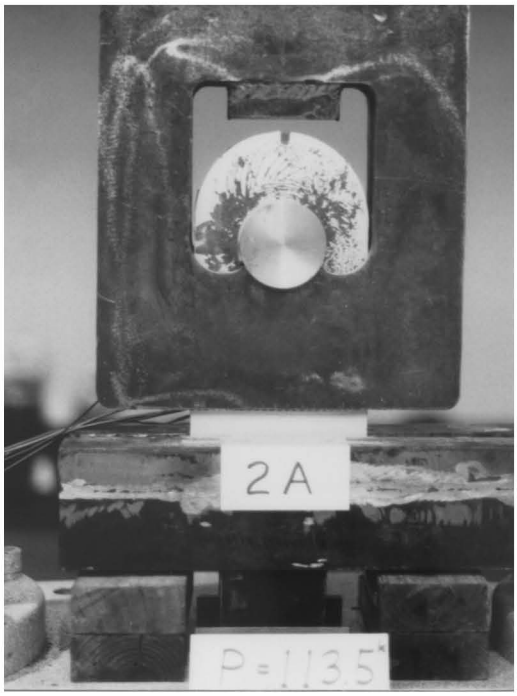

Fig. A39 - Specimen 2-A
at 113.5 kips

Fig. A40 - Specimen 2-A
After Failure

Table A12

Test Readings of Specimen 2-A

Load in Kips	Pin Deflection in Inches	Strain $(x10^{-3})$, inches/inch					
		Gage #1	Gage #2	Gage #3	Gage #4	Gage #5	Gage #6
1.0	0.197						
2.5	0.210	0.0524	0.1268	0.1444	0.1527	0.1214	0.1684
5.0	0.213	0.1097	0.3129	0.3496	0.2668	0.2056	0.2967
7.5	0.217	0.1645	0.4907	0.5426	0.3511	0.2648	0.3937
10.0	0.222	0.2233	0.6725	0.7342	0.4275	0.3167	0.4829
12.5	0.225	0.2527	0.8397	0.9083	0.4838	0.3510	0.5510
15.0	0.229	0.2910	1.009	1.083	0.5403	0.3863	0.6188
17.5	0.232	0.3379	1.177	1.253	0.5951	0.4206	0.6854
20.0	0.235	0.3776	1.345	1.416	0.6500	0.4534	0.7643
22.5	0.239	0.4141	1.511	1.575	0.7017	0.4829	0.8422
25.0	0.242	0.4740	1.674	1.728	0.7499	0.5100	0.9121
27.5	0.245	0.5521	1.834	1.879	0.7943	0.5351	0.9664
30.0	0.248	0.6235	1.993	2.029	0.8357	0.5592	1.028
32.5	0.251	0.6721	2.155	2.181	0.8765	0.5838	1.088
35.0	0.254	0.7178	2.315	2.330	0.9149	0.6078	1.151
37.5	0.257	0.7722	2.477	2.477	0.9506	0.6318	1.209
40.0	0.260	0.8378	2.641	2.624	0.9515	0.6563	1.263
42.5	0.263	0.9103	2.801	2.769	0.9724	0.6807	1.291
45.0	0.265	1.001	2.963	2.916	0.9978	0.7057	1.323
47.5	0.268	1.149	3.125	3.068	1.009	0.7306	1.353
50.0	0.270	1.291	3.285	3.215	1.026	0.7546	1.386
52.5	0.273	1.362	3.436	3.364	1.045	0.7792	1.404
55.0	0.275	1.458	3.580	3.547	1.071	0.8028	1.433
57.5	0.278	1.555	3.838	3.734	1.210	0.8253	1.467
60.0	0.281	1.619	4.223	3.949	1.273	0.8471	1.502

Table A12 (con't.)

Test Readings of Specimen 2-A

Load in Kips	Pin Deflection in Inches	Strain $(x10^{-3})$, inches/inch					
		Gage #1	Gage #2	Gage #3	Gage #4	Gage #5	Gage #6
62.5	0.283	1.701	4.572	4.246	1.301	0.8683	1.536
65.0	0.286	1.784	4.994	4.437	1.317	0.8881	1.568
67.5	0.289	1.868	5.422	4.728	1.335	0.9062	1.596
70.0	0.293	1.983	5.801	5.379	1.345	0.9209	1.621
72.5	0.296	2.115	6.105	5.806	1.360	0.9299	1.644
75.0	0.304	2.266	6.514	7.534	1.354	0.9256	1.643
77.5	0.320	2.665	10.93	18.64	1.343	0.9097	1.622
80.0	0.335	3.058		27.14	1.362	0.9270	1.629
82.5	0.349	3.926		31.94	1.362	0.9420	1.650
85.0	0.363	4.614		37.06	1.356	0.9723	1.675
87.5	0.380	6.412		42.22	1.380	1.001	1.705
90.0	0.397	9.189		45.59	1.397	1.024	1.741
92.5	0.418	11.23			1.399	1.046	1.777
95.0	0.438	13.22			1.400	1.068	1.809
97.5	0.458	14.79			1.405	1.089	1.831
100.0	0.481	16.36			1.412	1.110	1.844
102.5		17.99			1.446	1.128	1.872
105.0		20.04			1.538	1.145	1.917
107.5		22.08			1.576	1.161	1.948
110.0		24.41			1.594	1.176	1.949
112.5		27.36			1.636	1.187	1.958
115.0		30.76			1.714	1.198	2.072
120.0					5.492	1.216	4.836
122.5					8.663	1.211	7.337

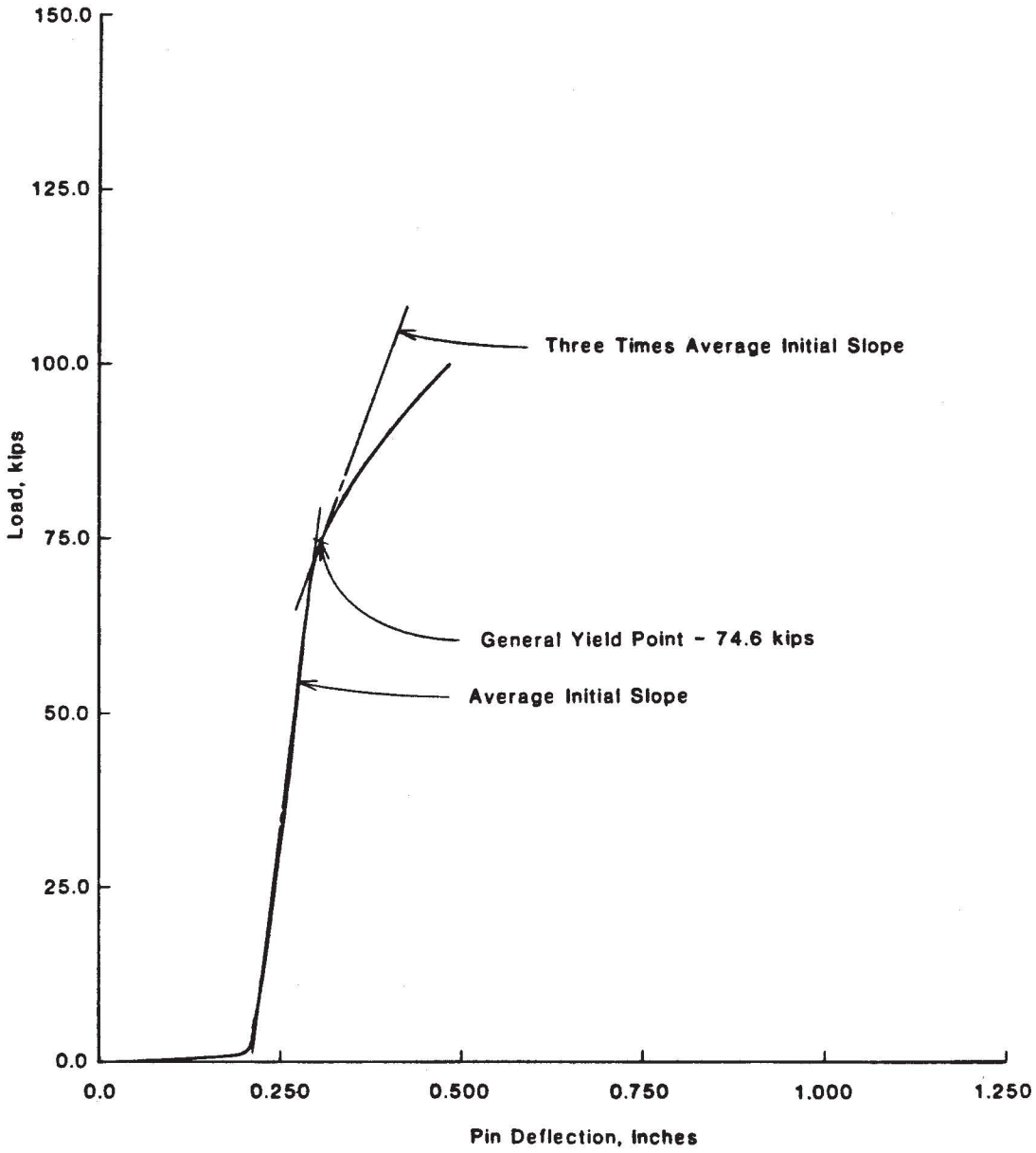

Fig. A41 - Load vs. Pin Deflection - Specimen 2-A

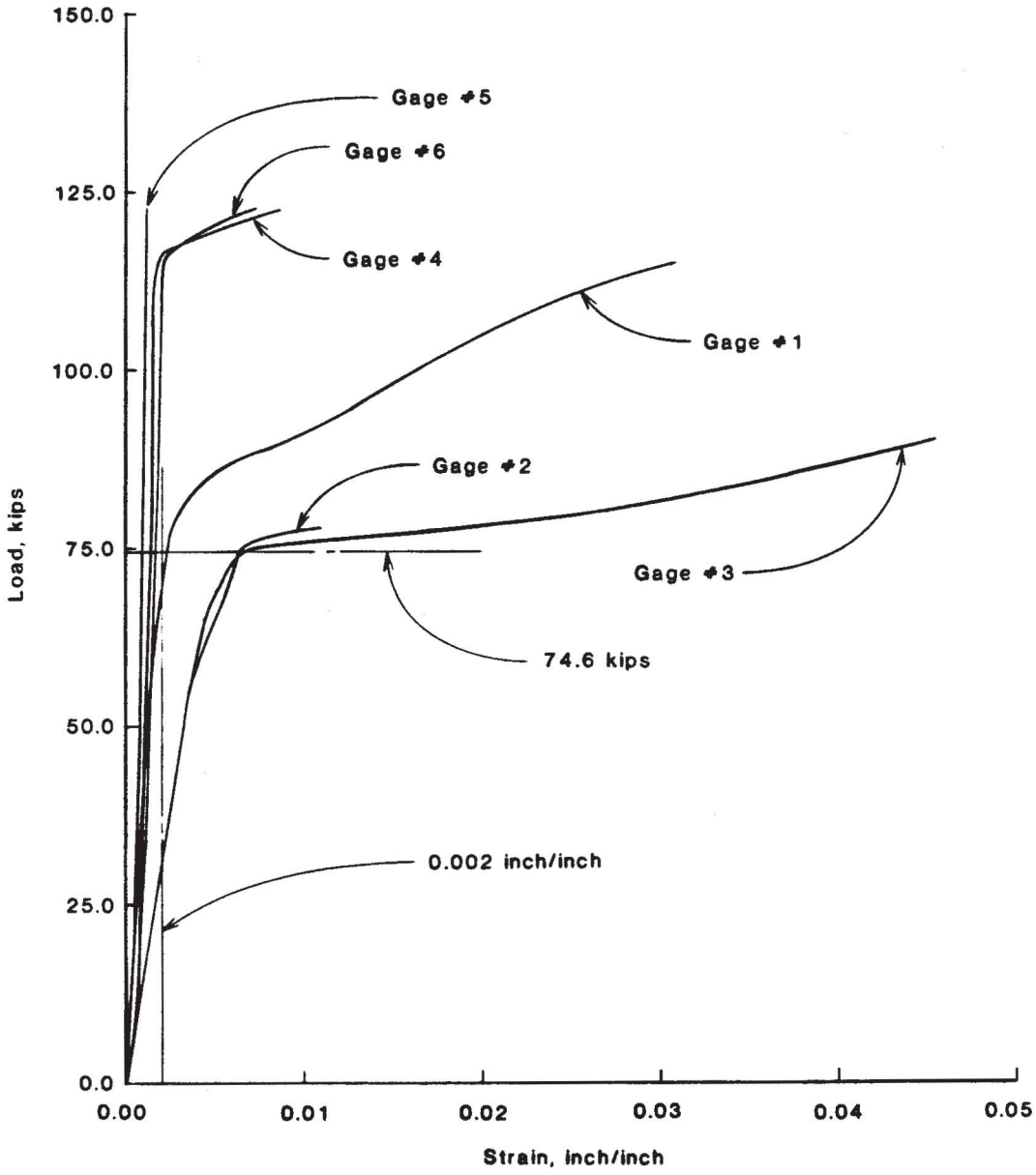

Fig. A42 - Load vs. Strain - Specimen 2-A

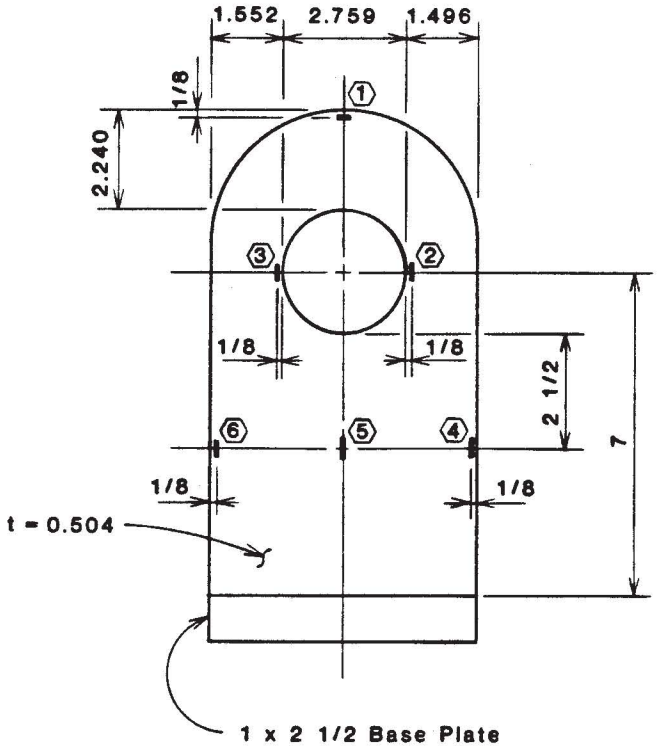

Notes:

| indicates strain gage

Dimensions are in inches. 1 in = 25.4 mm

Fig. A43 - As-built Dimensions of Specimen 2-B

Table A13

Summary of Results of Test 2-B

Item	Value
D_h/D_p	1.71
Yield Load, kips	59.3
Failure Load, kips	115.2
Location of Failure	Dishing

Note: 1 kip = 4.45 kN

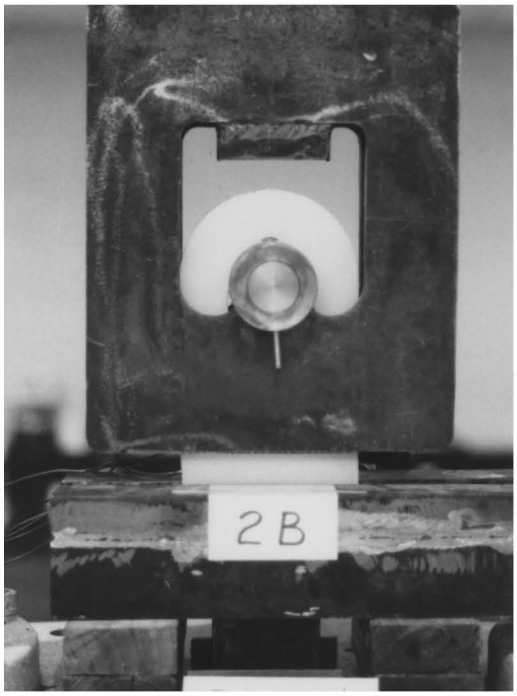

Fig. A44 - Specimen 2-B
at 0.0 kips

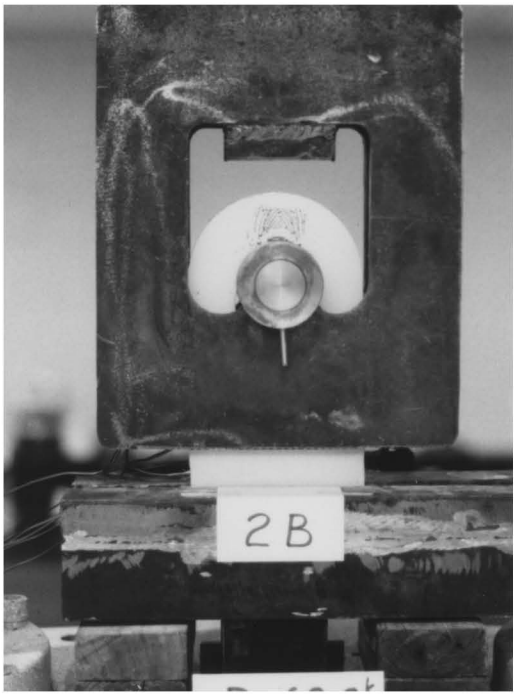

Fig. A45 - Specimen 2-B
at 60.0 kips

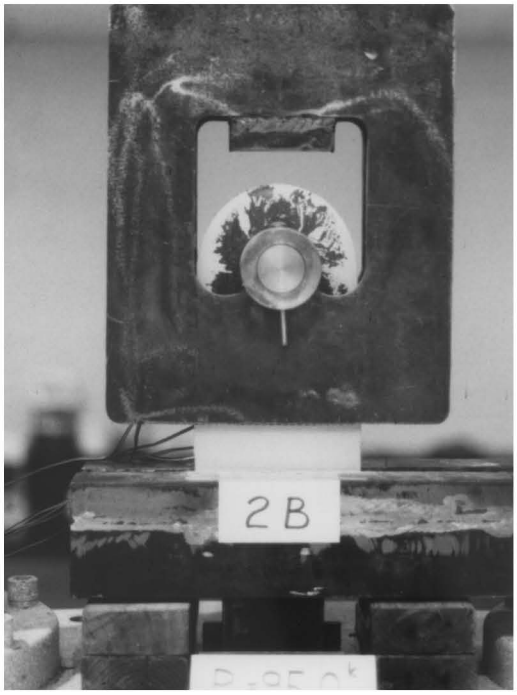

Fig. A46 - Specimen 2-B
at 95.0 kips

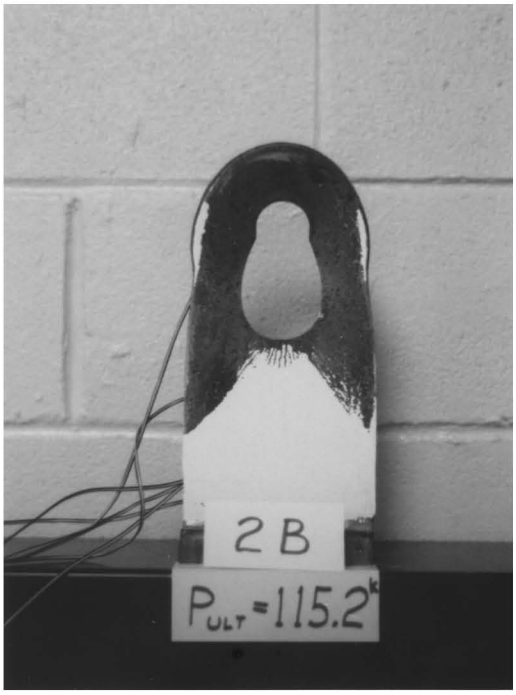

Fig. A47 - Specimen 2-B
After Failure

Table A14

Test Readings of Specimen 2-B

Load in Kips	Pin Deflection in Inches	Strain $(x10^{-3})$, inches/inch					
		Gage #1	Gage #2	Gage #3	Gage #4	Gage #5	Gage #6
1.0	0.164						
2.5	0.173	0.0459	0.2810	0.2801	0.2053	0.1637	0.2102
5.0	0.180	0.1021	0.4952	0.4923	0.3686	0.2889	0.3730
7.5	0.184	0.1696	0.6591	0.6542	0.4801	0.3666	0.4864
10.0	0.187	0.2463	0.7761	0.7702	0.5358	0.3930	0.5476
12.5	0.191	0.3250	0.9019	0.8955	0.5882	0.4141	0.6058
15.0	0.195	0.4023	1.030	1.026	0.6376	0.4331	0.6611
17.5	0.199	0.4815	1.164	1.162	0.6929	0.4561	0.7198
20.0	0.204	0.5632	1.301	1.303	0.7477	0.4781	0.7771
22.5	0.209	0.6459	1.440	1.446	0.8025	0.5001	0.8333
25.0	0.214	0.7409	1.581	1.591	0.8544	0.5222	0.9225
27.5	0.220	0.8843	1.733	1.748	0.9034	0.5442	1.023
30.0	0.226	1.070	1.875	1.894	0.9440	0.5632	1.075
32.5	0.232	1.185	2.029	2.054	0.9817	0.5853	1.151
35.0	0.239	1.296	2.192	2.223	1.014	0.6063	1.245
37.5	0.245	1.431	2.352	2.390	1.038	0.6268	1.312
40.0	0.252	1.655	2.523	2.570	1.056	0.6484	1.396
42.5	0.259	1.906	2.686	2.758	1.077	0.6714	1.468
45.0	0.266	2.173	2.841	2.903	1.090	0.6890	1.526
47.5	0.274	2.553	2.950	3.074	1.107	0.7071	1.574
50.0	0.283	4.446	3.153	3.190	1.123	0.7194	1.633
52.5	0.294	7.740	3.710	3.623	1.141	0.7291	1.708
55.0	0.306	9.662	4.584	4.234	1.194	0.7404	1.751
57.5	0.319		6.302	5.292	1.265	0.7448	1.804
60.0	0.335		11.23	9.191	1.304	0.7458	1.852

Table A14 (con't.)

Test Readings of Specimen 2-B

Load in Kips	Pin Deflection in Inches	Strain $(x10^{-3})$, inches/inch					
		Gage #1	Gage #2	Gage #3	Gage #4	Gage #5	Gage #6
62.5	0.355		17.41	14.56	1.309	0.7561	1.889
65.0	0.377		25.34	19.88	1.308	0.7727	1.913
67.5	0.402		30.15		1.328	0.7894	1.932
70.0	0.424		34.30		1.336	0.8021	1.958
72.5	0.447		38.84		1.337	0.8133	1.981
75.0	0.474		43.25		1.333	0.8236	1.995
77.5	0.500		49.41		1.325	0.8382	2.010
80.0	0.526		53.37		1.319	0.8465	2.028
82.5	0.554		59.27		1.320	0.8578	2.057
85.0	0.583		65.40		1.324	0.8681	2.092
87.5	0.612				1.338	0.8786	2.093
90.0	0.644				1.376	0.8888	2.079
92.5					1.446	0.8982	2.095
95.0					1.655	0.9085	2.151
97.5					2.885	0.9188	2.324
100.0					5.466	0.9310	3.090
105.0					9.507	0.9540	8.028
107.5					11.75	0.9648	11.27
110.0					13.49	0.9658	13.52
115.0					15.76	0.8943	16.30

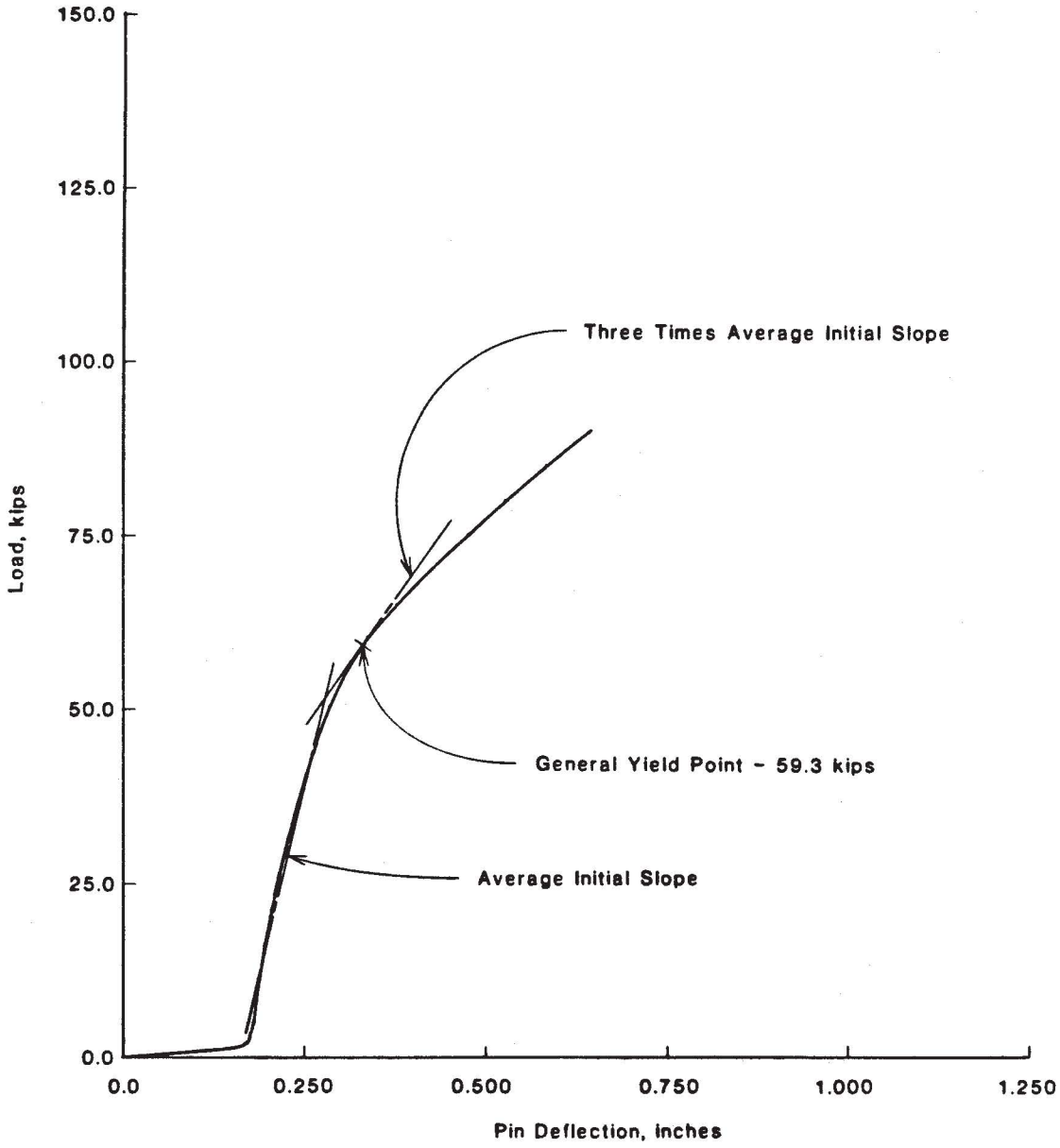

Fig. A48 - Load vs. Pin Deflection - Specimen 2-B

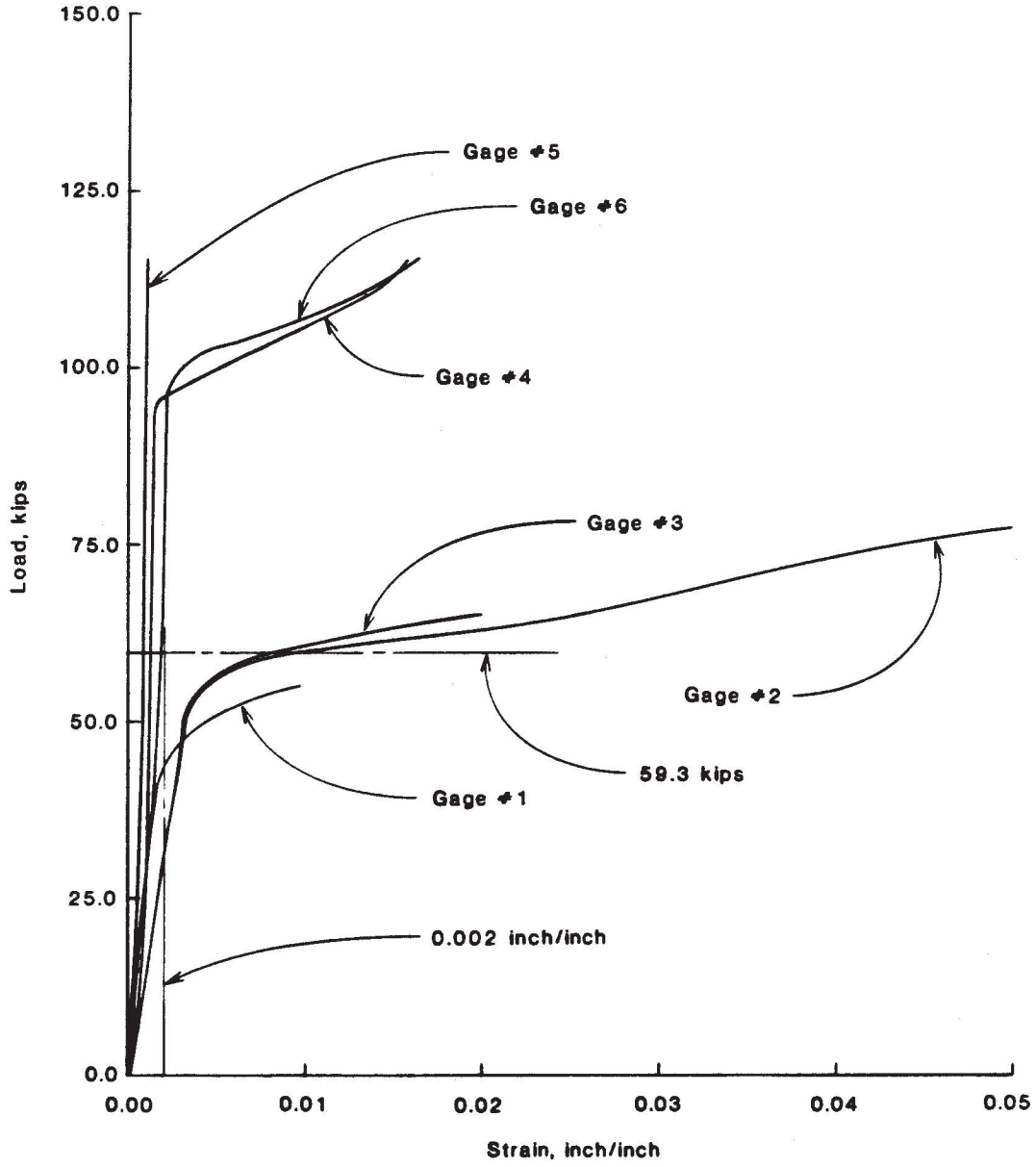

Fig. A49 - Load vs. Strain - Specimen 2-B

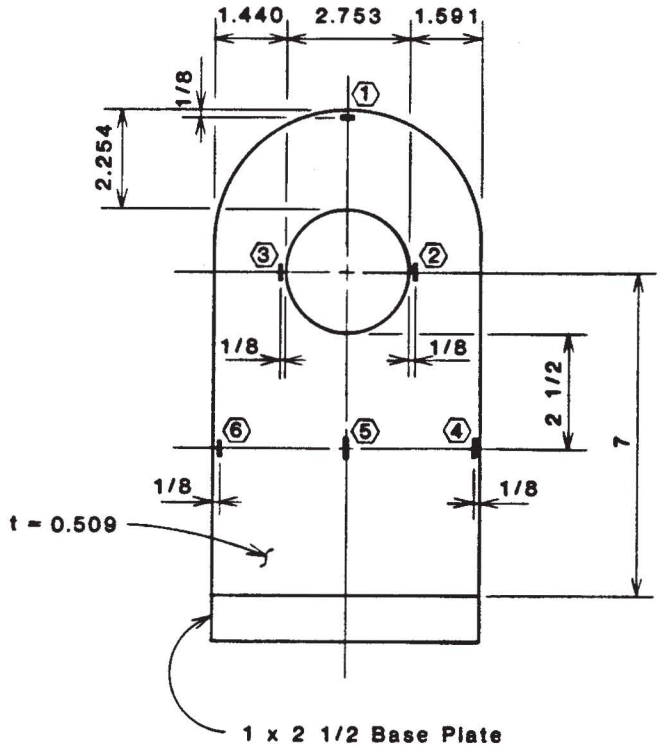

Notes:

▮ indicates strain gage

Dimensions are in inches. 1 in = 25.4 mm

Fig. A50 - As-built Dimensions of Specimen 2-C

Table A15

Summary of Results of Test 2-C

Item	Value
D_h/D_p	2.02
Yield Load, kips	58.6
Failure Load, kips	113.3
Location of Failure	Dishing

Note: 1 kip = 4.45 kN

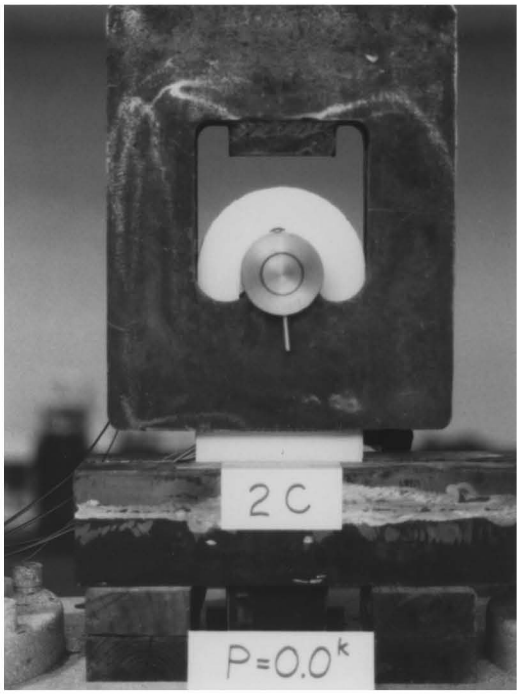

Fig. A51 - Specimen 2-C
at 0.0 kips

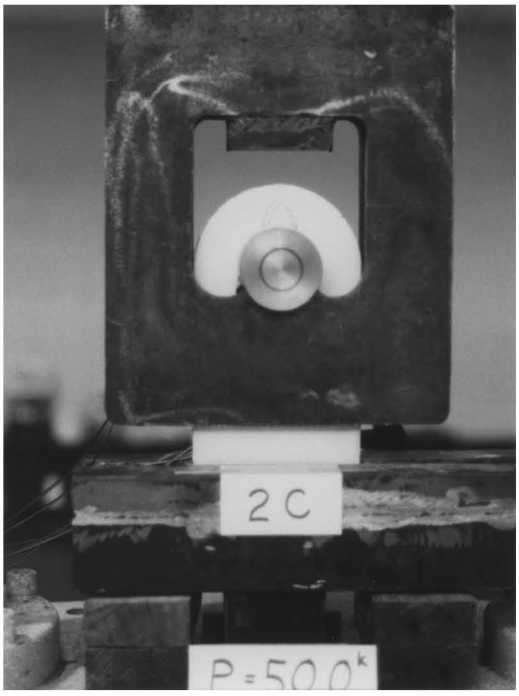

Fig. A52 - Specimen 2-C
at 50.0 kips

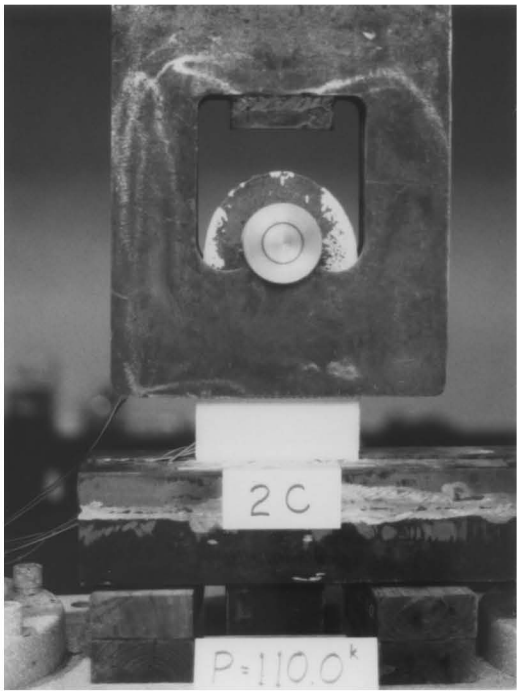

Fig. A53 - Specimen 2-C
at 110.0 kips

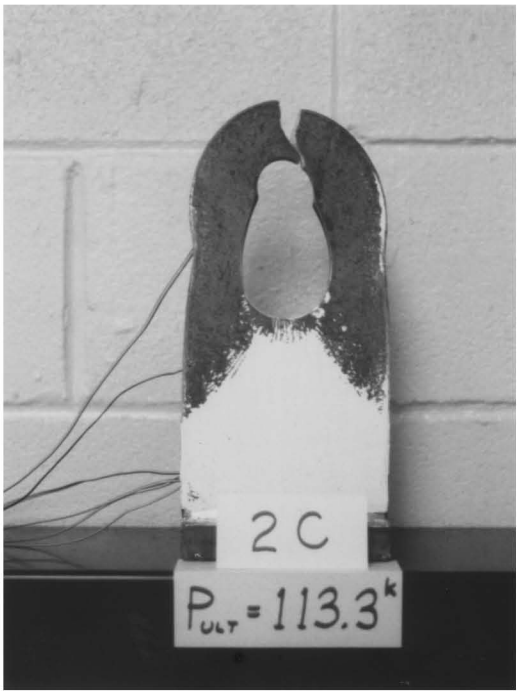

Fig. A54 - Specimen 2-C
After Failure

Table A16

Test Readings of Specimen 2-C

Load in Kips	Pin Deflection in Inches	Strain $(x10^{-3})$, inches/inch					
		Gage #1	Gage #2	Gage #3	Gage #4	Gage #5	Gage #6
1.0	0.219						
2.5	0.228	0.0509	0.2520	0.2598	0.1702	0.1336	0.1805
5.0	0.238	0.1018	0.4757	0.4987	0.3647	0.2931	0.3832
7.5	0.245	0.1561	0.6693	0.6981	0.5323	0.4258	0.5556
10.0	0.251	0.2178	0.8335	0.8575	0.6573	0.5174	0.6836
12.5	0.256	0.2825	1.015	1.032	0.7771	0.6032	0.8048
15.0	0.260	0.3462	1.190	1.200	0.8866	0.6798	0.8951
17.5	0.264	0.4236	1.371	1.370	0.9844	0.7465	0.9433
20.0	0.269	0.5188	1.564	1.550	1.095	0.8015	1.050
22.5	0.275	0.6085	1.720	1.694	1.196	0.8378	1.109
25.0	0.282	0.7146	1.898	1.856	1.336	0.8767	1.186
27.5	0.288	0.8329	2.080	2.019	1.467	0.9131	1.262
30.0	0.296	0.9587	2.266	2.185	1.546	0.9495	1.332
32.5	0.303	1.111	2.455	2.353	1.621	0.9847	1.392
35.0	0.311	1.285	2.652	2.525	1.685	1.019	1.448
37.5	0.319	1.487	2.857	2.705	1.752	1.051	1.502
40.0	0.327	1.706	3.069	2.884	1.799	1.082	1.547
42.5	0.336	1.931	3.267	3.033	1.864	1.112	1.589
45.0	0.345	2.292	3.509	3.515	1.956	1.142	1.630
47.5	0.355	2.952	3.776	4.071	2.040	1.167	1.676
50.0	0.366	5.929	4.358	4.654	2.123	1.189	1.728
52.5	0.380	8.847	5.138	5.419	2.181	1.203	1.768
55.0	0.395	11.60	6.436	6.394	2.264	1.214	1.805
57.5	0.412	14.15	8.674	9.329	2.349	1.217	1.837
60.0	0.433	16.39	11.91	13.94	2.421	1.211	1.865

Table A16 (con't.)

Test Readings of Specimen 2-C

Load in Kips	Pin Deflection in Inches	Strain $(x10^{-3})$, inches/inch					
		Gage #1	Gage #2	Gage #3	Gage #4	Gage #5	Gage #6
62.5	0.456			19.61	2.466	1.210	1.864
65.0	0.483			26.49	2.506	1.209	1.874
67.5	0.512				2.524	1.212	1.882
70.0	0.541				2.549	1.217	1.899
72.5	0.572				2.571	1.220	1.916
75.0	0.603				2.592	1.222	1.930
77.5	0.635				2.612	1.224	1.939
80.0	0.669				2.626	1.225	1.939
82.5	0.704				2.625	1.225	1.940
85.0	0.742				2.633	1.226	1.936
87.5	0.784				2.655	1.226	1.932
90.0	0.821				2.701	1.230	1.937
92.5					2.834	1.228	1.945
95.0					3.718	1.225	2.010
97.5					5.535	1.224	2.417
100.0					6.963	1.227	3.507
102.5					8.351	1.233	5.602
105.0					10.02	1.242	8.192
107.5					11.43	1.256	10.14
110.0					12.83	1.279	11.73
112.5					14.57	1.325	

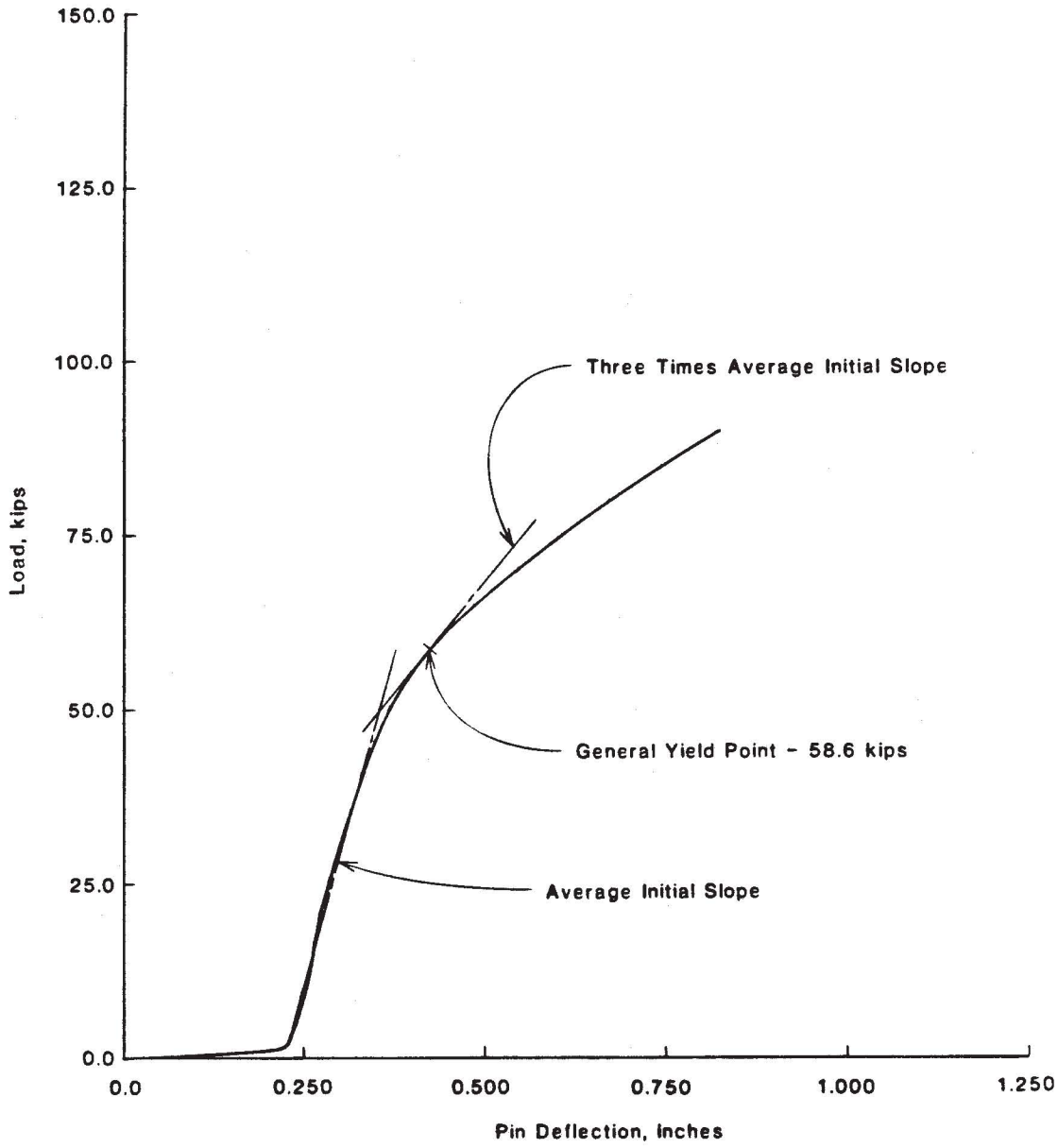

Fig. A55 - Load vs. Pin Deflection - Specimen 2-C

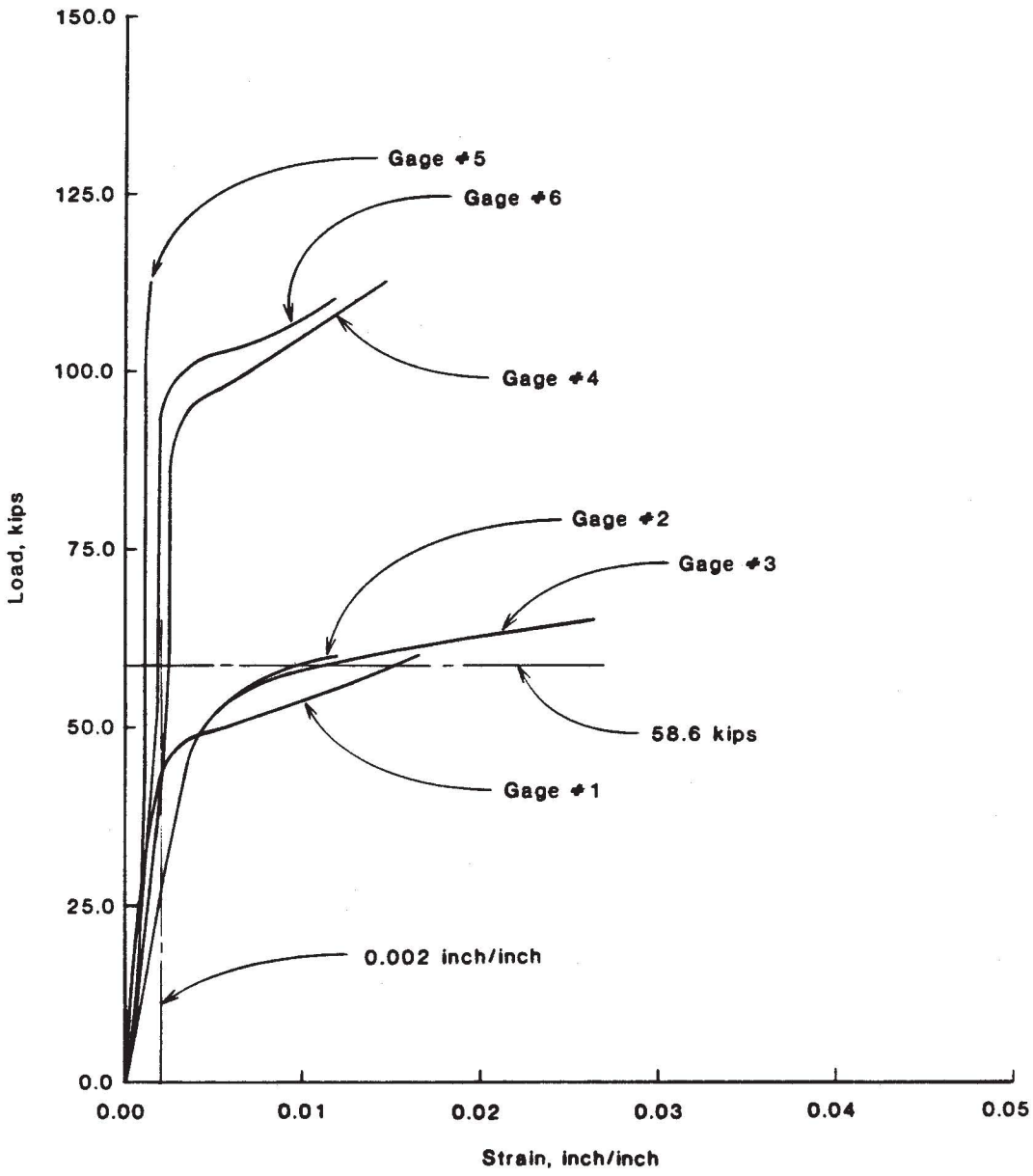

Fig. A56 - Load vs. Strain - Specimen 2-C

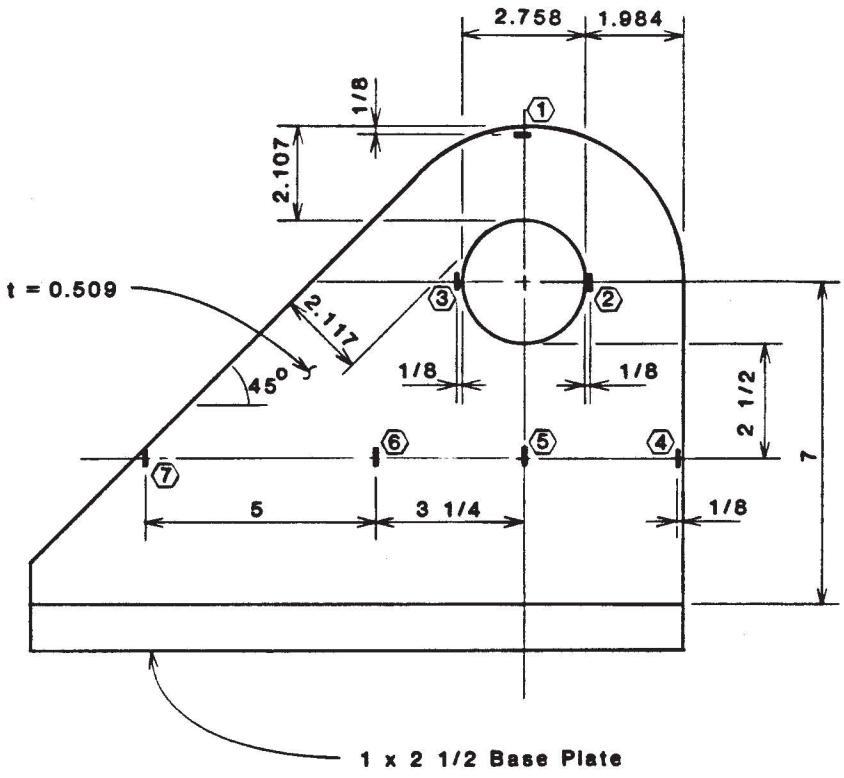

Notes:

▌ indicates strain gage

Dimensions are in inches. 1 in = 25.4 mm

Fig. A57 – As-built Dimensions of Specimen 3-A

Table A17

Summary of Results of Test 3-A

Item	Value
D_h/D_p	1.01
Yield Load, kips	90.0
Failure Load, kips	134.8
Location of Failure	Beyond

Note: 1 kip = 4.45 kN

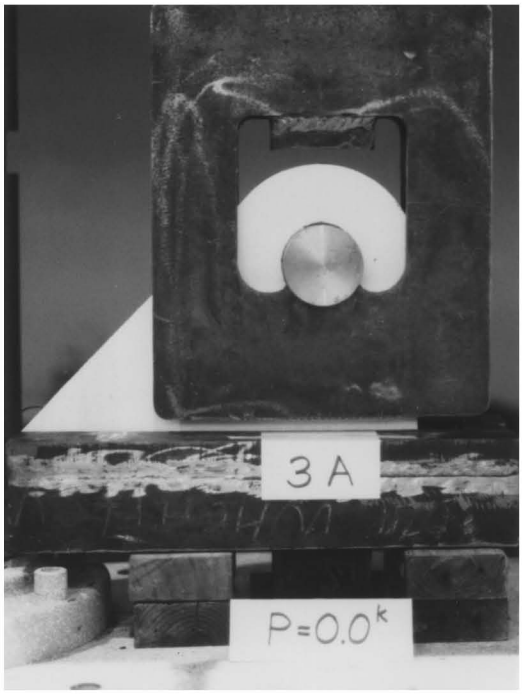

Fig. A58 - Specimen 3-A
at 0.0 kips

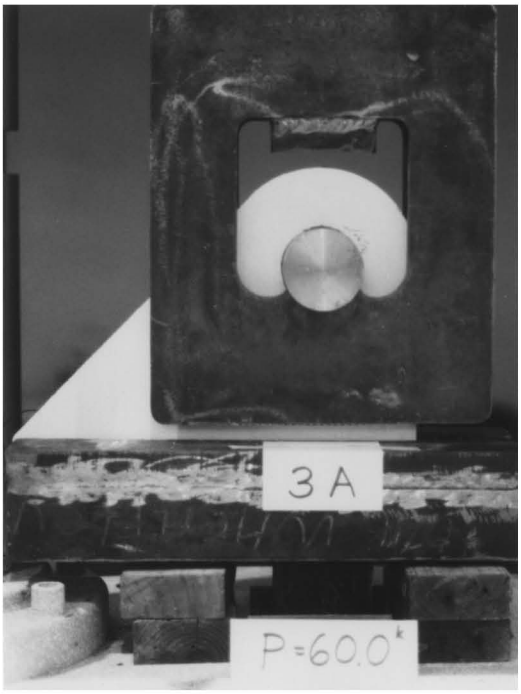

Fig. A59 - Specimen 3-A
at 60.0 kips

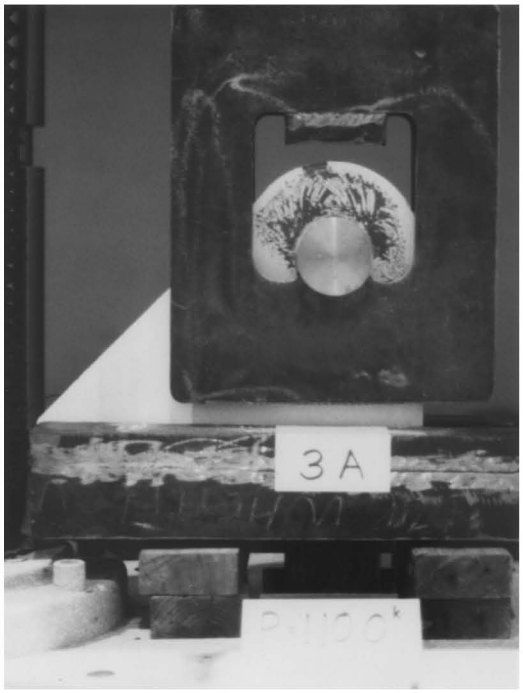

Fig. A60 - Specimen 3-A
at 110.0 kips

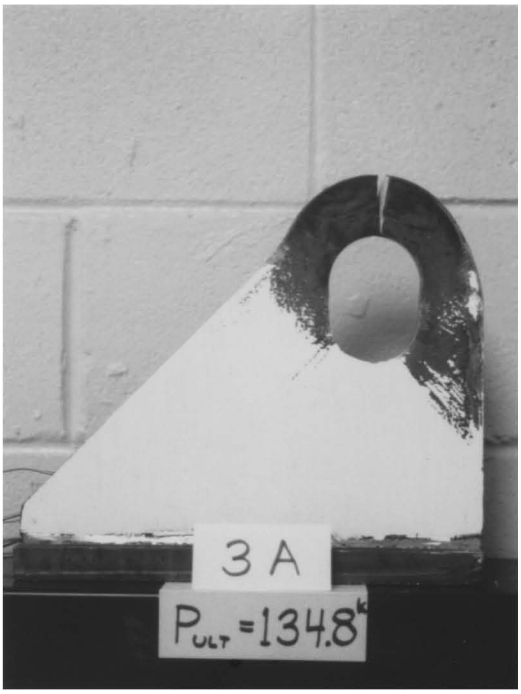

Fig. A61 - Specimen 3-A
After Failure

Table A18

Test Readings of Specimen 3-A

Load in Kips	Pin Deflection in Inches	Strain $(x10^{-3})$, inches/inch						
		Gage #1	Gage #2	Gage #3	Gage #4	Gage #5	Gage #6	Gage #7
1.0	0.049							
2.5	0.055	0.0597	0.1267	0.1321	0.0284	0.0127	0.0313	0.0112
5.0	0.061	0.1160	0.2315	0.2667	0.0533	0.0245	0.0572	0.0181
7.5	0.067	0.1679	0.3289	0.3881	0.0783	0.0342	0.0793	0.0259
10.0	0.072	0.2193	0.4219	0.5003	0.1067	0.0406	0.0935	0.0293
12.5	0.079	0.2722	0.5003	0.5987	0.1292	0.0372	0.0998	0.0298
15.0	0.087	0.3226	0.5796	0.7006	0.1512	0.0352	0.1081	0.0308
17.5	0.093	0.3745	0.6634	0.8075	0.1757	0.0352	0.1174	0.0337
20.0	0.101	0.4147	0.7330	0.8888	0.1957	0.0362	0.1258	0.0357
22.5	0.106	0.4680	0.8379	1.023	0.2295	0.0440	0.1424	0.0391
25.0	0.112	0.5156	0.9291	1.133	0.2589	0.0514	0.1561	0.0426
27.5	0.117	0.5596	1.019	1.240	0.2878	0.0592	0.1708	0.0450
30.0	0.122	0.6057	1.115	1.353	0.3186	0.0695	0.1855	0.0474
32.5	0.127	0.6532	1.213	1.463	0.3504	0.0812	0.2011	0.0504
35.0	0.131	0.7002	1.311	1.572	0.3827	0.0939	0.2158	0.0519
37.5	0.136	0.7526	1.412	1.679	0.4150	0.1057	0.2285	0.0533
40.0	0.141	0.8172	1.516	1.779	0.4405	0.1120	0.2373	0.0528
42.5	0.145	0.8951	1.635	1.874	0.4713	0.1213	0.2476	0.0528
45.0	0.150	0.9974	1.768	1.957	0.5051	0.1321	0.2588	0.0528
47.5	0.154	1.111	1.906	2.031	0.5403	0.1458	0.2720	0.0543
50.0	0.158	1.229	2.020	2.091	0.5721	0.1610	0.2872	0.0563
52.5	0.163	1.349	2.154	2.236	0.6045	0.1781	0.3034	0.0587
55.0	0.166	1.500	2.256	2.356	0.6339	0.1942	0.3200	0.0612
57.5	0.170	1.687	2.351	2.416	0.6637	0.2124	0.3371	0.0641
60.0	0.175	1.980	2.992	2.506	0.6906	0.2305	0.3538	0.0656

Table A18 (con't.)

Test Readings of Specimen 3-A

Load in Kips	Pin Deflection in Inches	Strain $(x10^{-3})$, inches/inch						
		Gage #1	Gage #2	Gage #3	Gage #4	Gage #5	Gage #6	Gage #7
62.5	0.179	2.211	3.285	2.613	0.7284	0.2476	0.3714	0.0680
65.0	0.183	2.548	3.582	2.791	0.7827	0.2652	0.3885	0.0695
67.5	0.188	2.889	3.739	3.071	0.8351	0.2823	0.4066	0.0700
70.0	0.194	3.536	3.773	3.195	0.8713	0.2960	0.4222	0.0685
72.5	0.201	4.701	3.790	3.383	0.8992	0.3087	0.4379	0.0675
75.0	0.210	6.653	3.904	3.523	0.9252	0.3210	0.4516	0.0656
77.5	0.219	10.76	4.135	3.824	0.9546	0.3352	0.4673	0.0641
80.0	0.231	14.20	4.759	4.389	0.9888	0.3537	0.4843	0.0617
82.5	0.245	16.98	6.064	5.331	1.023	0.3733	0.5029	0.0592
85.0	0.256	19.09	7.814	6.858	1.058	0.3943	0.5225	0.0578
87.5	0.270	21.37	9.926	9.480	1.119	0.4163	0.5445	0.0553
90.0	0.284	23.47	12.12	12.18	1.171	0.4296	0.5621	0.0534
92.5	0.300	26.18	14.97	15.30	1.229	0.4438	0.5812	0.0514
95.0	0.313	28.71	17.80	18.11	1.280	0.4589	0.5998	0.0509
97.5	0.331	31.87		21.62	1.324	0.4824	0.6199	0.0489
100.0	0.348	34.98		25.24	1.360	0.5103	0.6414	0.0465
102.5				28.93	1.400	0.5378	0.6635	0.0445
105.0					1.442	0.5636	0.6854	0.0421
107.5					1.488	0.5866	0.7084	0.0406
110.0					1.535	0.6052	0.7299	0.0402
115.0					1.659	0.6444	0.7755	0.0402
117.5					1.770	0.6649	0.7989	0.0402
120.0					1.922	0.6874	0.8224	0.0416
122.5					2.159	0.7035	0.8444	0.0431
125.0					2.562	0.7191	0.8668	0.0451

Table A18 (con't.)

Test Readings of Specimen 3-A

Load in Kips	Pin Deflection in Inches	Strain $(x10^{-3})$, inches/inch						
		Gage #1	Gage #2	Gage #3	Gage #4	Gage #5	Gage #6	Gage #7
127.5					3.836	0.7328	0.8898	0.0490
130.0					6.125	0.7441	0.9133	0.0543
132.5					8.635	0.7490	0.9379	0.0627

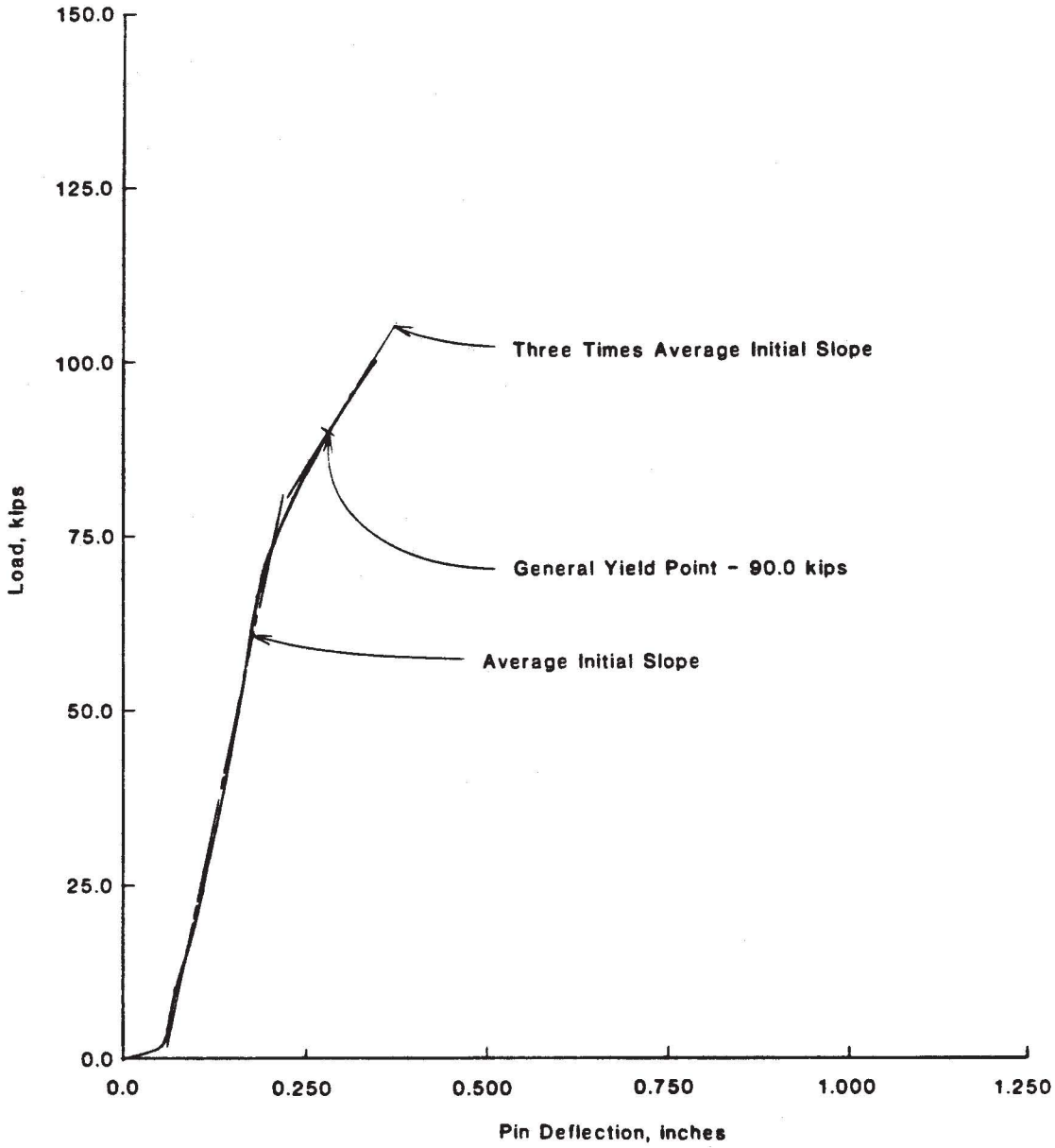

Fig. A62 - Load vs. Pin Deflection - Specimen 3-A

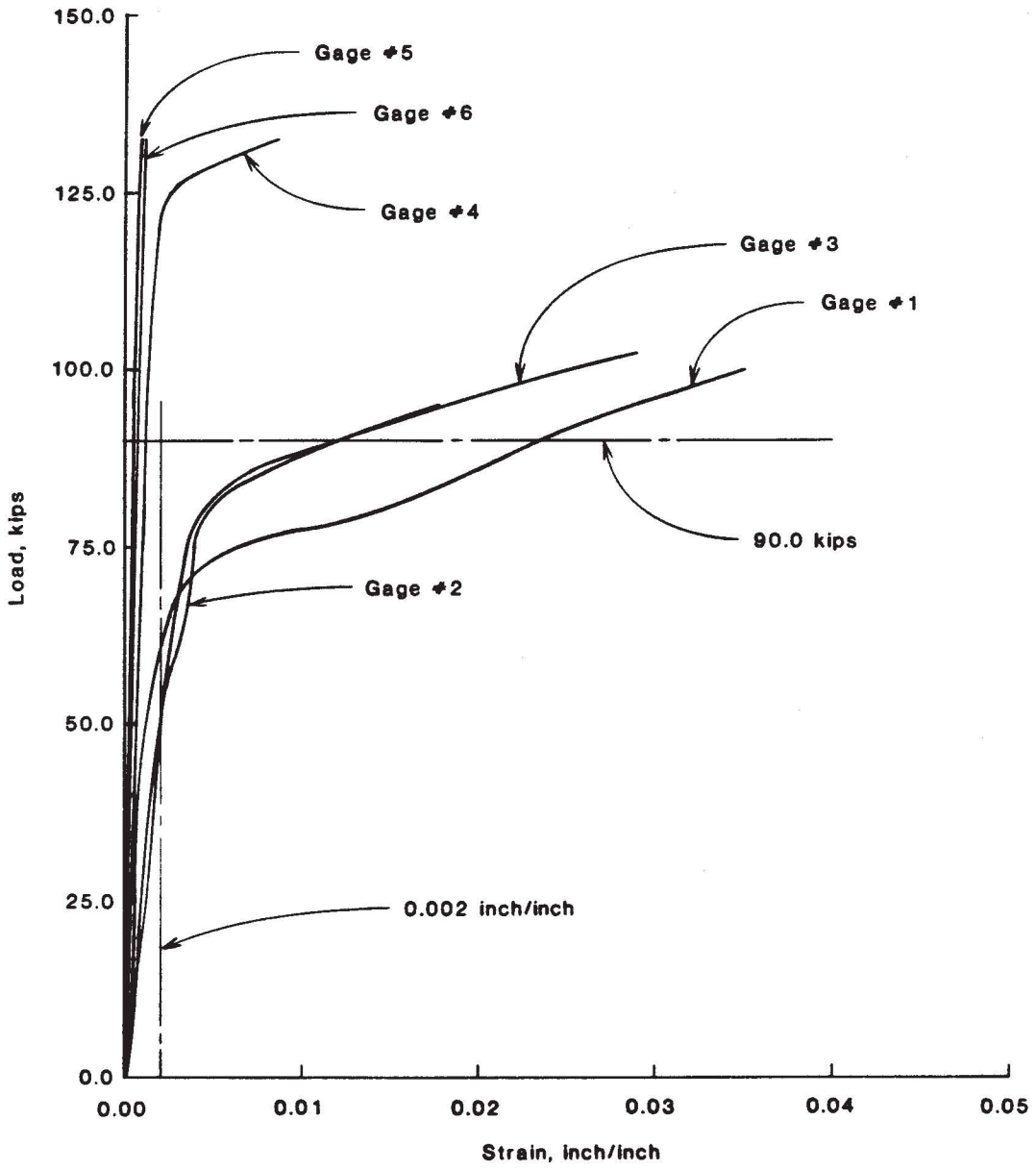

Fig. A63 - Load vs. Strain - Specimen 3-A

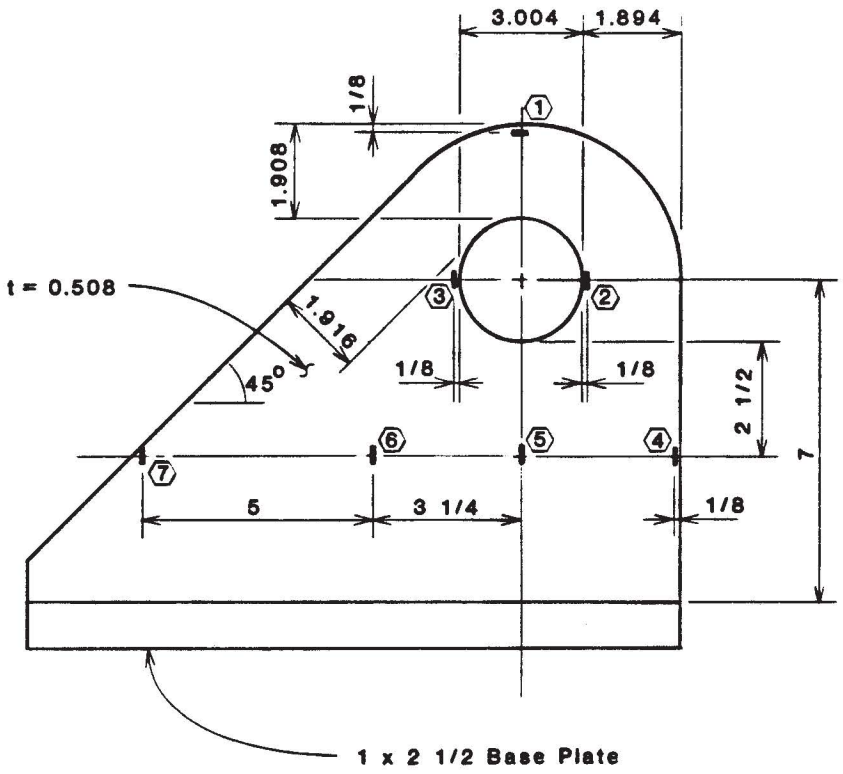

Notes:

▌ indicates strain gage

Dimensions are in inches. 1 in = 25.4 mm

Fig. A64 - As-built Dimensions of Specimen 3-B

Table A19

Summary of Results of Test 3-B

Item	Value
D_h/D_p	1.86
Yield Load, kips	74.5
Failure Load, kips	104.5
Location of Failure	Dishing

Note: 1 kip = 4.45 kN

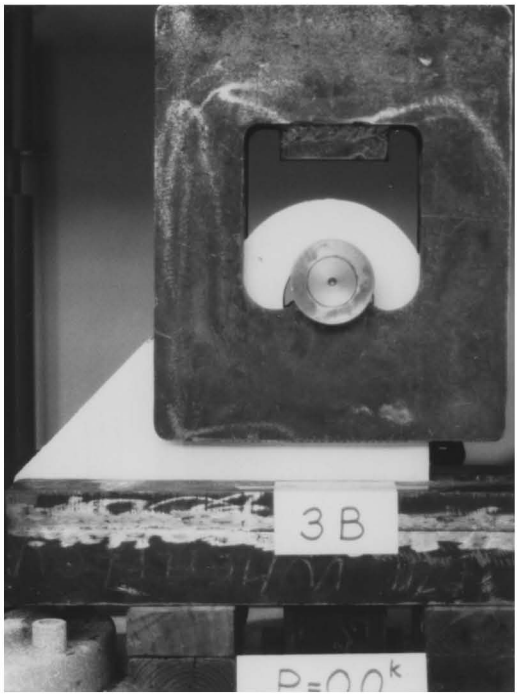

Fig. A65 - Specimen 3-B
at 0.0 kips

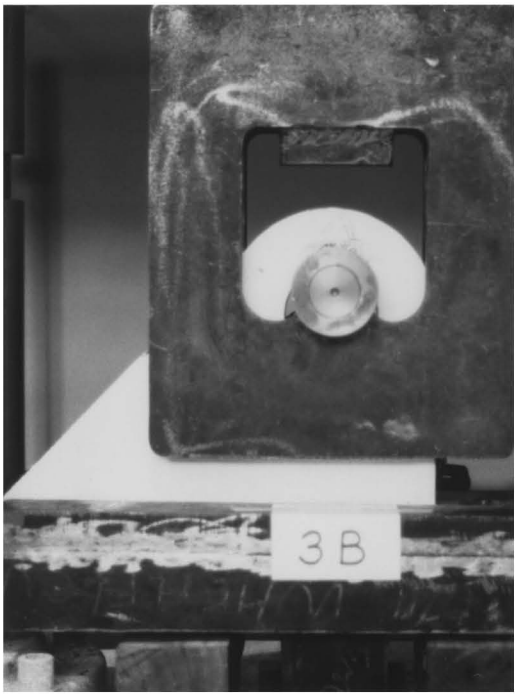

Fig. A66 - Specimen 3-B
at 50.0 kips

Fig. A67 - Specimen 3-B
at 102.5 kips

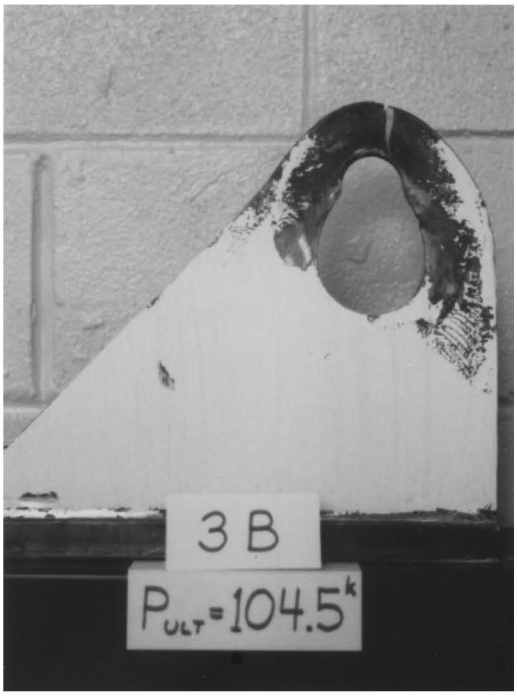

Fig. A68 - Specimen 3-B
After Failure

Table A20

Test Readings of Specimen 3-B

Load in Kips	Pin Deflection in Inches	Strain $(x10^{-3})$, inches/inch				
		Gage #1	Gage #2	Gage #3	Gage #4	Gage #6
1.0	0.145					
2.5	0.176	0.1140	0.1456	0.1234	0.0319	0.0046
5.0	0.197	0.2425	0.2504	0.2079	0.0595	0.0050
7.5	0.210	0.3698	0.3711	0.3052	0.0973	0.0116
10.0	0.221	0.5182	0.8585	0.4271	0.1475	0.0245
12.5	0.232	0.5845	1.143	0.4805	0.1697	0.0299
15.0	0.241	0.6799	1.624	0.5662	0.1965	0.0350
17.5	0.251	0.7959	2.106	0.7029	0.2276	0.0412
20.0	0.260	0.9175	2.503	0.8564	0.2611	0.0489
22.5	0.270	1.056	3.209	1.075	0.2985	0.0583
25.0	0.279	1.218	3.740	1.279	0.3390	0.0676
27.5	0.287	1.393	4.279	1.490	0.3819	0.0785
30.0	0.296	1.588	4.792	1.708	0.4274	0.0902
32.5	0.304	1.806	5.198	1.906	0.4752	0.1018
35.0	0.313	2.043	5.606	2.126	0.5199	0.1135
37.5	0.322	2.301	5.927	2.338	0.5694	0.1255
40.0	0.331	2.582	6.251	2.695	0.6259	0.1384
42.5	0.340	2.882	6.542	2.944	0.6788	0.1523
45.0	0.350	3.619	6.885	3.252	0.7306	0.1667
47.5	0.363	6.348	7.268	3.627	0.7905	0.1850
50.0	0.377	10.03	7.769	3.962	0.8461	0.2009
52.5	0.393	15.75	8.435	4.402	0.9029	0.2180
55.0	0.410	20.07	9.207	5.004	0.9498	0.2359
57.5	0.428	23.86	10.01	5.749	0.9666	0.2531
60.0	0.446	28.05	10.88	6.519	0.9764	0.2706

Table A20 (con't.)

Test Readings of Specimen 3-B

Load in Kips	Pin Deflection in Inches	Strain $(x10^{-3})$, inches/inch				
		Gage #1	Gage #2	Gage #3	Gage #4	Gage #6
62.5	0.466		11.85	7.298	1.004	0.2877
65.0	0.485		12.97	8.196	1.059	0.3055
67.5	0.507		14.76	9.167	1.098	0.3222
70.0	0.531		18.79	10.59	1.139	0.3404
72.5	0.562			12.94	1.164	0.3612
75.0	0.592			15.34	1.202	0.3834
77.5	0.622			17.67	1.243	0.4057
80.0	0.651			20.20	1.280	0.4290
82.5	0.688			22.80	1.306	0.4505
85.0	0.723			25.71	1.322	0.4743
87.5	0.763			28.74	1.331	0.5000
90.0	0.804			31.69	1.377	0.5265
92.5				34.90	1.507	0.5545
95.0				38.09	1.903	0.5838
97.5				41.82	3.357	0.6150
100.0				46.11	5.194	0.6548
102.5				51.83	6.605	0.7039

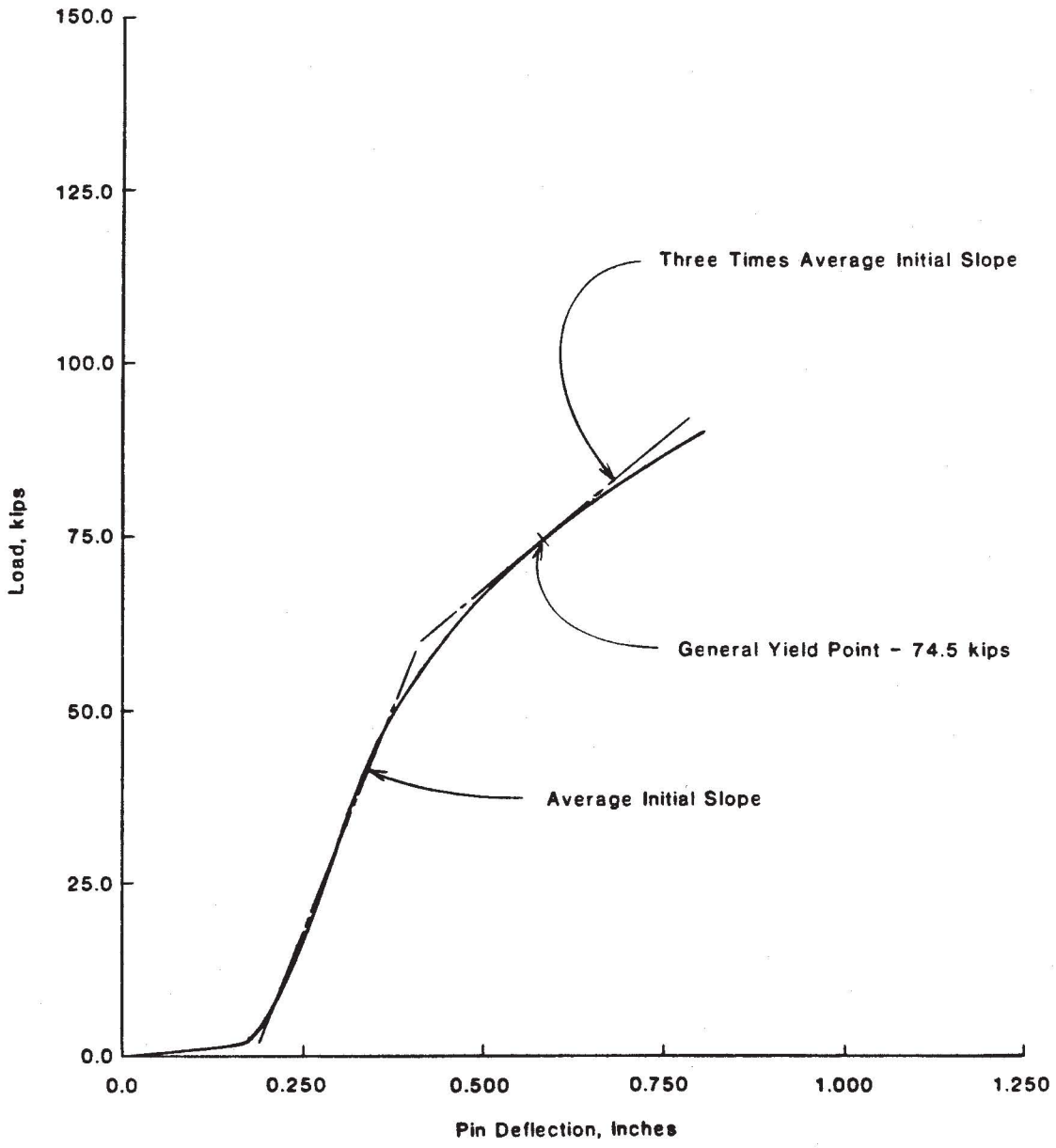

Fig. A69 - Load vs. Pin Deflection - Specimen 3-B

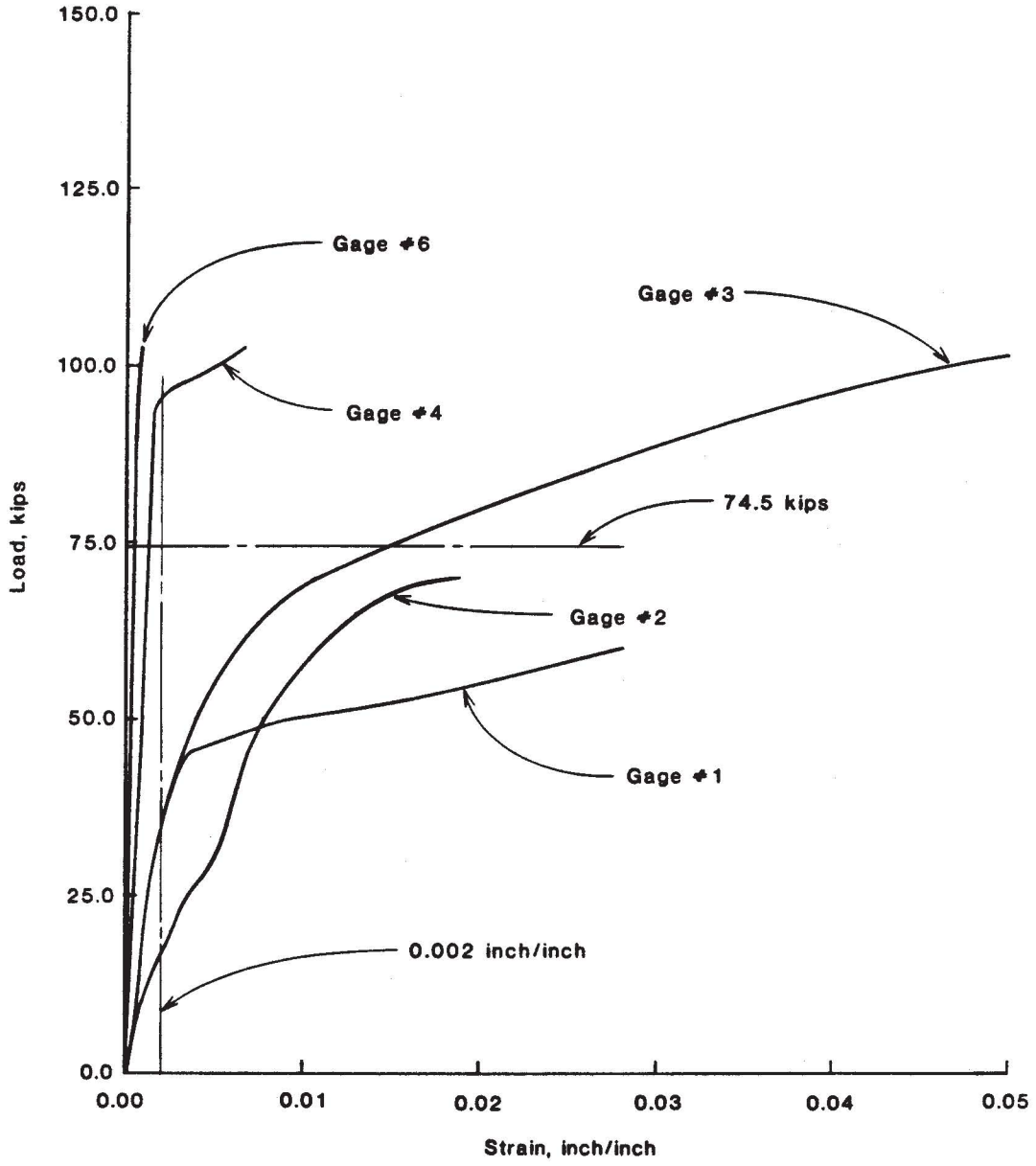

Fig. A70 - Load vs. Strain - Specimen 3-B

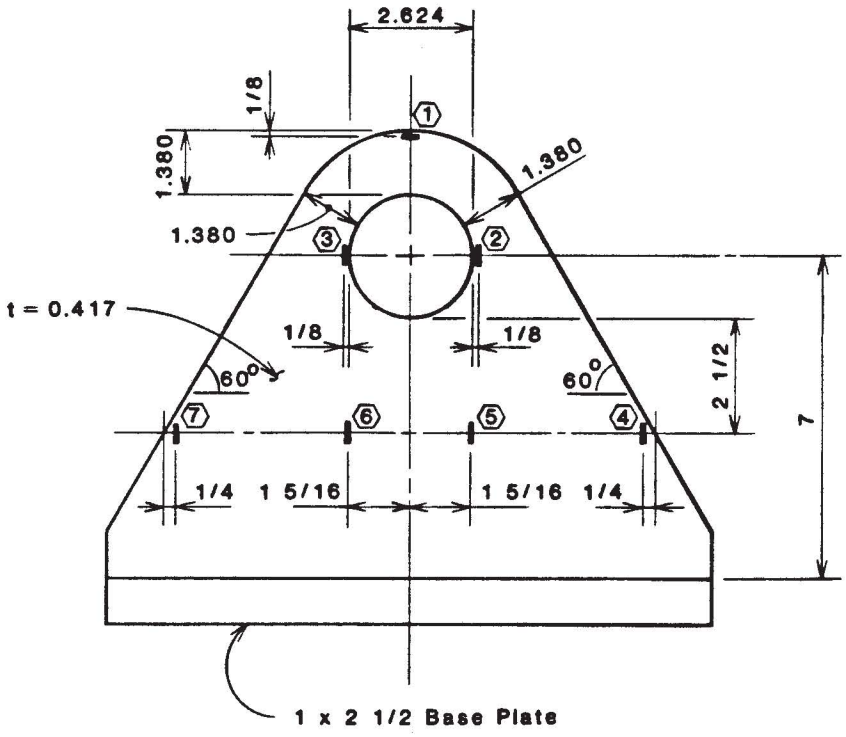

Notes:

▮ indicates strain gage

Dimensions are in inches. 1 in = 25.4 mm

Fig. A71 - As-built Dimensions of Specimen 4-A

Table A21

Summary of Results of Test 4-A

Item	Value
D_h/D_p	1.32
Yield Load, kips	69.6
Failure Load, kips	92.7
Location of Failure	Shear

Note: 1 kip = 4.45 kN

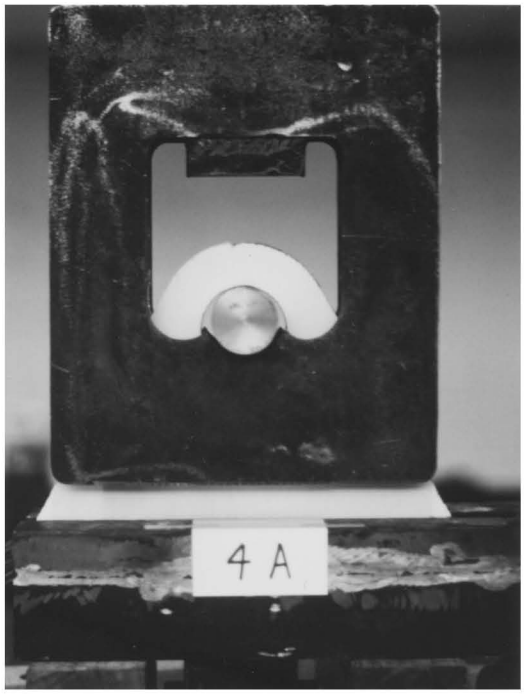

Fig. A72 - Specimen 4-A
at 0.0 kips

Fig. A73 - Specimen 4-A
at 45.0 kips

Fig. A74 - Specimen 4-A
at 80.0 kips

Fig. A75 - Specimen 4-A
After Failure

Table A22

Test Readings of Specimen 4-A

Load in Kips	Pin Deflection in Inches	Strain $(x10^{-3})$, inches/inch						
		Gage #1	Gage #2	Gage #3	Gage #4	Gage #5	Gage #6	Gage #7
0.5	0.189							
2.5	0.221	0.1718	0.2435	0.2514	0.0059	0.0191	0.0250	0.0118
5.0	0.247	0.3191	0.4969	0.5078	0.0535	0.0795	0.0908	0.0633
7.5	0.264	0.5024	0.7392	0.7530	0.0849	0.1286	0.1473	0.1046
10.0	0.274	0.6650	0.8720	0.8867	0.0893	0.1458	0.1684	0.1173
12.5	0.283	0.8897	1.005	1.022	0.0830	0.1536	0.1831	0.1257
15.0	0.290	1.063	1.108	1.127	0.0825	0.1620	0.1959	0.1374
17.5	0.295	1.273	1.232	1.254	0.0874	0.1777	0.2155	0.1576
20.0	0.300	1.521	1.357	1.384	0.0967	0.1968	0.2391	0.1826
22.5	0.305	1.806	1.486	1.515	0.1065	0.2160	0.2636	0.2096
25.0	0.310	2.138	1.622	1.651	0.1178	0.2352	0.2887	0.2361
27.5	0.315	2.521	1.758	1.788	0.1276	0.2523	0.3118	0.2612
30.0	0.319	2.921	1.900	1.932	0.1370	0.2685	0.3354	0.2857
32.5	0.323	3.332	2.050	2.085	0.1473	0.2867	0.3599	0.3108
35.0	0.328	3.770	2.201	2.239	0.1576	0.3049	0.3835	0.3358
37.5	0.332	4.249	2.356	2.394	0.1679	0.3226	0.4071	0.3594
40.0	0.336	4.797	2.516	2.555	0.1792	0.3417	0.4311	0.3825
42.5	0.340	5.400	2.680	2.717	0.1905	0.3614	0.4552	0.4051
45.0	0.345	6.300	2.857	2.883	0.2018	0.3815	0.4803	0.4267
47.5	0.350	8.448	3.055	3.056	0.2131	0.4007	0.5044	0.4473
50.0	0.356	11.81	3.256	3.232	0.2258	0.4218	0.5284	0.4690
52.5	0.362	16.14	3.455	3.406	0.2371	0.4419	0.5530	0.4891
55.0	0.369	21.08	3.642	3.568	0.2470	0.4621	0.5766	0.5078
57.5	0.375	26.09	3.816	3.719	0.2553	0.4817	0.5997	0.5255
60.0	0.383	31.97	3.981	3.859	0.2612	0.5009	0.6213	0.5402

Table A22 (con't.)

Test Readings of Specimen 4-A

Load in Kips	Pin Deflection in Inches	Strain $(x10^{-3})$, inches/inch						
		Gage #1	Gage #2	Gage #3	Gage #4	Gage #5	Gage #6	Gage #7
62.5	0.392	38.59	4.143	3.997	0.2661	0.5205	0.6444	0.5549
65.0	0.403	44.61	4.273	4.111	0.2690	0.5382	0.6645	0.5667
67.5	0.416		4.418	4.246	0.2720	0.5589	0.6877	0.5785
70.0	0.429		4.574	4.409	0.2754	0.5800	0.7118	0.5894
72.5	0.446		4.776	4.647	0.2779	0.6031	0.7378	0.5982
75.0	0.463		5.079	5.008	0.2789	0.6282	0.7649	0.6051
77.5	0.484		5.536	5.553	0.2775	0.6558	0.7946	0.6102
80.0	0.507		6.222	6.349	0.2731	0.6869	0.8282	0.6117
82.5			7.219	7.448	0.2657	0.7222	0.8659	0.6092
85.0			8.418	8.725	0.2563	0.7610	0.9066	0.6042
87.5				10.53	0.2367	0.8092	0.9558	0.5890
90.0				13.23	0.2048	0.8726	1.020	0.5605
92.5				18.42	0.1454	0.9657	1.113	0.5030

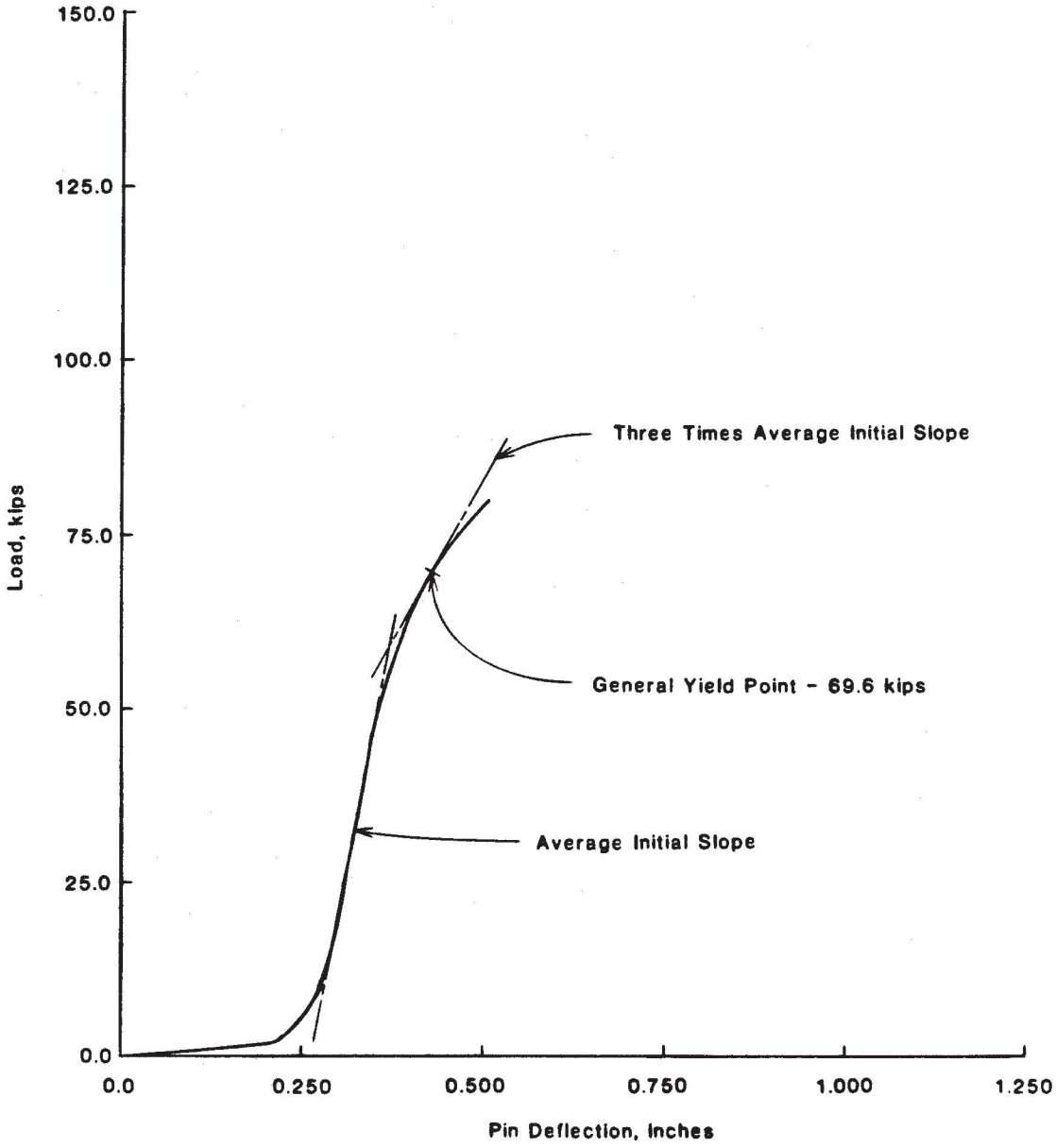

Fig. A76 - Load vs. Pin Deflection - Specimen 4-A

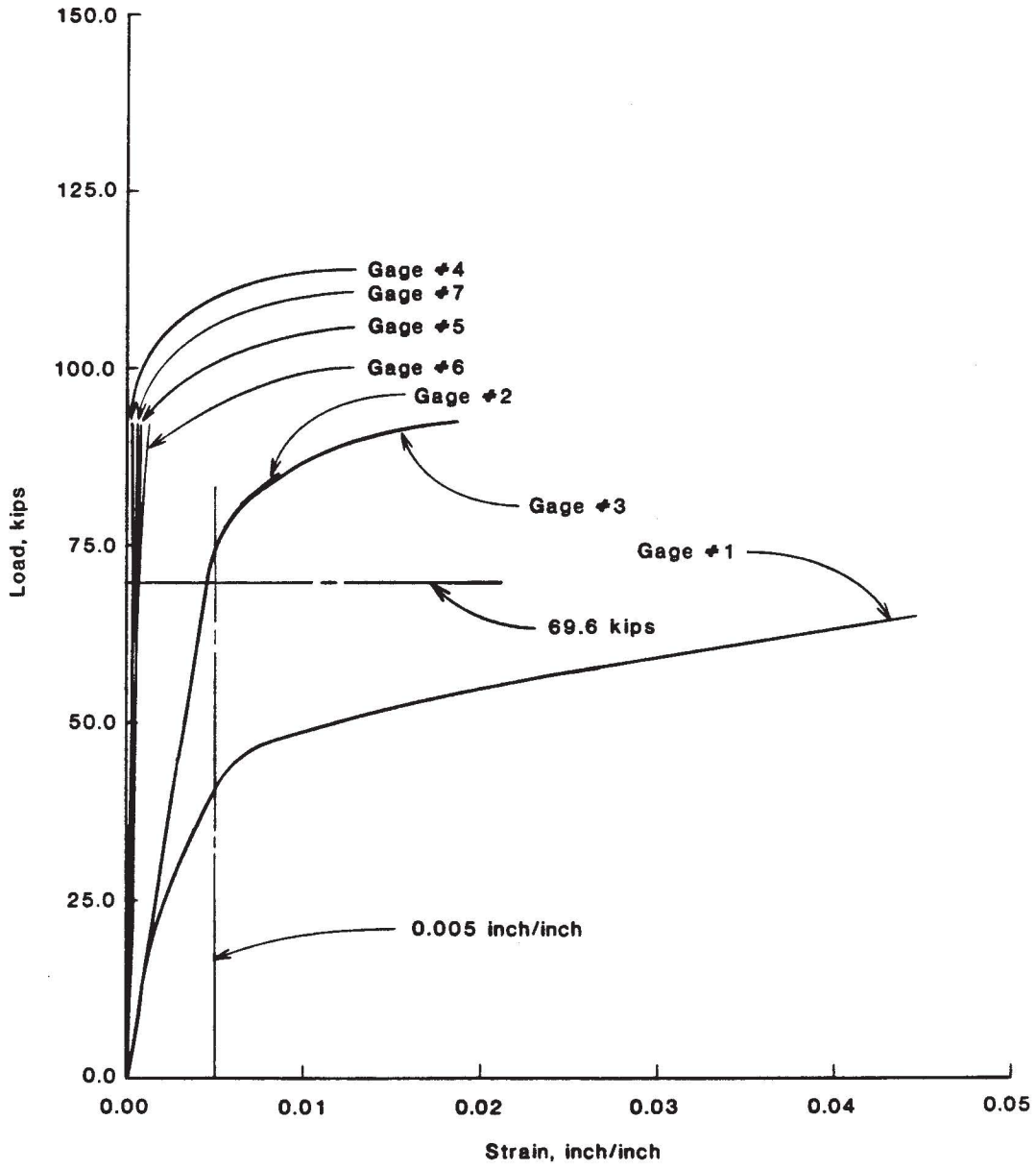

Fig. A77 - Load vs. Strain - Specimen 4-A

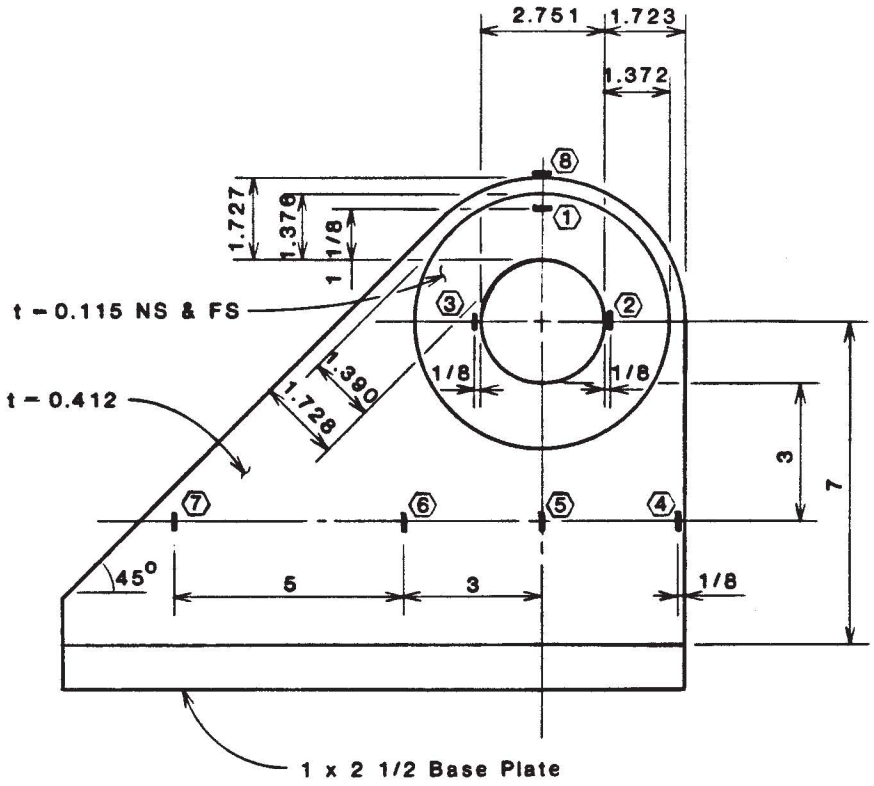

Notes:

▌ indicates strain gage

Dimensions are in inches. 1 in = 25.4 mm

Fig. A78 - As-built Dimensions of Specimen 5-A

Table A23

Summary of Results of Test 5-A

Item	Value
D_h/D_p	1.00
Yield Load, kips	139.8
Failure Load, kips	167.2
Location of Failure	Side

Note: 1 kip = 4.45 kN

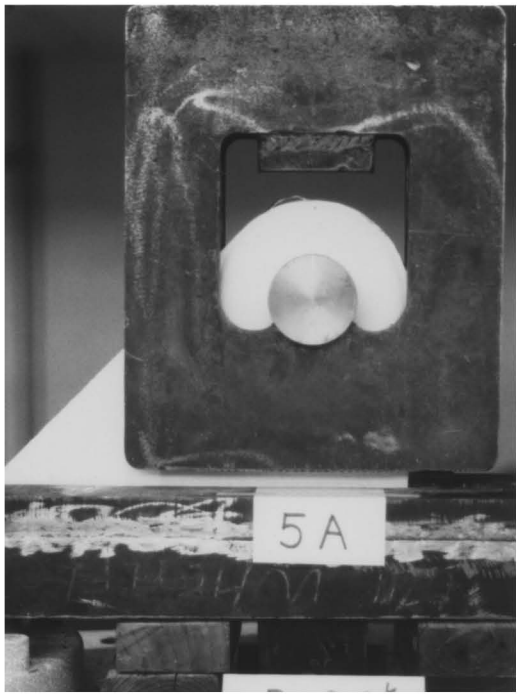

Fig. A79 - Specimen 5-A
at 0.0 kips

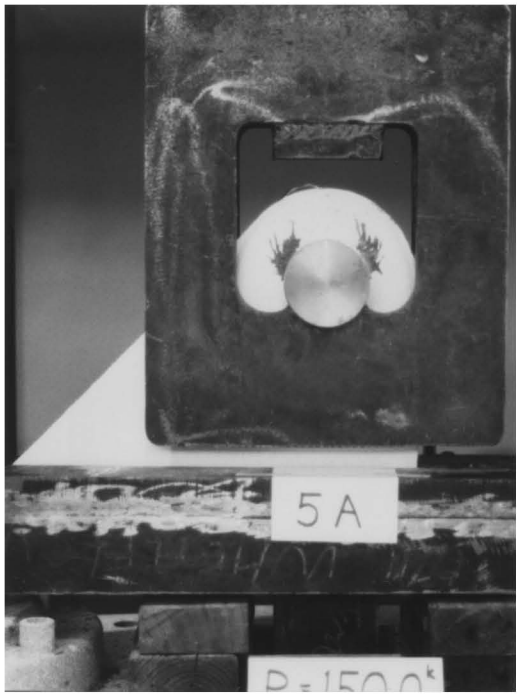

Fig. A80 - Specimen 5-A
at 150.0 kips

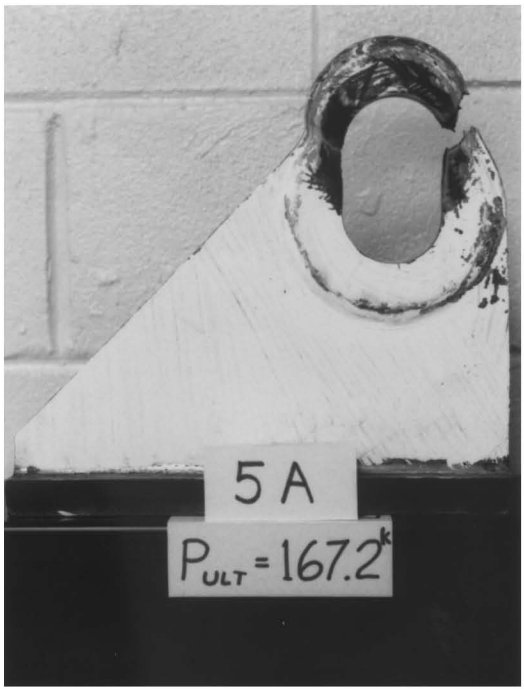

Fig. A81 - Specimen 5-A
After Failure

Table A24

Test Readings of Specimen 5-A

Load in Kips	Pin Deflection in Inches	Strain $(x10^{-3})$, inches/inch							
		Gage #1	Gage #2	Gage #3	Gage #4	Gage #5	Gage #6	Gage #7	Gage #8
1.0	0.035								
2.5	0.067		0.1760	0.3900	0.0327	0.0530	0.0701	0.0498	0.0226
5.0	0.088	0.0717	0.2906	0.5747	0.0495	0.0662	0.0861	0.0533	0.0838
7.5	0.100	0.1441	0.4052	0.7393	0.0732	0.0806	0.1013	0.0568	0.1492
10.0	0.109	0.2142	0.5225	0.8992	0.1044	0.1005	0.1203	0.0614	0.2111
12.5	0.118	0.2797	0.6410	1.058	0.1391	0.1215	0.1418	0.0665	0.2711
15.0	0.125	0.3389	0.7588	1.227	0.1753	0.1445	0.1632	0.0716	0.3312
17.5	0.131	0.3982	0.8833	1.388	0.2135	0.1706	0.1866	0.0758	0.3904
20.0	0.137	0.4536	1.007	1.485	0.2509	0.1963	0.2084	0.0797	0.4485
22.5	0.142	0.5086	1.137	1.569	0.2899	0.2236	0.2306	0.0836	0.5078
25.0	0.147	0.5608	1.265	1.630	0.3293	0.2501	0.2521	0.0867	0.5671
27.5	0.152	0.6104	1.396	1.668	0.3687	0.2763	0.2720	0.0890	0.6268
30.0	0.157	0.6787	1.528	1.721	0.4069	0.3024	0.2915	0.0913	0.6861
32.5	0.161	0.7314	1.660	1.730	0.4451	0.3277	0.3102	0.0933	0.7462
35.0	0.165	0.7610	1.794	2.102	0.4821	0.3531	0.3293	0.0945	0.8059
37.5	0.170	0.8401	1.930	2.431	0.5199	0.3787	0.3487	0.0965	0.8678
40.0	0.174	0.8457	2.061	2.784	0.5564	0.4044	0.3677	0.0977	0.9370
42.5	0.178	0.8654	2.195	3.259	0.5933	0.4296	0.3863	0.0985	1.003
45.0	0.183	0.9400	2.326	3.611	0.6301	0.4559	0.4049	0.0998	1.070
47.5	0.187	1.087	2.397	4.050	0.6663	0.4816	0.4240	0.1009	1.142
50.0	0.190	1.134	2.476	4.425	0.7037	0.5085	0.4427	0.1013	1.208
52.5	0.193								
55.0	0.198	1.203	2.569	5.293	0.7774	0.5591	0.4789	0.1021	1.370
57.5	0.202	1.307	2.581	5.684	0.8140	0.5837	0.4956	0.1017	1.446
60.0	0.205	1.420	2.596	6.152	0.8499	0.6078	0.5124	0.1017	1.516

Table A24 (con't.)

Test Readings of Specimen 5-A

Load in Kips	Pin Deflection in Inches	Strain $(x10^{-3})$, inches/inch							
		Gage #1	Gage #2	Gage #3	Gage #4	Gage #5	Gage #6	Gage #7	Gage #8
62.5	0.209	1.495	3.157	6.467	0.8877	0.6308	0.5299	0.1006	1.590
65.0	0.213	1.516	3.383	6.683	0.9255	0.6550	0.5467	0.1006	1.654
67.5	0.217	1.545	3.659	6.903	0.9645	0.6788	0.5634	0.0998	1.723
70.0	0.221	1.587	4.030	7.129	1.005	0.7021	0.5802	0.0986	1.793
72.5	0.225	1.685	4.350	7.356	1.054	0.7286	0.5989	0.0975	1.852
75.0	0.228	1.790	4.724	7.484	1.097	0.7512	0.6144	0.0963	1.905
77.5	0.231	1.890	5.039	7.713	1.151	0.7757	0.6320	0.0947	1.963
80.0	0.234	1.959	5.373	7.900	1.207	0.7995	0.6483	0.0936	2.023
82.5	0.238	1.985	5.841	8.127	1.270	0.8241	0.6659	0.0924	2.088
85.0	0.242	2.042	6.228	8.318	1.332	0.8471	0.6819	0.0909	2.149
87.5	0.245	2.118	6.600	8.590	1.395	0.8716	0.6990	0.0893	2.215
90.0	0.248	2.203	6.941	8.890	1.459	0.8950	0.7161	0.0877	2.281
92.5	0.252	2.275	7.364	9.123	1.524	0.9180	0.7325	0.0854	2.347
95.0	0.255	2.358	7.856	9.427	1.586	0.9417	0.7496	0.0835	2.415
97.5	0.258	2.435	8.353	9.687	1.645	0.9666	0.7667	0.0815	2.483
100.0	0.261	2.528	8.905	9.944	1.705	0.9896	0.7835	0.0792	2.556
102.5	0.264								
105.0	0.268	2.772	10.02	10.46	1.823	1.035	0.8174	0.0742	2.732
107.5	0.271	2.928	10.50	10.81	1.886	1.057	0.8345	0.0718	2.833
110.0	0.274	3.072	10.86	11.13	1.941	1.081	0.8524	0.0691	2.912
112.5	0.277	3.235	11.38	11.56	1.993	1.103	0.8680	0.0660	3.003
115.0	0.280	3.380	11.89	11.95	2.052	1.127	0.8859	0.0637	3.108
117.5	0.284	3.538	12.36	12.33	2.111	1.148	0.9023	0.0598	3.224
120.0	0.287	3.687	12.77	12.67	2.165	1.166	0.9171	0.0567	3.337
122.5	0.292	3.866	13.20	13.10	2.228	1.185	0.9331	0.0528	3.453

Table A24 (con't.)

Test Readings of Specimen 5-A

Load in Kips	Pin Deflection in Inches	Strain $(x10^{-3})$, inches/inch							
		Gage #1	Gage #2	Gage #3	Gage #4	Gage #5	Gage #6	Gage #7	Gage #8
125.0	0.296	4.023	13.78	13.51	2.288	1.204	0.9487	0.0492	3.586
127.5	0.300	4.283	14.13	14.12	2.353	1.221	0.9643	0.0457	3.745
130.0	0.304	4.475	14.36	14.69	2.411	1.239	0.9792	0.0418	3.892
132.5	0.308	4.675	14.64	15.21	2.468	1.258	0.9959	0.0387	4.038
135.0	0.314	5.105	14.80	15.90	2.535	1.269	1.009	0.0329	4.259
137.5	0.324	5.989	14.87	16.49	2.615	1.273	1.018	0.0259	4.534
140.0	0.334	6.851	14.93	16.84	2.685	1.284	1.030	0.0193	4.910
142.5	0.349	7.553	15.03	17.39	2.756	1.293	1.041	0.0108	6.409
145.0	0.363	9.398	15.31	17.91	2.829	1.307	1.054	0.0041	7.534
147.5	0.386	16.63		18.67	2.913	1.325	1.070		8.943
150.0	0.410	25.65		20.11	2.995	1.345	1.088		

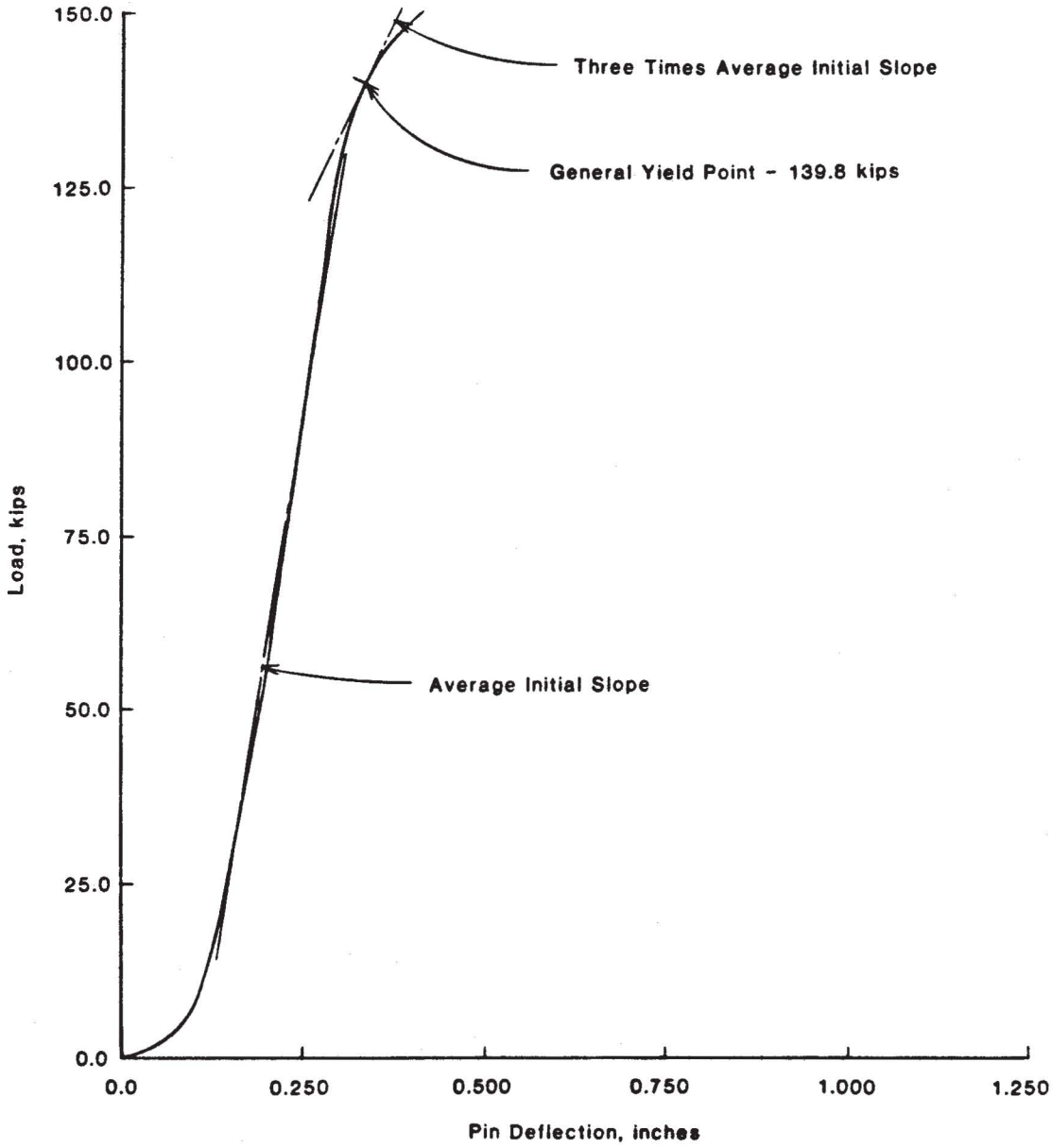

Fig. A82 - Load vs. Pin Deflection - Specimen 5-A

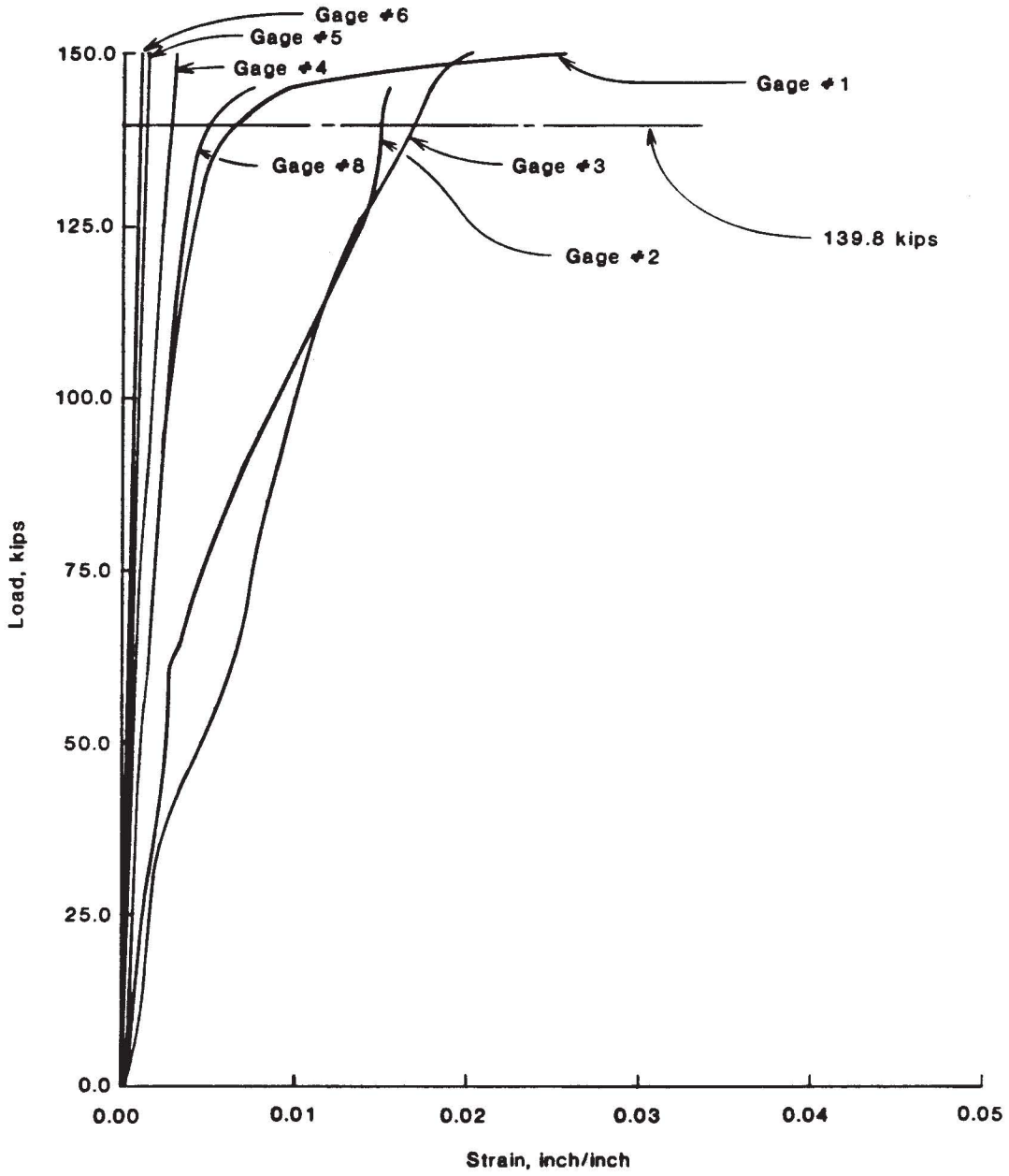

Fig. A83 - Load vs. Strain - Specimen 5-A

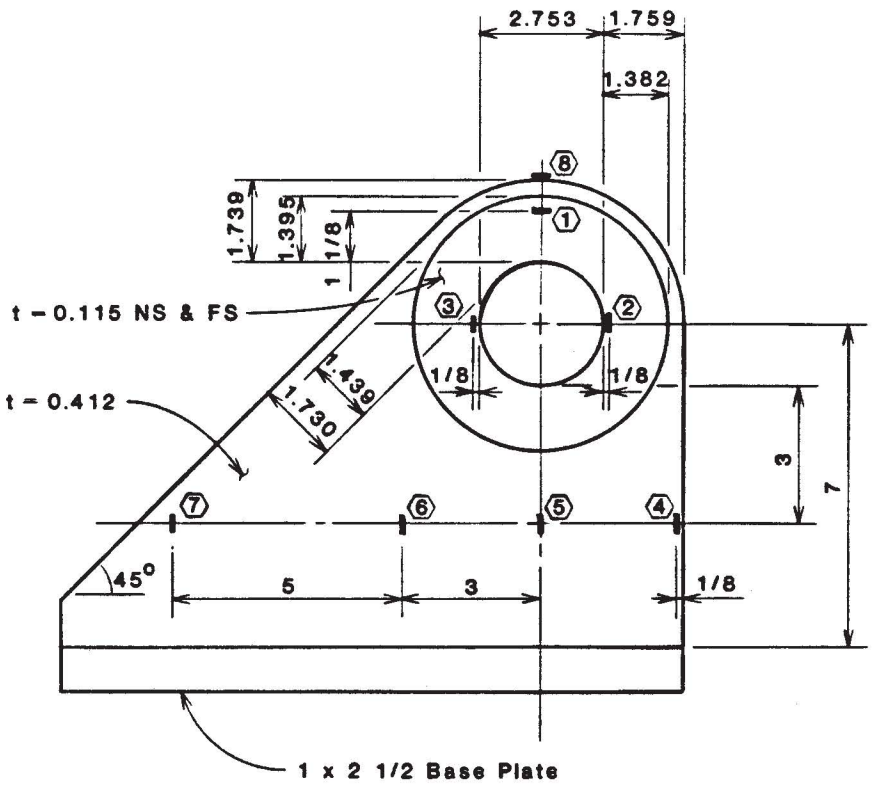

Notes:

▌ indicates strain gage

Dimensions are in inches. 1 in = 25.4 mm

Fig. A84 - As-built Dimensions of Specimen 5-B

Table A25

Summary of Results of Test 5-B

Item	Value
D_h/D_p	1.70
Yield Load, kips	110.0
Failure Load, kips	123.6
Location of Failure	Beyond

Note: 1 kip = 4.45 kN

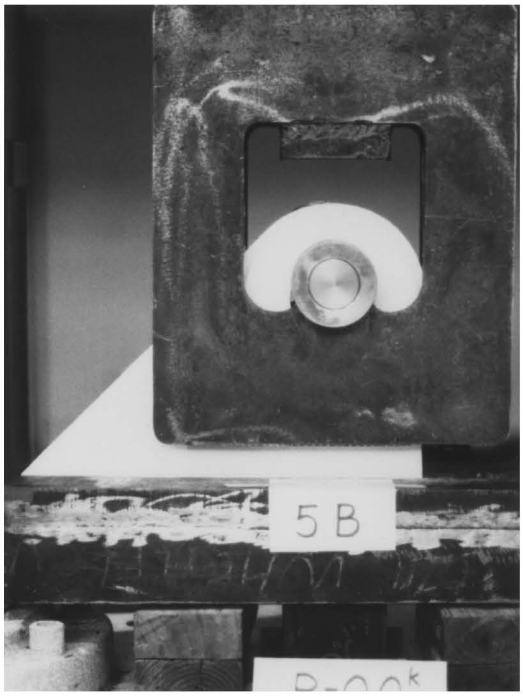

Fig. A85 - Specimen 5-B
at 0.0 kips

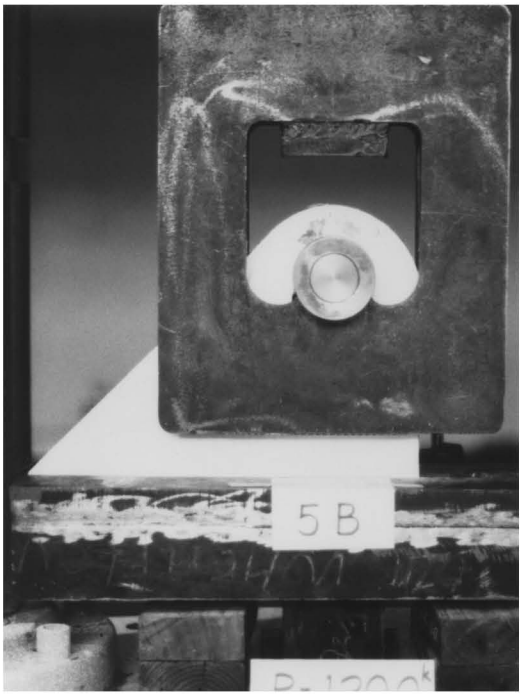

Fig. A86 - Specimen 5-B
at 120.0 kips

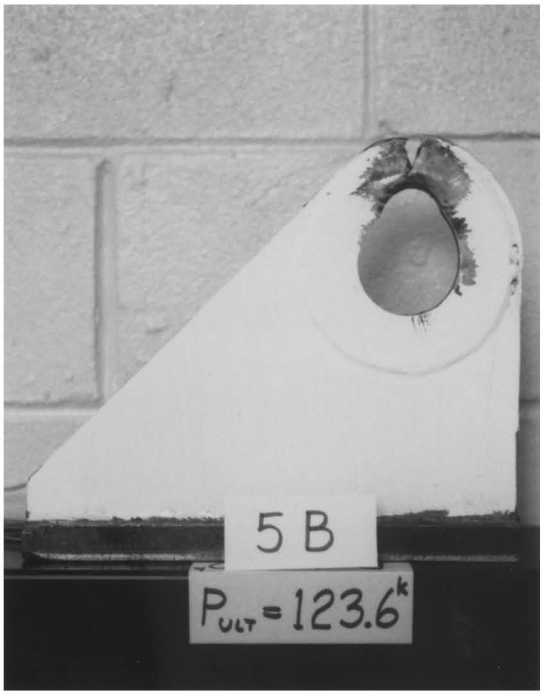

Fig. A87 - Specimen 5-B
After Failure

Table A26

Test Readings of Specimen 5-B

Load in Kips	Pin Deflection in Inches	Strain $(x10^{-3})$, inches/inch				
		Gage #1	Gage #2	Gage #3	Gage #4	Gage #8
1.0	0.033					
2.5	0.055					
5.0	0.076	0.1138	0.0058	0.0577		0.2257
7.5	0.081	0.1895	0.0644	0.1470		0.3439
10.0	0.102	0.2682	0.1411	0.2506		0.4528
12.5	0.113	0.3541	0.2343	0.3722	0.0098	0.5681
15.0	0.121	0.4274	0.3266	0.4904	0.0382	0.6829
17.5	0.130	0.5006	0.4198	0.6135	0.0689	0.8012
20.0	0.139	0.5710	0.5175	0.7430	0.1109	0.9194
22.5	0.148	0.6335	0.6142	0.8877	0.1558	1.036
25.0	0.156	0.6965	0.7133	1.027	0.2032	1.150
27.5	0.163	0.7473	0.8154	1.161	0.2486	1.264
30.0	0.171	0.8328	1.313	1.298	0.2959	1.378
32.5	0.179	0.9427	1.868	1.450	0.3438	1.493
35.0	0.186	0.9965	2.432	1.603	0.3921	1.615
37.5	0.193	1.059	3.082	1.669	0.4443	1.751
40.0	0.200	1.153	3.818	1.721	0.4990	1.888
42.5	0.206	1.217	4.672	1.723	0.5556	2.036
45.0	0.212	1.285	5.521	1.730	0.6126	2.187
47.5	0.219	1.300	6.468	1.729	0.6727	2.333
50.0	0.226	1.323	7.484	2.194	0.7337	2.495
52.5	0.233	1.350	8.574	2.381	0.7968	2.678
55.0	0.239	1.381	9.480	2.575	0.8593	2.858
57.5	0.246	1.404	10.31	2.739	0.9242	3.065
60.0	0.253	1.385	11.22	2.870	0.9882	3.312

Table A26 (con't.)

Test Readings of Specimen 5-B

Load in Kips	Pin Deflection in Inches	Strain $(x10^{-3})$, inches/inch				
		Gage #1	Gage #2	Gage #3	Gage #4	Gage #8
62.5	0.260	1.707	12.10	3.040	1.055	3.577
65.0	0.267	2.273	12.93	3.191	1.125	3.885
67.5	0.274	2.947	13.79	3.386	1.196	4.228
70.0	0.280	3.715	14.69	3.598	1.273	4.629
72.5	0.287	4.579	15.67	3.745	1.360	5.135
75.0	0.294	5.642	16.40	3.850	1.437	5.594
77.5	0.302	7.408	17.27	4.016	1.557	6.712
80.0	0.310	9.471	17.72	4.154	1.667	8.278
82.5	0.318	12.23	17.86	4.295	1.781	10.81
85.0	0.327	14.36	17.98	4.375	1.899	14.43
87.5	0.336	15.80	18.07	4.413	2.016	18.52
90.0	0.347	16.95	18.15	4.425	2.139	23.23
92.5	0.359	18.07	18.19	4.518	2.267	
95.0	0.370	19.20	18.23	4.741	2.384	
97.5	0.384	20.57	18.28	5.290	2.507	
100.0	0.400		18.39	7.637	2.637	
102.5	0.416		18.49	10.30	2.762	
105.0	0.433		18.61	13.14	2.888	
107.5	0.453		18.69	16.38	3.014	
110.0	0.475		18.89	19.64	3.144	
112.5	0.500		19.36	22.96	3.274	
115.0	0.529		19.98	26.15	3.398	
117.5	0.564		20.92	28.76	3.518	
120.0	0.603		22.36	32.16	3.622	
122.5	0.658		24.30	36.65	3.713	

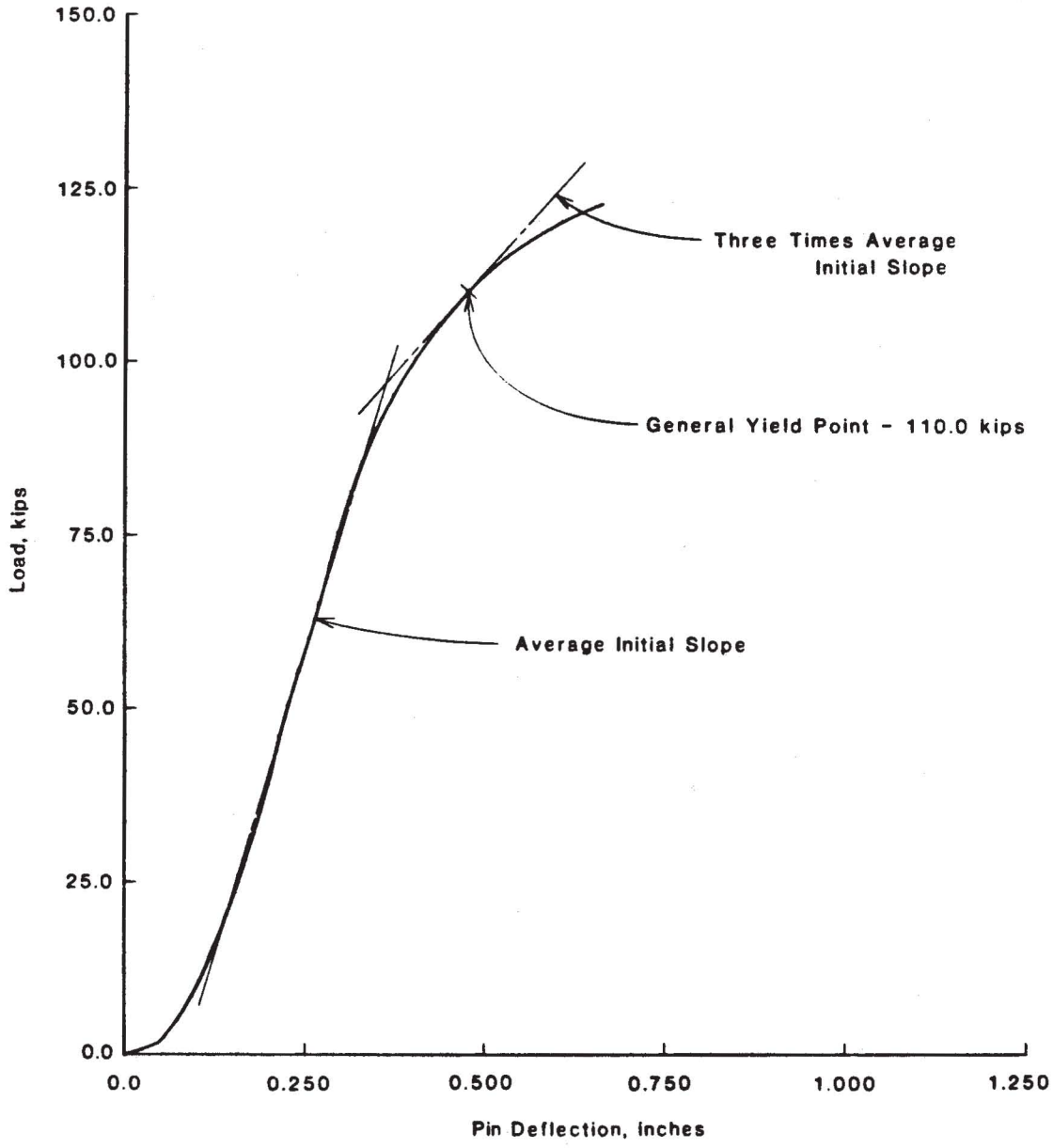

Fig. A88 - Load vs. Pin Deflection - Specimen 5-B

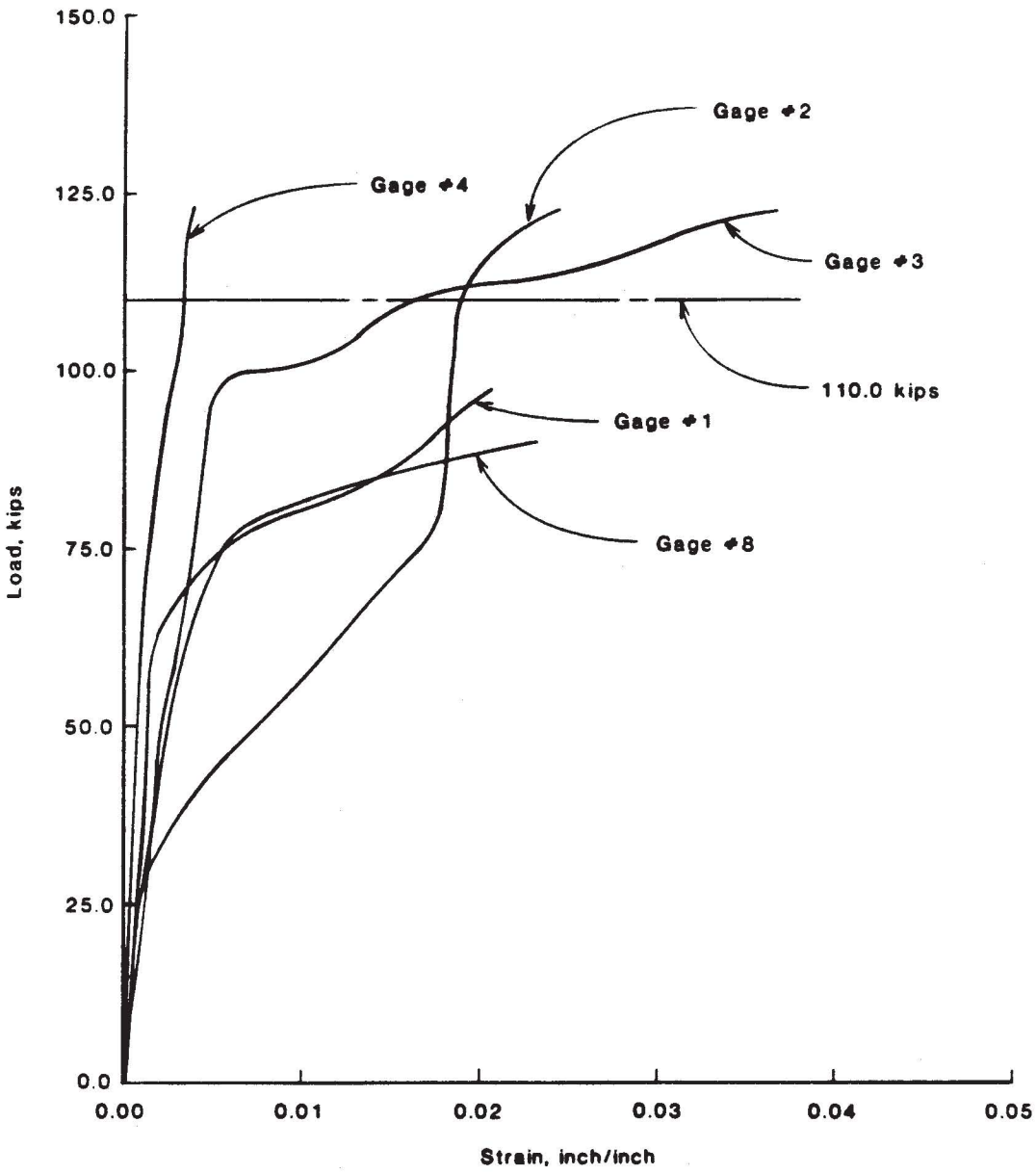

Fig. A89 - Load vs. Strain - Specimen 5-B